DE NOVO DESIGN OF

ANTIMICROBIAL PEPTIDES FOR APPLICATION

AS ANTI-INFECTIVE AGENTS

JASMEET SINGH KHARA

(*B. Sc Pharm (Hons.), NUS*)

A THESIS SUBMITTED FOR

THE DEGREE OF JOINT DOCTOR OF PHILOSOPHY

DEPARTMENT OF PHARMACY

NATIONAL UNIVERSITY OF SINGAPORE

AND

DEPARTMENT OF MEDICINE

IMPERIAL COLLEGE LONDON

2016

Declaration

I hereby declare that this thesis is my original work and it has been written by me in its entirety. I have duly acknowledged all the sources of information which have been used in the thesis.

This thesis has also not been submitted for any degree in any university previously.

_____

Jasmeet Singh Khara

05 August 2016

ACKNOWLEDGEMENTS

I am indebted to my supervisors Associate Professor Pui Lai Rachel Ee, Dr. Yang Yi-Yan, Professor Paul R Langford, Dr. Sandra M Newton and Dr. Brian D Roberston for all their patience, guidance and support over the past four years. Their invaluable advice and feedback has not only proven instrumental at all stages of my doctoral research, but also contributed significantly towards my own personal development. It has truly been a great learning experience, with not one, but five supervisors, and a privilege to have been part of this inter-disciplinary collaboration.

I am also grateful to the past and present members of the Ee Research Group, National University of Singapore (NUS), including Dr. Ong Zhan Yuin, Dr. Li Yan, Dr. Zhang Luqi, Dr. Priti Bahety, Ashita Nair, Wang Ying, Sybil Obuobi and Lim Fang Kang for all their insightful scientific input, friendship and for being there to render assistance whenever required. I would also like to acknowledge the contributions of members of the Drug and Gene Delivery Group at the Institute of Bioengineering and Nanotechnology (IBN, Biomedical Research Council, Agency for Science, Technology and Research, Singapore), especially Dr. Liu Shao Qiong, Dr. Ke Xi Yu, Dr. Yang Chuan, Dr. Jeremy Tan, Dr. Zhi Xiang Voo, and Dr. Nikken Wiradharma.

I would like to express my sincere gratitude to those in the Section of Paediatrics, Department of Medicine, Imperial College London (ICL), including Sena Plevnik, Dr. Melissa Shea Hamilton, Dr. Yanwen Li, Dr. Mingshi Li, Dr. Victoria Wright, Dr. Janine Bosse, and all members of

I would like to thank all my friends and family for their unwavering support throughout the years including my brother and sister for always being there to talk to, and my mother for all her sacrifices, for always believing in me and for never stopping us from pursuing our dreams. Finally, I would like to thank my wife, Dalvin, for her patience, love, encouragement and for being my pillar of support throughout these years. This thesis is dedicated to all of you.

LIST OF PUBLICATIONS AND PRESENTATIONS

The presented thesis is based on the following peer-reviewed journal articles:

1. **Khara JS**, Wang Y, Ke XY, Liu S, Newton SM, Langford PR, Yang YY, Ee PL. Anti-mycobacterial activities of synthetic cationic α-helical peptides and their synergism with rifampicin. Biomaterials. 2014;35:2032-8.

2. **Khara JS**, Lim FK, Wang Y, Ke XY, Voo ZX, Yang YY, Lakshminarayanan R, Ee PL. Designing α-helical peptides with enhanced synergism and selectivity against *Mycobacterium smegmatis*: Discerning the role of hydrophobicity and helicity. Acta Biomater. 2015;28:99-108.

3. **Khara JS**, Priestman M, Uhia I, Hamilton MS, Krishnan N, Wang Y, Yang YY, Langford PR, Newton SM, Robertson BD, Ee PL. Unnatural amino acid analogues of membrane-active helical peptides with anti-mycobacterial activity and improved stability. J Antimicrob Chemother. 2016;71:2181-91.

4. **Khara JS**, Obuobi S, Wang Y, Hamilton MS, Robertson BD, Newton SM, Yang YY, Langford PR, Ee PL. Disruption of drug-resistant biofilms using *de novo* designed short synthetic α-helical antimicrobial peptides with idealized facial amphiphilicity. *Under review*.

The presented thesis is also based on the following book chapter:

5. **Khara JS**, Ee PL. Nature-inspired multifunctional host defense peptides with dual antimicrobial-immunomodulatory activities. In: Santambrogio L, editor. Biomaterials in Regenerative Medicine and the Immune System. Switzerland: Springer International Publishing; 2015. p. 95-112.

The author has also contributed to the following publications:

6. Wang Y, Ke XY, **Khara JS**, Bahety P, Liu S, Seow SV, Yang YY, Ee PL. Synthetic modifications of the immunomodulating peptide thymopentin to confer anti-mycobacterial activity. Biomaterials. 2014;35:3102-9.

7. Wang Y, Rezk AR, **Khara JS**, Yeo LY, Ee PL. Stability and efficacy of synthetic cationic antimicrobial peptides nebulized using high frequency acoustic waves. Biomicrofluidics. 2016;10:034115.

8. Battersby AJ, **Khara JS**, Wright VJ, Levy O, Kampmann B. Antimicrobial proteins and peptides in early life: Ontogeny and translational opportunities. Front. Immunol. 2016;7:309.

9. Wang Y, Ke XY, Voo ZX, Yap SL, Yang C, Gao S, Liu S, Venkataraman S, Obuobi S, **Khara JS**, Yang YY, Ee PL. Biodegradable functional polycarbonate micelles for controlled release of amphotericin B. Acta Biomater. 2016;46:211-220.

10. **Khara JS**, Krishnan N, Yang YY, Langford PR, Newton SM, Robertson BD, Ee PL. Beta-sheet forming peptides with *in vitro*, intracellular and anti-biofilm activities against *Mycobacterium tuberculosis*. *In preparation*.

The work presented in this thesis has also been presented at the following conferences:

1. **Khara JS**, Krishnan N, Yang YY, Langford PR, Newton SM, Robertson BD, Ee PL. β-sheet forming peptides with *in vitro*, intracellular and anti-biofilm activities against *Mycobacterium tuberculosis*. *IV International Conference on Antimicrobial Research*. Malaga, Spain. 29th June-1st July 2016. Oral Presentation.

2. **Khara JS**, Newton SM, Yang YY, Langford PR, Robertson BD, Ee PL. *De novo* design of short synthetic anti-mycobacterial peptides. *The 2016 TB Summit*. London, UK. 21st-23rd June 2016. Oral Presentation.

3. **Khara JS**, Newton SM, Krishnan N, Uhía I, Priestman M, Langford PR, Ee PL, Robertson BD. Targeting the mycobacterial membrane using novel antimicrobial peptides for tuberculosis therapy. *The Acid Fast Club Winter Meeting*. London, UK. 8th Jan 2016. Oral Presentation.

4. **Khara JS**, Uhía I, Priestman M, Newton SM, Langford PR, Ee PL, Robertson BD. Dynamic time-lapse microscopic studies employing microfluidic-based technology reveal the killing kinetics and mechanisms of synthetic peptides in different pathogenic bacteria. *Antibiotic Resistance and Antibiotic Alternatives*. London, UK. 3rd-5th Nov 2015. Oral Presentation.

5. **Khara JS**, Priestman M, Newton SM, Langford PR, Ee PL, Robertson BD. Shedding light on the antimicrobial mechanism of synthetic peptides using microfluidic live-cell imaging technology. *International Meeting on Antimicrobial Peptides*. London, UK. 5th-7th September 2015. Poster Presentation.

6. **Khara JS**, Lim FK, Wang Y, Ke XY, Voo ZX, Yang YY, Lakshminarayanan R, Ee PL. Designing antimicrobial peptides with enhanced synergism and selectivity against drug-susceptible and multidrug-resistant tuberculosis: Insights from mechanistic-based studies. *Gordon Research Conference on Antimicrobial Peptides*. Lucca (Barga), Italy. 3rd-8th May 2015. Poster Presentation.

7. **Khara JS**, Lakshminarayanan R, Ee PL. Tackling the weak link: Lysine replacement enhances stability of potent anti-mycobacterial

peptides. *Antibiotic Alternatives for the New Millennium*. London, UK. 5th-7th Nov 2014. <u>Poster Presentation</u>.

8. **Khara JS**, Lim FK, Wang Y, Ke XY, Voo ZX, Yang YY, Lakshminarayanan R, Ee PL. An investigation of hydrophobicity and alpha-helicity on the activities of synthetic cationic antimicrobial peptides in mycobacteria. *European Congress of Clinical Microbiology and Infectious Diseases.* Barcelona, Spain, 10th-13th May 2014. <u>Poster Presentation</u>.

9. **Khara JS**, Wang Y, Ke XY, Liu S, Newton SM, Langford PR, Yang YY, Ee PL. Anti-mycobacterial activities of synthetic cationic α-helical peptides and synergistic effect in combination with rifampicin against various mycobacterial strains. *NUS-ITB Symposium.* Singapore. 12th Nov 2013. <u>Poster Presentation</u>.

TABLE OF CONTENTS

SUMMARY

Host defence peptides (HDPs) have been proposed as blueprints for the development of new antimicrobials to combat drug-resistant infections. To enhance their clinical utility, short synthetic analogues have been designed by fine-tuning their selectivity to preferentially interact with microbial over mammalian cells. However, the strategies employed by the majority of these studies are largely empirical and synthetic peptides derived from natural HDPs possess high sequence similarity, which may promote cross-resistance when applied as therapeutic agents. Adopting a *de novo* approach enables the rational design of short synthetic antimicrobial peptides (AMPs), whilst mitigating concerns of resistance development to naturally occurring innate immune peptides. Thus, the overall aim of this thesis is to rationally design novel short synthetic cationic AMPs using a *de novo* approach and evaluate their efficacy and safety in anti-infective applications. We hypothesised that rationally designed synthetic AMPs, comprising of repeated sequences corresponding to the hydrophobic periodicity of natural α-helical peptides, can be safely and effectively applied in tuberculosis mono- and combination therapy, and in the treatment and prevention of drug-resistant biofilms and endotoxemia.

To test our hypothesis, we explored four specific aims:

(1) Rationally design and evaluate short cationic α-helical AMPs for their cytotoxicity, and anti-mycobacterial activity alone and in combination with first line anti-tubercular drugs.

(2) Investigate the influence of hydrophobicity and helicity of α-helical AMPs on the anti-mycobacterial mechanisms of action and synergistic interactions in combination therapy.

(3) Examine the impact of various unnatural amino acid substitutions on the stability and anti-mycobacterial selectivity of synthetic α-helical AMPs.

(4) Assess the effect of sequence pattern and length on the biological activity of multifunctional α-helical peptides with idealised facial amphiphilicity.

In **Specific Aim 1**, we described the rational design of short synthetic amphipathic α-helical peptides, and studied the effect of various N- and C-terminal modifications on cytotoxicity, anti-mycobacterial activity and synergism with rifampicin. It was demonstrated that the peptides were effective against both drug-susceptible and MDR-TB, displayed minimal cytotoxicity, interacted synergistically with rifampicin against *M. smegmatis* and BCG, and that such combination treatment could delay the emergence of rifampicin resistance. In **Specific Aim 2**, six α-helical peptides were designed with varied hydrophobicity and helical characters and evaluated for their anti-mycobacterial mechanisms and synergism with rifampicin. It was found that increasing hydrophobicity beyond a certain threshold was detrimental to cell selectivity, and that enhancements in hydrophobicity and helicity improved synergism and increased the rate and extent of peptide-mediated membrane permeabilisation. In **Specific Aim 3**, several unnatural amino acid-modified peptides were assessed for their *in vitro* and intracellular activity against *M.*

tuberculosis, and their ability to resist protease degradation. We demonstrated that L to D amino acid substitutions proved most effective in enhancing cell selectivity, and that the D-isomer was stable to trypsin degradation and could reduce the intracellular bacterial burden of both drug-susceptible and MDR-TB. In **Specific Aim 4**, we presented the rational design of α-helical peptides with idealised facial amphiphilicity, and evaluated the influence of peptide length and sequence on the antimicrobial, anti-biofilm and anti-endotoxin activities. The peptide with the optimal composition was found to be a broad-spectrum and potent inhibitor of both drug-susceptible and MDR bacteria, able to suppress biofilm growth after 24 h and disrupt mature biofilms within 2 h of treatment, and also suppress the production of LPS-induced pro-inflammatory mediators to levels of unstimulated controls at low micromolar concentrations.

In conclusion, the findings of this thesis have supported the hypothesis that rationally designed synthetic AMPs, adopting α-helical conformations, are safe and effective in TB mono- and combination therapy, and in the treatment and prevention of drug-resistant biofilms and endotoxemia. Thus, the *de novo* designed peptides presented herein should be evaluated *in vivo* using animal models to establish their clinical potential for various anti-infective applications.

LIST OF TABLES

LIST OF FIGURES

Figure 5.10. Extracellular ATP release in a concentration-dependent manner after exposure of *M. smegmatis* to II for 2 h. Peptide-induced membrane damage is accompanied by leakage of intracellular content due to compromised membrane integrity. Data expressed as mean ± S.E.M. for three independent experiments.

Figure 5.11. Plot of viable CFU after treatment of *M. smegmatis* with various concentrations of II. 100% reduction in bacterial burden was observed at 2x, 4x and 8x MIC, suggestive of a bactericidal mechanism of action at these concentrations. Data expressed as mean ± S.E.M. for three independent experiments.

Figure 6.1. CD spectra demonstrating α-helical secondary conformations of II and its synthetic analogues with unnatural amino acid substitutions in 25 mM SDS micelle solution. Data are expressed as the mean of three runs per peptide.

Figure 6.2. Toxicity profiles of synthetic peptides modified with unnatural amino acids against (a) human red blood cells and (b) the mouse macrophage cell line RAW 264.7. (c) Viability of RAW 264.7 cells after 4 days of treatment with II-D. Peptides displayed minimal haemolytic activity and cytotoxicity against mammalian cells at various concentrations tested. Data are expressed as mean ± S.D. for two independent experiments.

Figure 6.3. Inhibitory activity of synthetic peptides against BCG at concentrations of 4x MIC following 6 h treatment with trypsin at a ratio of 1:100. Only the unmodified peptide, II, did not inhibit bacterial growth after 7 days. Data are expressed as mean ± S.D. for two independent experiments.

Figure 6.4. Killing efficiencies of antimicrobial peptide II-D against (a) H37Rv, (b) Mtb 411 and (c) CSU87 following treatment for 7 days at various concentrations. Data are expressed as mean ± S.D. for two independent experiments.

Figure 6.5. Intracellular killing of the drug-susceptible clinical isolate Mtb 411 by (a) antimicrobial peptide II-D and (b) rifampicin, and the MDR clinical isolate CSU87 by (c) antimicrobial peptide II-D and (d) moxifloxacin. Data expressed as mean ± S.D. and are representative of two independent experiments. (* $p \leq 0.05$, ** $p \leq 0.01$, *** $p \leq 0.001$, **** $p \leq 0.0001$).

Figure 6.6. Time-lapse fluorescence microscopy images of BCG following treatment with antimicrobial peptide II-D at (a) 4x MIC and (b) 8x MIC in the presence of the membrane-impermeable dye, PI. Peptide-mediated membrane disruption promoted uptake of PI into bacterial cells. Scale bar = 10 μm.

Figure 6.7. Flow cytometric analysis of the proportion of bacterial cells positively stained by the membrane-impermeable dye PI after 3 h exposure to different antimicrobials. Controls consisted of (a) H37Rv and (d) CSU87 treated with media alone. H37Rv was treated with (b) rifampicin and (c) II-D, while CSU87 with (e) moxifloxacin and (f) II-D at 4x MIC concentrations. II-

D induced a significant shift in the percentage of H37Rv and CSU87 taking up PI, suggestive of membrane permeabilising mechanisms of action. The levels of PI uptake for negative controls, rifampicin and moxifloxacin, were similar to that of media. Data are representative of three independent experiments.

Figure 6.8. The ability of antimicrobial peptide II-D to promote (a) NO and (b) TNF-α production in unstimulated RAW 264.7 mouse macrophage cells following 24 h treatment. II-D did not induce NO or TNF-α when compared to positive controls consisting of cells stimulated with 100 ng mL^{-1} LPS. Data are expressed as mean $\pm$ S.D. for two independent experiments.

Figure 6.9. Killing efficiencies of antimicrobial peptides (a) II-D and (b) FITC-II-D against BCG following treatment for 7 days at various concentrations. II-D had killing efficiencies of > 98% and > 99% at 31.3 and 62.5 mg L^{-1}, respectively, while FITC-II-D had killing efficiencies of > 99% at both 250 and 500 mg L^{-1}. Data are expressed as mean $\pm$ S.E.M. for three independent experiments.

Figure 6.10. (a) Fluorescence microscopy images of BCG treated with 500 mg L^{-1} FITC-labelled II-D for 2 h using the CellASIC ONIX Microfluidic Platform. Scale bar = 10 μm (inset scale bar = 5 μm). Confocal microscopy images following incubation of 500 mg L^{-1} FITC-labelled II-D for 2 h with (b) BCG-mCherry and (c) BCG in the presence of 2 μg mL^{-1} membrane dye FM4-64. Scale bar = 2 μm.

Figure 6.11. Fluorescence intensity profiles of BCG-mCherry along the cell length (dashed lines) showing (a) entry of FITC-II-D into the cytoplasm while (b) and (c) represent unaffected cells. Fluorescence intensity profiles of BCG along the cell width (dashed lines) showing presence of FITC-II-D in the bacterial membrane segments (d) and (e). Images were acquired following 2 h treatment with 500 mg L^{-1} of antimicrobial peptide FITC-II-D. Scale bar = 2 μm.

Figure 7.1. Helical wheel projection of α-helical peptides with idealised facial amphiphilicity, possessing the backbone sequence $(X_1Y_1Y_2X_2)_n$, where X_1 and X_2 are hydrophobic amino acids, Y_1 and Y_2 are cationic amino acids, and n is the number repeat units.

Figure 7.2. CD spectra representing α-helical propensity of peptides with the backbone sequence (a) $(LKKL)_n$ (b) $(IKKI)_n$ and (c) $(WKKW)_n$ in 25 mM SDS micelle solution, where n = 2, 2.5 and 3. Data are expressed as the mean of three runs per peptide.

Figure 7.3. Haemolytic activity of synthetic α-helical peptides possessing (a) 2 repeat units, (b) 2.5 repeat units and (c) 3 repeat units tested against blood from two healthy donors. Peptides induced minimal haemolysis at concentrations corresponding to the respective MICs. Data are expressed as mean $\pm$ S.D. for two independent experiments.

Figure 7.4. Killing efficiency of antimicrobial peptide L12 against (a) *E. coli*, (b) *S. aureus*, (c) *P. aeruginosa* and (d) *K. pneumoniae* following treatment for 18 h at concentrations corresponding to 0, 0.5x, 1x, 2x and 4x MIC. Data are expressed as mean ± S.D. for two independent experiments.

Figure 7.5. Time-lapse fluorescence microscopy images of *E. coli* (a, b, c) and *S. aureus* (d, e, f) following treatment with (a and d) media alone, (b and e) L12 at 4x MIC and (c and f) L12 at 8x MIC in the presence of the membrane impermeable dye, PI. The uptake of PI into bacterial cells within minutes of exposure supports the rapid membrane-lytic antimicrobial mechanisms of the synthetic peptides. No uptake of PI was observed in negative controls while a concentration dependent increase in the proportion of fluorescent bacteria was evident with peptide treatment. Scale bar = 10 μm.

Figure 7.6. (a) Inhibition of drug-susceptible and drug-resistant *P. aeruginosa* and *S. aureus* biofilms formation following overnight exposure to L12. (b) IVIS imaging and (c) radiance quantification of biofilm growth inhibition of bioluminescent *P. aeruginosa* treated with L12 overnight. (d) Cell viabilities of pre-formed PA-W25 and MRSA 252 biofilms after treatment with L12 for 2 h. (e) IVIS imaging and (f) radiance quantification of pre-formed biofilm disruption of bioluminescent *P. aeruginosa* exposed to L12 for 2 h. Rows in (b) and (e) represent individual replicates. L12 inhibits biofilm formation at 1x and 2x MIC, and effectively disrupts pre-established biofilms at supra-MIC levels. (* $p \leq 0.05$, ** $p \leq 0.01$, *** $p \leq 0.001$, **** $p \leq 0.0001$).

Figure 7.7. The ability of *de novo* designed peptides to (a) bind LPS within 30 min exposure and (b) restrict LPS-stimulated NO production following 24 h treatment with peptides at various concentrations. The synthetic peptides L12 and W12 strongly bound LPS and effectively inhibited NO production at sub-MIC concentrations of 3.9 μM. (* $p \leq 0.05$, ** $p \leq 0.01$, *** $p \leq 0.001$, # $p \leq 0.0001$). (c) The effect of synthetic peptides on viability of RAW 264.7 mouse macrophage cells following 24 h treatment with peptides at various concentrations. Data are expressed as mean ± S.E.M. for three independent experiments.

LIST OF ABBREVIATIONS

ABSSSI	Acute bacterial skin and skin structure infection
ADC	Albumin-dextrose-catalase
AHU	Animal Handling Unit
Ala	Alanine
AMP	Antimicrobial peptide
AMR	Antimicrobial resistance
ANOVA	One-way analysis of variance
Arg	Arginine
ATP	Adenosine triphosphate
BHI	Brain heart infusion
BMAP-18	Bovine myeloid antimicrobial peptide-18
BRC	Biomedical Research Centre
CA	Cecropin A
CCR6	CC chemokine receptor 6
CD	Circular dichroism
CFU	Colony forming unit
CHCA	α-cyano-4-hydroxycinnamic acid
CLSM	Confocal laser scanning microscopy
CSA	Cationic steroid antibiotics
CV	Crystal violet
CXCR-3	CXC chemokine receptor type 4
Cys	Cysteine
D2S	Dexamethasone-spermine
Dab	2,4-diaminobutyric acid

Dap	2,3-diaminopropionic acid
diS-C$_3$-5	3',3'-dipropylthiadicarbocyanine
DMEM	Dulbecco's Modified Eagle's medium
DMSO	Dimethyl sulfoxide
DOPE	1,2-dioleoyl-sn-glycero-3-phosphoethanolamine
DOPG	1,2-dioleoyl-sn-glycero-3-phospho-(1'-rac-glycerol)
ELISA	Enzyme-linked immune sorbent assay
EPS	Extracellular polymeric substance
FBS	Fetal bovine serum
FDA	Food and Drug Administration
FE-SEM	Field emission scanning electron microscopy
FICI	Fractional inhibitory concentration index
FILM	Facility for Imaging by Light Microscopy
FITC	Fluorescein isothiocyanate
FPRL1	Formyl peptide receptor–like 1
GDP	Gross Domestic Product
GM	Geometric mean
hBD	Human β-defensins
HC$_{50}$	Haemolysis concentration, 50%
HDAMP	Histidine derived antimicrobial peptide
HDP	Host defence peptide
His	Histidine
HNP	Human neutrophil peptide
IL	Interleukin
Ile	Isoleucine

iNOS	Inducible nitric oxide synthase
LAL	Limulus Amebocyte Lysate
LB	Bovine lactoferricin
LD50	Lethal dose, 50%
Leu	Leucine
LPS	Lipopolysaccharide
LTA	Lipoteichoic acid
LUV	Large unilamellar vesicles
Lys	Lysine
MAC	*M. avium* complex
MALDI	Matrix-assisted laser desorption/ionisation
MAPK	Mitogen-activated protein kinases
MCP-1	Monocyte chemoattractant protein-1
MDR	Multidrug-resistant
Met	Methionine
MIC	Minimum inhibitory concentration
MIP-3α	Macrophage inflammatory protein-3α
MOI	Multiplicity of infection
mPE	Meta-phenylene ethynylene
MRSA	Methicillin-resistant *Staphylococcus aureus*
MS	Mass spectroscopy
MSSA	Methicillin-susceptible *Staphylococcus aureus*
MTT	3-(4,5-Dimethylthiazol-yl)-diphenyl tetrazolium bromide
M_W	Molecular weight
ND	Not determined

NO	Nitric oxide
OADC	Oleic acid-ADC
Orn	Ornithine
OUCRU	Oxford University Clinical Research Unit
PBS	Phosphate-buffered saline
pDC	Plasmacytoid dendritic cell
PG-1	Protegrin-1
PI	Propidium iodide
PLC	Phospholipase C
PMN	Polymorphonucleocyte
Pro	Proline
RBC	Red blood cell
RP-HPLC	Reversed-phase high-performance liquid chromatography
SAMP	Synthetic AMP
SD	Standard deviation
SDS	Sodium dodecyl sulphate
SELDI	Surface-enhanced laser desorption/ionisation
SEM	Standard error of mean
Ser	Serine
SI	Selectivity index
TB	Tuberculosis
TDM	Trehalose-6,6'-dimycolate
TFA	Trifluoroacetic acid
TLR	Toll-like receptor
TNF-α	Tumour necrosis factor-α

TOF	Time-of-flight
TPCK	N-tosyl-L-phenylalanyl chloromethyl ketone
t_R	Retention time
Trp	Tryptophan
Val	Valine
VAP	Ventilator-associated pneumonia
VCAM-1	Vascular cell adhesion molecule 1
WHO	World Health Organisation
XDR	Extensively drug-resistant

CHAPTER 1: Introduction

1.1. Antimicrobial resistance: An overview

The widespread emergence of antimicrobial resistance (AMR) over the past several decades is rapidly becoming a global health emergency, especially given the dwindling number of new antibiotics undergoing clinical development [1]. In Europe and the US alone, at least 50,000 deaths are attributed to antimicrobial-resistant infections each year [2]. While the development of resistance by microorganisms to new drugs is unavoidable due to natural evolutionary processes, the indiscriminate use of antibiotics in both humans and livestock has inadvertently accelerated the selection of resistant pathogens [1, 3]. Inevitably, AMR diminishes drug efficacy which results in significant complications, higher costs, poorer treatment outcomes, and consequently, higher mortality rates [1].

Recently, the discovery of bacterial resistance to what was reported as "the last line antibiotic", colistin, has fuelled speculation that the world could be on the brink of the post-antibiotic era, an age where common ailments and infections could prove deadly [4]. By the middle of the 21st century, AMR is expected to pose a greater threat to human health than cancer, resulting in over 10 million deaths a year [2]. Without any firm action, the economic burden of AMR is projected to cost the world up to 100 trillion USD with a reduction in global Gross Domestic Product (GDP) of between 2 to 3.5% by 2050 [2]. Hence measures to curb the spread of resistance to existing antibiotics, while developing therapeutics with novel mechanisms of action, will be instrumental in tackling the escalating threat of AMR [1].

1.1.1. The burden and management of tuberculosis

Even though mortality and incidence rates have steadily declined since the World Health Organisation (WHO) declared tuberculosis (TB) as a global public health emergency over 20 years ago, it now ranks alongside HIV as the leading cause of death from an infectious disease worldwide, with 9.6 million new cases and 1.5 million deaths in 2014 [5]. Multidrug-resistant TB (MDR-TB), defined as resistance to at least rifampicin and isoniazid, two of the most effective first-line anti-tubercular drugs, accounted for 3.3% of the new cases and 20% of the previously treated cases [5]. Approximately 9.7% of MDR-TB cases are extensively drug-resistant TB (XDR-TB), an even more severe form of the disease, defined as resistance to rifampicin, isoniazid, at least one fluoroquinolone, and a second line injectable (amikacin, kanamycin or capreomycin) [5]. The WHO recently developed a new framework (The End TB Strategy) to succeed the Millennium Development Goals, aimed at reducing TB death and incidence rates in 2035 by 95% and 90% respectively, in comparison to 2015 [6]. However, given that second-line drugs only cure an estimated 60% of MDR-TB, and 40% of XDR-TB, resistant strains of *Mycobacterium tuberculosis* pose a significant challenge to global efforts in controlling TB [7].

The standard regimen for drug-susceptible TB comprises a cocktail of four drugs administered in two separate phases. The two-month long intensive phase consists of isoniazid, rifampicin, ethambutol and pyrazinamide, followed by a four-month continuation phase with isoniazid and rifampicin [8]. Although highly effective when adhered to strictly, the lengthy and

complex nature of this six-month regimen inevitably gives rise to patient compliance issues [9]. Moreover, inadequate dosing or inappropriate treatment conditions are associated with higher mortality rates and the development of MDR-TB [10]. The treatment of MDR-TB requires a combination of second- and third-line anti-tubercular agents which are not only more costly and toxic, but also less effective and entail prolonged treatment durations of 18 to 24 months [8]. While two new drugs, bedaquiline and delamanid, have recently been approved for MDR-TB treatment, rifampicin was the last first-line drug to be developed in 1967. Thus, there is an urgent need for novel anti-mycobacterial compounds that are more potent, less toxic, and effective against both MDR and XDR-TB, with the aim of shortening treatment regimens and improving treatment outcomes [6, 10, 11].

1.1.2. The discovery of new antibiotics

The serendipitous discovery of penicillin by Alexander Fleming in 1928 heralded the dawn of the antibiotic era, and has proven vital in saving countless number of lives as it enabled the effective control of bacterial infections [12]. However, it was the systematic screening approach pioneered by Selman Waksman in the 1940s, and subsequently termed as the 'Waksman platform', which proved widely successful in uncovering major antibiotic classes [13]. These discoveries spurred the golden era of antibiotic discovery from 1940 to 1960, a period which accounts for a vast majority of the antibiotics we use today [12]. Since then however, there has been a dearth in the discovery of novel classes of antibiotics [12, 13].

In a time when the development of new classes of antibiotics is imperative, paradoxically, antibiotic pipelines are shrinking. A combination of high failure rates in drug research, uncertainty of future market size for a new antibiotic due to ever-changing resistance patterns, and the prospect of achieving profitability only decades after initial financial outlay, have served as financial disincentives for pharmaceutical companies to invest in the R&D of new antibiotics [14]. With approximately two-thirds of the 37 antibiotics under development still in phase one or two clinical trials [15], only a handful may eventually obtain market approval [16]. With regards to TB, there are currently only eight new or repurposed drugs undergoing late phase clinical trials [5]. Even then, withdrawals due to efficacy concerns following post-market surveillance and emergence of resistance for follow-on compounds without novel mechanisms of action will increase attrition rates [14]. Hence, there is an urgent need to expand the size and quality of the current antibiotic pipeline to provide effective therapeutics for drug-resistant and biofilm-related infections.

1.2. Natural antimicrobial peptides

1.2.1. Structure and diversity

Natural antimicrobial peptides (AMPs) have long been regarded as fundamental pillars of human immunity that are indispensable components of both the adaptive and innate immune systems. The first in a series of landmark studies, which put the spotlight on AMPs was the discovery of cecropins in 1980 from the haemolymph of the moth *Hyalophora cecropia* [17]. Further revelations of the existence of α-defensins in human neutrophils [18], and

magainins in the skin of the frog *Xenopus laevis* [19], were suggestive of the ubiquitous presence of such defence molecules among eukaryotes, possessing broad-spectrum antimicrobial activity. Since then, over 2000 AMPs have been isolated and characterised to date from various plants and animal species including vertebrates such as amphibians, reptiles, birds, mammals, fish, and arthropods such as insects and crustaceans. Given the multiplicity of sources, it is no surprise that AMPs adopt diverse conformations, belonging to four main structural classes: α-helical, β-sheet, extended structures enriched with a particular amino acid and loop peptides (Figure 1.1) [20]. Despite the exceptional disparities in sequence and configuration, AMPs are innately similar with a high proportion of hydrophobic and cationic residues, adopting amphipathic structures upon folding, which have been implicated in their ability to kill microbes [21].
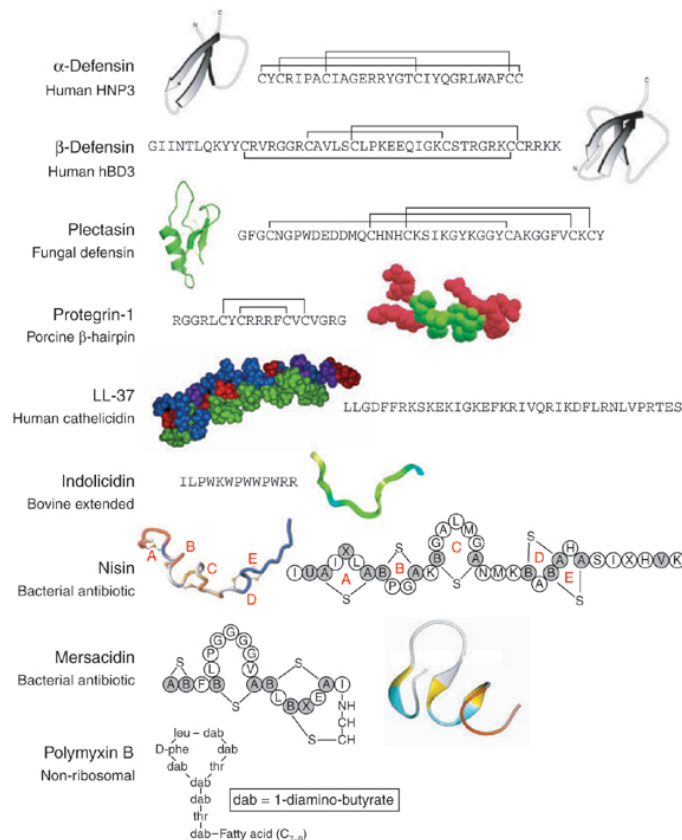
Figure 1.1. Structure and sequences of naturally occurring antimicrobial peptides. Reproduced with permission from [22]. Copyright (2006) Nature Publishing Group.

1.2.2. Mechanisms of action

1.2.2.1. Direct antimicrobial activity

AMPs are revered for their potential as anti-infective agents due to their broad-spectrum of activity encompassing bacteria, fungi, viruses and parasites [22]. Although the exact mechanisms of action remain unclear, the cationic and amphiphilic regions of AMPs are widely understood to be influential in their direct microbicidal activity. These positively charged peptides initially accumulate on the bacterial surface, mediated largely by electrostatic interactions with anionic polymers, such as lipopolysaccharide (LPS) and lipoteichoic acids (LTA) in Gram-negative and Gram-positive bacteria,

6

respectively. Subsequent pore formation has been explained *via* several complex models including the toroidal-pore or barrel-stave mechanisms or detergent-like membrane solubilisation as espoused by the "carpet-like" mechanism [22, 23]. Penetration of peptides into the lipid bilayer, driven by their inherent hydrophobicity, triggers membrane disruption that provokes homeostatic imbalances and loss of cellular content, culminating in cell death. However, the bacterial membrane may not necessarily be the sole target of AMPs as some traverse the lipid bilayer, without inducing membrane permeabilisation, and inhibit enzymatic activity or impede cell wall, nucleic acid, or protein synthesis [23-25]. Importantly, these bactericidal mechanisms are not limited to drug-susceptible bacteria, but also target their drug-resistant counterparts including methicillin-resistant *Staphylococcus aureus* (MRSA), vancomycin-resistant *Enterococcus faecalis*, MDR *Pseudomonas aeruginosa* and *M. tuberculosis* [24]. In addition, the rapid membrane-lytic mechanisms of AMPs has been suggested to diminish their propensity for resistance development, while their ability to synergise with conventional antibiotics underlines their potential as adjuvants in combinatorial drug therapies for infection control [21, 26].

1.2.2.2. Immune modulating effects

AMPs are increasingly understood to play a multifaceted role in the regulation of the immune system. Figure 1.2 highlights the diverse biological functions of AMPs, comprising a multitude of immunomodulatory properties including endotoxin neutralising ability, induction of cytokine and/or chemokine

7

production, modulation of dendritic cell and T cell immune response, and promotion of wound healing and angiogenesis [27].
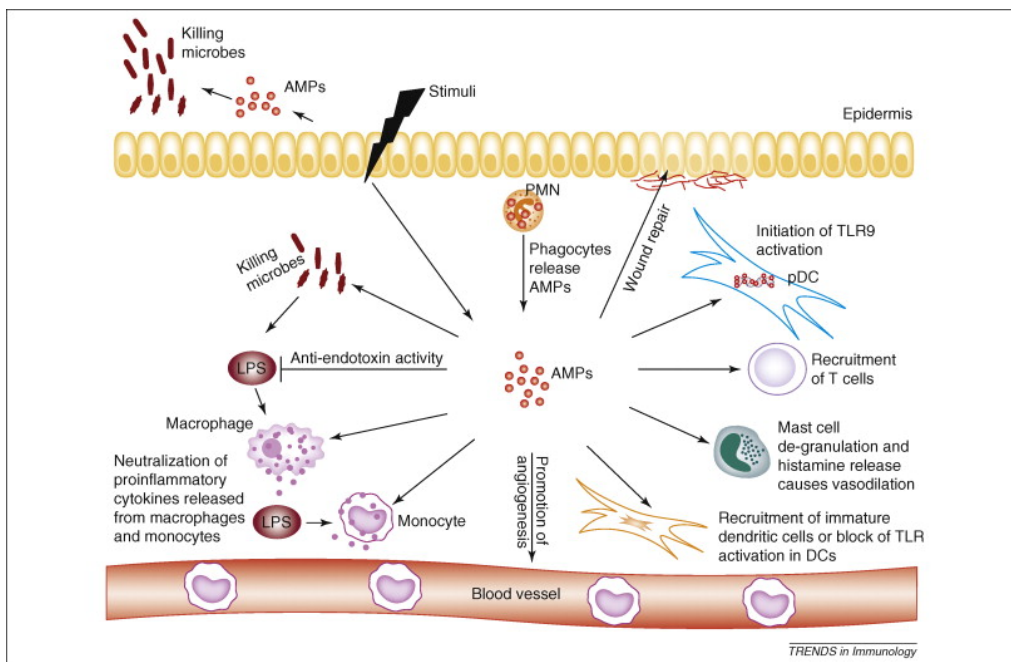
Figure 1.2. Multiple functions of antimicrobial peptides in host defence ranging from activation of innate immune cells (monocytes, macrophages, neutrophils and epithelial cells), stimulation of cytokine and chemokine production, promotion of dendritic and T cells migration, and modulation of TLR signalling. Abbreviations: AMP, antimicrobial peptide; DC, dendritic cell; LPS, lipopolysaccharide; pDC, plasmacytoid dendritic cell; PMN, polymorphonucleocyte; TLR, Toll-like receptor. Reproduced with permission from [27]. Copyright (2009) Elsevier B.V.

1.2.3. Biological functions of host defence peptides

The term host defence peptide (HDP) has been increasingly applied to accurately describe peptides exhibiting immune-regulating properties in addition to direct antimicrobial activity. Of the countless HDPs prevalent in humans and mammals, human defensins and cathelicidins are the two most well characterised. The following section explores the direct antibacterial activity and immunomodulatory activity of cathelicidins and human defensins.

1.2.3.1. HDPs as antimicrobials

The only member of the cathelicidin family to be isolated from humans is the α-helical peptide, hCAP-18. Existing as a pro-peptide, hCAP-18 undergoes proteolytic cleavage at the C-terminal region to produce a 37 amino acid domain, widely known as LL-37. This cationic peptide has demonstrated potent inhibitory activity against a broad range of Gram-positive and Gram-negative bacteria *in vitro* [28]. Furthermore, the successful elimination of both MDR *Acinetobacter baumannii* and MRSA *in vitro* following treatment with LL-37, highlights the potential utility of this peptide in eradicating drug-resistant infections [28, 29]. LL-37 has been found to be inactive against *M. tuberculosis in vitro* up to concentrations of 50 mg L^{-1} [30]. However, in *M. tuberculosis* infected macrophages, LL-37 exhibited moderate anti-mycobacterial activity after 24 hours when added exogenously at concentrations of 15 to 25 mg L^{-1} [31]. This observed intracellular activity also translated into *in vivo* efficacy when treatment with 32 μg of LL-37, three times per week for four weeks was found to significantly reduce bacterial burden in the lungs of mice infected with *M. tuberculosis*, as compared to untreated controls ($p < 0.05$) [32]. Despite its inherent poor activity *in vitro*, the anti-mycobacterial activity of LL-37 is augmented *in vivo*, indicative of potential underlying immunomodulatory mechanisms.

On the other hand, the two major classes of human defensins are comprised of α- and β- defensins, each containing six cysteine (Cys) residues which form three pairs of disulfide bonds. The fundamental distinction resides in the connectivity of these disulfide bonds, with linkages between Cys residues in

positions 1 to 6, 2 to 4 and 3 to 5 in α-defensins, but in positions 1 to 5, 2 to 4 and 3 to 6 in β-defensins. In a similar fashion to cathelicidins, proteolysis of the precursor pro-peptide liberates the active element of defensins. Early work on α-defensins, or human neutrophil peptides (HNP), in the mid-1980s revealed that HNP 1-3 mixture was not only effective against Gram-positive and Gram-negative bacteria, but also displayed antifungal and antiviral properties [18]. Follow on studies extended this spectrum of activity to include various mycobacterial strains. HNP-1 exhibited bactericidal activity against *M. tuberculosis* while HNP-1, HNP-2 and HNP-3 were found to effectively eradicate *M. avium* complex (MAC) *in vitro* [33, 34]. Treatment of *M. tuberculosis* infected macrophages with 40 mg L^{-1} HNP-1 also showed strong bactericidal activity with 98% killing after 3 days [35]. *In vivo* however, a much lower dose of 5 μg per mouse once weekly for 4 weeks resulted in significant reduction in mycobacterial burden in the lungs ($p < 0.001$) [36].

The human β-defensins (hBD) were also effective in eradicating Gram-positive and Gram-negative bacteria, though hBD-2 demonstrated ~10 fold greater activity than hBD-1 [37]. However, their ability to reduce bacterial load was severely undermined upon exposure to high salt concentrations of NaCl. Interestingly, hBD-3 emerged as a promising candidate for the treatment of nosocomial infections, buoyed by evidence of its rapidly bactericidal activity against MDR clinical isolates of *S. aureus*, *Enterococcus faecium*, *P. aeruginosa*, *Stenotrophomonas maltophilia*, and *A. baumannii* [38]. Combination treatment with HDPs has been shown to induce synergism and improve antimicrobial efficiency as compared to treatment with a lone

agent. The addition of hBD-1, hBD-2, hBD-3 and LL-37 in various permutations revealed that a combination of two or more HDPs was essential in eliciting synergistic interactions against *S. aureus* and *E. coli* [39]. A separate study evaluating the effect of combining sub-lethal doses of HNP-1 and LL-37 on their antimicrobial potency found that combination of both agents augmented the killing of *S. aureus* and *E. coli* [40]. These findings suggest that though devoid of activity when present alone at sub-inhibitory concentrations, combination of defensins with other HDPs can produce synergistic modulation of antibacterial activity in order to exert a bactericidal response.

1.2.3.2. HDPs as immune modulators

Facilitating the chemotaxis of a myriad of immune cells remains one of the principal functions of HDPs. This chemotactic activity is induced either directly by chemokine production or indirectly *via* the activation of receptors. The ability of LL-37 to promote receptor-mediated chemotaxis of various immune cells has been widely established. LL-37 has demonstrated direct chemoattractant properties for mast cells, with cell migration mediated *via* the Gi protein-phospholipase C (PLC) signalling pathway [41]. LL-37 was also found to be chemotactic for various leucocytes such as monocytes, neutrophils, eosinophils and T lymphocytes [42, 43]. The involvement of the formyl peptide receptor–like 1 (FPRL1) proved central to the recruitment of human leucocytes in mounting an immune response.

In pioneering research aimed at elucidating the chemotactic properties of human defensins, Yang *et al.* revealed that hBD-2 was a potent inducer of both T cell and immature dendritic cell migration through interactions with CC chemokine receptor 6 (CCR6) [42]. In a follow on study, the team determined that α-defensins, HNP-1 and HNP-2, were similarly chemotactic for both immature human dendritic cells and T lymphocytes, though independent of CCR6 activation [44]. Both dendritic and T cells are key modulators of adaptive immune responses. Taken together, these findings serve to reinforce the critical role of α- and β- defensins in both innate and adaptive immunity. HNP-1 and HNP-3 were also found to be chemoattractants for mast cells, T lymphocytes and macrophages while HNP-1 and HNP-2 were implicated as essential mediators of monocyte migration [45, 46]. Macrophage recruitment by HNP-1 was initiated following signal transduction by $G\alpha_i$ proteins and mitogen-activated protein kinases (MAPK) [46].

Besides their chemotactic activities, HDPs can elicit pro- or anti-inflammatory responses, dependent on the extent of cytokine induction or inhibition in different cell types. LL-37 effectively inhibited the release of the pro-inflammatory cytokine, tumour necrosis factor-α (TNF-α), from macrophages while inducing anti-inflammatory chemokine monocyte chemoattractant protein-1 (MCP-1). In epithelial cells, however, MCP-1 production was antagonised, while significant induction of interleukin-8 (IL-8) was observed. The immunomodulatory activity of LL-37 was achieved partly through the up-regulation of chemokine receptors including CCR2, CXC chemokine receptor type 4 (CXCR-4) and IL-8RB [47]. HNP-1, HNP-2 and HNP-3 increased

TNF-α and IL-1 release from human monocytes while down regulating the expression of IL-10, a known inhibitor of cytokine production. Moreover, the reduction in vascular cell adhesion molecule 1 (VCAM-1) expression in endothelial cells could potentially enhance HNP-mediated chemotaxis of leucocytes [48]. The stimulation of keratinocytes by hBD-2 and hBD-3 induced an array of pro-inflammatory cytokines and chemokines including IL-6, IL-10, IP-10, MCP-1, macrophage inflammatory protein-3α (MIP-3α) and RANTES [49]. The G protein and PLC signalling pathways were found to be involved in the potentiation of this stimulatory effect.

1.3. Limitations of HDPs

The clinical development of HDPs has been largely limited to topical applications as anti-infectives in skin diseases, rosacea, oral candidiasis and diabetic foot ulcers [50, 51]. There are several pertinent issues related to toxicity and stability which need to be resolved before peptides can be successfully applied as therapeutics [21, 22]. Firstly, peptides are vulnerable to degradation by proteases in the blood, resulting undesirable pharmacokinetic properties due to their relatively short *in vivo* half-lives [50]. To overcome this limitation, stability-enhancing modifications including peptide cyclisation, N-terminal acetylation, unnatural or D-amino acid substitutions, and the development of peptidomimetics have been proposed [22, 26]. Secondly, the complex interactions of HDPs with the immune system, as a consequence of their diverse biological functions (Figure 1.2), could result in undesirable systemic toxicities during therapeutic administration [22, 51]. As such, investigations into the more subtle cytotoxic effects of HDPs including

degranulation of mast cells and induction of apoptosis could facilitate the development of safer peptide analogues [22, 51], although this is not in the scope of this thesis. Instead, the design of synthetic AMPs which bear minimal resemblance to the sequences of HDPs, could be explored as a means of reducing undesirable immune activation, and in turn circumventing unwanted side effects.

Another major barrier is the high cost of manufacturing, as solid phase chemical synthesis of peptides can cost between $100 to $600 per gram [22]. Natural peptides tend to have long sequences (> 20 amino acids) and complex secondary structures, further complicating synthesis and increasing costs, thereby hindering large-scale production [51]. While novel approaches are being explored to reduce the manufacturing costs of peptide therapeutics, the development of shorter synthetic HDP analogues could also provide an effective means of minimising costs [22].

A significant draw of AMPs lies in the diminished propensity of microbes to develop resistance against these compounds in comparison to conventional antibiotics [52]. Given that AMPs non-specifically target the cytoplasmic membrane, it has been suggested that reconfiguration of the bacterial membrane, an energetically unfavourable and seemingly unlikely process, would be necessary for resistance development [21]. The improbability of microbial resistance developing against AMPs was demonstrated *in vitro* when efforts to generate pexiganan resistance against *S. aureus* and *S. epidermidis* proved unsuccessful [53]. In contrast, a 64-fold increase in the

minimum inhibitory concentration (MIC) of mupirocin after seven passages, and a >1000-fold increase in the MIC of fusidic acid after 14 passages, was observed against *S. aureus* [53]. Similarly, exposure of *P. aeruginosa* and MRSA to sub-inhibitory concentrations of protegrin-1 (PG-1) failed to induce resistance after 11 and 18 passages, respectively [54]. Treatment of *P. aeruginosa* with gentamicin, and MRSA with norfloxacin, under similar conditions, produced remarkably different results with 190-fold and 85-fold increase in MIC, respectively [54]. However, these studies have only selected for resistance over a relatively short period and it has been suggested that prolonged exposure to AMPs at high concentrations, when applied therapeutically, would almost certainly promote the development of resistance [55]. Such a situation, when it arises, would have severe implications for human health due to cross-resistance to innate HDPs [22, 55].

1.4. Clinical application of HDPs

Although many HDP-based therapeutics have been evaluated clinically over the past few decades, none have been approved for use in the clinic to date [50]. The development of promising drug candidates including iseganan, pexiganan, and omiganan, undergoing late stage phase III trials was hampered either due to a lack of efficacy, various regulatory barriers, poor clinical trial design or commercial considerations. The development of pexiganan for the treatment of diabetic foot ulcers was dealt a major blow back in 1999 when the drug was not approved US Food and Drug Administration (FDA) [56]. Citing ethical concerns over the trial design and lack of evidence demonstrating superiority over conventional therapies, the FDA did not deem

the drug approvable. As such, dwindling resources coupled with a shift in commercial priorities of its pharmaceutical partner forced Magainin Pharmaceuticals to cease operations. However, Dipexium Pharmaceuticals recently initiated phase III trials for the pexiganan cream, Locilex, in the treatment of diabetic foot ulcers (NCT01590758 and NCT01594762).

Omiganan was also unsuccessful in receiving FDA approval for the treatment of catheter-associated infections following phase III trials due to its failure to meet its primary clinical endpoint. Despite demonstrating statistically significant efficacy in the prevention of both catheter colonisation and microbiologically confirmed infections, it did not satisfactorily meet the primary clinical endpoint of 'physician determined infections' [56]. This failure prompted Cutanea Life Sciences to explore other potential indications, with the recently initiated phase II and III studies for the treatment of acne vulgaris (NCT02571998) and rosacea (NCT02576860), respectively.

The development of iseganan, the first antimicrobial peptide to be evaluated as an oral decontaminant, was also discontinued by Intrabiotics following Phase 3 trials which did not significantly reduce ventilator-associated pneumonia (VAP) among surviving patients [57]. The trial was halted early due a higher rate of VAP and death in the arm receiving iseganan as compared to placebo, although this was not shown to be statistically significant. The investigators attributed this failure to the short contact time between iseganan in solution and the pathogens [58]. In addition, ethical issues surrounding the design of

the trial were also raised as patients in the control arm received placebo rather than the best available treatment option [58].

In other instances, commercial considerations have seen promising lead compounds being shelved despite strong preclinical evidence of therapeutic efficacy. Plectasin was one such antibiotic which saw its clinical development come to a halt following a licensing agreement between Novozymes and Sanofi-Aventis in 2008. The relatively small market size of pneumococcal infections failed to justify the financial investment required for the clinical development of this narrow-spectrum antibiotic [59]. Successful efforts to extend the plectasin's spectrum of activity have led to the development a broad-spectrum derivative NZ2114, and despite announcing plans to initiate Phase 1 trials in 2010, no progress has been made since [59].

Natural AMPs have been studied for the past 25 years and their importance as antimicrobials and immunomodulators is well established. Although none have been approved as drugs, there are more than 10 phase II and III clinical trials using AMPs or their inducers, currently in progress or recently completed [60]. Table 1.1 provides a summary of the AMPs being actively pursued in clinical development [61]. Compared to a total of about 37 new antibiotics which are mostly analogues of old drug classes in clinical development, there is indeed significant emphasis on AMP therapeutics in this space as a novel class of antibiotics. Importantly, the industry estimates that the proportion of peptides in pharma will grow faster (9.4% annual growth in 2012–2018) than the global industry (3–6% annual growth in 2012–2016)

[62]. This is contrary to longstanding scepticism about this class of molecules being unstable and hence ineligible for drug development and inferior to small molecules. The difference is that with rapid advancement of peptide science, computer-aided analysis and combinatorial chemistry, we now have the means to modify and produce clinically relevant artificial variants and alternatives. While there are no AMPs currently being evaluated in clinical studies for application in TB chemotherapy, our background work has indeed provided strong support for this approach in the TB context.

Table 1.1. Synthetic host defence peptides undergoing active clinical development. Reproduced with permission from [61]. Copyright (2015) Springer International Publishing.

Peptide[a]	Description	Clinical application	Phase	Status	Company	Ref/Reg no.[b]
Brilacidin (PMX30063)	Synthetic defensin mimetic	Treatment for acute bacterial skin and skin structure infections (ABSSSI) caused by *S. aureus*	II	In progress	Cellceutix Corporation	NCT02052388
HB1345	Synthetic lipohexapeptide	Anti-infective for skin infections such as acne	Pre-phase I	In progress	Helix BioMedix	http://helixbio medix.com/
LTX-109	Synthetic antimicrobial peptidomimetic (SAMP)	Treatment of nasal MRSA/MSSA infection	I/II	Completed	Lytix Biopharma	NCT01158235
		Impetigo	II	Completed		NCT01803035
Omiganan (CLS001)	Synthetic 12-mer peptide derived from indolicidin	Treatment of inflammatory papules and pustules associated with rosacea	II	Completed	Cutanea Life Sciences	NCT01784133
PAC-113	Synthetic 12-mer peptide from histatin	Treatment of oral candidiasis in HIV seropositive patient	IIb	Completed	Pacgen Biopharmaceuticals	NCT00659971
Pexiganan (MSI-78)	Synthetic 22-amino acid peptide isolated from the skin of the African Clawed Frog	Treatment of mild infections associated with diabetic foot ulcers	III	In progress	Dipexium Pharmaceuticals	NCT01590758 NCT01594762

[a] Research programs that were terminated or suspended indefinitely have been excluded
[b] Reference or registration numbers are obtained from http://clinicaltrials.gov

1.5. Design strategies for development of synthetic AMPs

In a bid to develop shorter synthetic peptide antibiotics with higher potency, greater intrinsic stability and lower toxicity, researchers are turning towards naturally occurring peptides for inspiration. One strategy utilises these molecules as a reference template for systematic modification by substitution, deletion or scrambling of amino acid sequences to produce structurally related compounds termed as congeners. When the intention is to strategically combine the vital domains of two or more individual compounds, the end product is either a conjugate (peptide-ligand) or a hybrid (peptide-peptide). Another emerging class of synthetic AMPs is peptidomimetics, designed to structurally resemble naturally occurring HDPs whilst addressing their inherent drawbacks. The following section closely examines the numerous approaches that have been utilised for the purposes of designing synthetic peptides endowed with superior killing and immune-regulating properties.

1.5.1. Peptide conjugates

In essence, this approach entails the coupling of a specific ligand or drug molecule to AMPs with the aim of imparting dual antibacterial and immunomodulating properties. Though straightforward in principle, the application of this design strategy has been limited thus far. Cationic steroid antibiotics (CSA), designed as synthetic mimics of the antibiotic polymyxin B, consist of steroid polyamine conjugates capable of killing both Gram-positive and Gram-negative bacteria [63]. Spermine, a polyamine that has been shown to possess broad-spectrum antibacterial activity, is inherently positively charged and bears a marked structural resemblance to cationic AMPs [64].

This polycation was covalently linked to dexamethasone, a corticosteroid with known anti-inflammatory and immunosuppressant properties, to give a disubstituted dexamethasone-spermine (D2S). Not only was this conjugate effective against *P. aeruginosa* and MRSA, D2S was further shown to inhibit the release of IL-6 and IL-8 from neutrophils exposed to LPS or LTA [65]. The conjugate also retained glucocorticoid activity suggesting that the anti-inflammatory activity of D2S was likely mediated *via* the engagement of glucocorticoid receptors.

Recently, conjugation of thymopentin (RKDVY), a synthetic pentapeptide corresponding to amino acid residues 32-36 from the thymus hormone thymopoietin, to the N- and C- terminus of a highly cationic AMP comprising of six arginine (Arg) residues to confer the molecule with immunomodulatory properties, has been reported [66]. Thymopentin, being an immunostimulant, replicates the biological activity of thymopoietin and promotes thymocyte differentiation and maturation. The resultant peptides, RR-11 (RKDVYRRRRRR) and RY-11 (RRRRRRKDVY), displayed potent bactericidal activity against both drug-susceptible and drug-resistant *M. smegmatis* while preserving the pro-inflammatory functions of thymopentin. Both RR-11 and RY-11 induced significant TNF-α release from macrophages which was found to be comparable to levels following stimulation with thymopentin alone.

Lipopeptide conjugates are also being explored for their potential as novel antibiotics with improved antibacterial and immunomodulatory properties.

The conjugation of lipophilic acyl chains of various lengths to 12 amino acid residue fragments of human lactoferrin, LF12, was shown to enhance antibacterial killing considerably [67]. Lipopeptides comprising of acyl chains 12 carbon units in length (LF12-C12) were deemed the optimal composition, with enhancements in activity of 50-fold and 75-fold against *E. coli* and *S. aureus*, respectively. Furthermore, LF12-C12 possessed a 12-fold superior endotoxin neutralising potency as compared to the parent peptide LF12. These results highlight the applicability of lipophilic modification to augment both antimicrobial and anti-inflammatory activity of AMPs.

1.5.2. Hybrid peptides

Hybridisation is a technique combining the functional domains of two or more naturally occurring peptides with the intention of enhancing selectivity by improving antibacterial activity while minimising cytotoxicity against mammalian cells. Liu *et al.* successfully employed this in the development of hybrid β-hairpin peptides by merging various segments derived from porcine cathelicidin PG-1, cecropin A (CA) isolated from haemolymph of *Hyalophora cecropia*, and a 25 amino acid peptide from the N-terminus of lactoferrin called bovine lactoferricin (LB) [68]. The resulting hybrid peptides, LB-PG and CA-PG, exhibited superior antibacterial efficiencies and broader antimicrobial spectra as compared to parental peptides. The enhancement in potency of the constructed hybrids was attributed in part to their greater net positive charge, amphiphilicity and propensity to adopt β-hairpin conformation. Moreover, LB-PG and CA-PG inhibited the expression and release of pro-inflammatory cytokines, TNF-α and inducible nitric oxide

synthase (iNOS), and chemokines, MIP-1α and MCP-1, from macrophages stimulated with LPS. This finding underlines their potential as anti-inflammatory agents to suppress cytokine production and mitigate over-stimulation of the immune system by bacterial endotoxins.

This design strategy has also been utilised to endow previously inactive peptides with enhanced antimicrobial and anti-endotoxic activities. An LPS binding motif, termed as β-boomerang motif, GWKRKRFG, was bereft of both antimicrobial and anti-endotoxic properties but provided promise due to its LPS-anchoring capabilities [69]. This boomerang motif was exploited to abolish LPS-induced aggregation, which traps peptides at the outer membrane and in turn limits their bactericidal activity. In a bid to salvage inactive peptides TA, TB and KL-12, synthetic peptides incorporating the β-boomerang motif at the C-terminus were constructed and the hybrids displayed remarkable improvement in activity against both Gram-positive and Gram-negative bacteria [70]. This modification also produced hybrids with superior endotoxin-neutralising abilities, with peptides TA and TB having previously demonstrated poor activity in neutralising LPS.

Synthetic hybrids may also be designed with the goal of incorporating the individual benefits of each fragment into a fusion product capable of manifesting desirable traits. Scudiero *et al.* set out to develop a hybrid peptide possessing the high salt tolerance capabilities of hBD-3 while preserving the antibacterial activity of hBD-1 [71]. Three analogues, 3N, IC and 3I consistently displayed the highest potency against *P. aeruginosa*, *E.coli* and *E.*

faecalis, even at high salt concentrations. The chemotactic activity of the analogues for neutrophils and monocytes was maintained relative to parent peptides hBD-1 and hBD-3.

1.5.3. Peptidomimetics

In the pursuit of developing novel therapeutics with comparable efficacies to AMPs whilst overcoming their shortcomings including poor *in vivo* stability and high manufacturing costs, investigators have focused their attention towards designing non-peptidic oligomers and polymers. Drawing inspiration from key structural features of natural AMPs, these molecules possess an inherent amphiphilic backbone and present net positive charges to mimic the biological functions of these peptides.

Magainin, an AMP isolated from the skin of African frog Xenopus laevis, provided the template for the development of peptide mimetic, meta-phenylene ethynylene (mPE), which was explored for its anti-biofilm activity against oral pathogens [72]. mPE effectively inhibited the growth of bacterial pathogens *S. aureus*, *Porphyromonas gingivalis*, and *S. mutans*, and prevented *S. mutans* biofilm formation. An assessment into the anti-inflammatory activity of this peptide mimetic revealed a considerable decline in TNF-α secretion following LPS stimulation of macrophages, indicative of preserved biological function. mPE was further evaluated for its application in periodontal disease and displayed inhibitory activity against both *A. actinomycetemcomitans* and *P. gingivalis* biofilms [73]. Low concentrations of 2 μg mL^{-1} adequately suppressed IL-1β and induced IL-8 release in

epithelial and myeloid cells, reiterating its potential utility as an anti-inflammatory agent in the management of other diseases.

CSAs represent another class of peptidomimetics resembling AMPs, with positive charges and hydrophobic residues on opposite faces giving rise to amphiphilic secondary conformations. Antimicrobial testing of analogues CSA-13, CSA-90 and CSA-92 against a wide array of bacterial strains found that these mimetics exhibited far superior antimicrobial activities than human cathelicidin LL-37 [74]. Furthermore, all three mimetics induced IL-8 release from keratinocytes, suggestive of dual antimicrobial and pro-inflammatory responses.

In an attempt to overcome challenges associated with poor solubility and complicated synthetic pathways, ultra-short histidine (His) derived AMPs (HDAMPs) were designed to possess both antimicrobial and anti-inflammatory activities. Comprising of one His and one or two Arg moieties, these peptidomimetics proved effective against both Gram-positive and Gram-negative bacteria, including MRSA [75]. HDAMPs also demonstrated immunosuppressive properties with LPS-neutralising ability and significantly inhibited the secretion of NO and TNF-α from macrophages stimulated with LPS.

Cyclic peptidomimetics comprising mainly of the cyclic lipo-α-AApeptides (N-acylated-N-aminoethyl peptides), on the other hand, displayed enhanced antimicrobial activities against both Gram-positive and Gram-negative

bacteria as compared to the linear analogue [76]. The ability of these peptidomimetics to suppress inflammatory responses was apparent from the inhibition of nitric oxide (NO) and TNF-α production, mediated by antagonising TLR4-induced nuclear factor kappa-light-chain-enhancer of activated B-cells (NF-kB).

1.5.4. Peptide congeners

A far more direct and common approach, in designing peptides with higher antimicrobial efficacy and reduced systemic toxicity, involves systematic manipulation of the amino acid sequence of peptides with known activity. Many naturally occurring peptides from mammals, amphibians and insects have served as AMP templates including cathelicidin LL-37, hBDs, lactoferrin, heparin and thrombin. Such template-based studies are carried out by either substituting specific amino acids within the parent peptide sequence, or truncating the N- and C-terminus of the parent peptide, or a combination of both these steps. These systematic modifications not only allow the investigation of crucial physiochemical parameters for improved potency and efficacy, but also seek to identify the shortest possible active domains of the parental peptides.

The effect of length, charge, helicity, hydrophobicity and amphiphilicity on antimicrobial and haemolytic activity of AMPs has been extensively evaluated and reviewed in-depth [77]. However, the modulating effect of these physicochemical parameters on the immunomodulatory functions of AMPs has been limited thus far. An investigation into the relationship between

hydrophobicity and LPS-neutralising activity of synthetic bovine myeloid antimicrobial peptide-18 (BMAP-18) revealed that both factors were linearly correlated. Increments in hydrophobicity of BMAP-18 analogues resulted in greater inhibition of NO and TNF-α production [78]. These findings were echoed in a separate study assessing the amino acid-substituted analogues of IG-19, corresponding to the α-helical region of cathelicidin LL-37, which also found that enhancements in peptide hydrophobicity showed significant linear correlation with improved LPS-binding activity [79].

Apart from overall peptide hydrophobicity, the pinpoint substitution of specific hydrophobic amino acids along a peptide sequence can potentiate both antimicrobial and anti-inflammatory activities. Swapping out a single serine (Ser) residue at position 9 along the hydrophobic face of LL-23 with valine (Val), rendered the weakly bactericidal and immunosuppressive peptide more active, with a pronounced reduction in the release of pro-inflammatory cytokines TNF-α and MCP-1 [80]. This point mutation directed the formation of a continuous hydrophobic face, which had previously been segregated by the hydrophilic Ser residue. Another study comparing two tryptophan (Trp)-substituted analogues uncovered that substitution of this hydrophobic amino acid at the amphipathic interface, rather than at the centre of the hydrophobic face, produced analogues with greater LPS-neutralising activity [79]. Taken together, these results highlight the importance of site-specific Trp substitutions and a continuous hydrophobic surface in directing the design of novel AMPs with improved selectivity and anti-inflammatory activity.

The substitution of D-amino acids into the peptide sequence is a practice usually aimed at decreasing the inherent cytotoxicity of AMPs, as well as improving their stability to proteolytic degradation. Interestingly however, a study investigating the effect of swapping the entire amino acid sequence from L- to D-isomers found that the D-analogue exhibited the greatest antimicrobial potency amongst all the peptides tested [81]. Notably, the D-analogue proved to be a stronger inhibitor of NO production and pro-inflammatory cytokines TNF-α and MIP-2 at all concentrations. In a separate study, several D-amino acid substituted analogues of an amphipathic α-helical peptide, K9L8W, were found to possess superior cell selectivity while maintaining potent anti-inflammatory activity [82]. Given the paucity of research in this regard, the benefits of such an approach to develop more potent anti-inflammatory agents while concurrently improving their antibacterial activity, warrants further investigation.

1.5.5. Genomic mining strategies

Recently, the first report on mycobacteriophage-derived AMPs found to exhibit potent antibacterial and immunoregulative properties has emerged [83]. The researchers systematically screened the complete genome of over 70 mycobacteriophages for peptides capable of inhibiting both the growth of *M. tuberculosis* and activity of trehalose-6,6'-dimycolate (TDM), an immunostimulant produced by virulent *M. tuberculosis* that induces inflammatory responses and pulmonary granuloma formation. Out of 200 shortlisted candidates, a 34 amino acid peptide, PK34, was found to possess the strongest anti-mycobacterial activity with an MIC of 50 mg L^{-1}. PK34 also

hampered the *in vitro* release of pro-inflammatory cytokines IFN-γ, TNF-α, MCP-1, IL-6, IL-10 and IL-12 in a concentration-dependent manner. *In vivo*, PK34's mitigating effect on *M. tuberculosis* granuloma formation and TDM-induced inflammatory response was likely mediated by blocking MAPK activation. Given the diversity of bacteriophages and the abundance of information nestled within their genomic sequences, such innovative approaches could provide the key to unlocking novel compounds in our quest to expand our arsenal of antibiotics.

1.5.6. De novo design strategies

The *de novo* design of AMPs is based upon an appreciation of the structural commonalities including cationic charge, hydrophobicity, and amphiphilicity, and the intricacies surrounding the folding of proteins into different secondary conformations. This minimalist approach entails the combination of bulky lipophilic and cationic amino acids, often using a generic sequence to generate short synthetic peptides, usually consisting of ≤ 20 amino acids [26]. Trp-rich peptides such as indolicidin and tritrpticin, and their synthetic analogues, have emerged as an important class of peptides due to their broad-spectrum of antimicrobial activity, even at very short peptide lengths [84]. Park *et al*. explored short Trp-rich AMPs bearing the sequence XXWXXWXXWXX-NH2, where X represents leucine (Leu) or lysine (Lys)/Arg, for their potential antibacterial and anti-endotoxin activities [85]. Several synthetic analogues possessed enhanced activity against *E. coli* and *S. aureus* while majority displayed superior killing properties against MRSA relative to indolicidin. These analogues also proved to be potent anti-inflammatory agents, evident

from their ability to strongly inhibit NO production and neutralise LPS. A separate study evaluating short peptides ranging from five to 11 amino acids revealed that the hexapeptide comprising of three Arg and three Trp residues was the most efficient motif for antimicrobial activity [86]. A follow-on study aimed at identifying the minimal motif or pharmacophore required to produce active antibacterial peptides, comprising solely of Arg and Trp, demonstrated that the tripeptide (WRW-NH$_2$) was moderately active against *S. aureus* [87]. In contrast, the tetra- and tripeptides were inactive against the Gram-negative *E. coli*, and a minimum of five residues (three hydrophobic and two cationic) were required for antibacterial activity.

A linguistic model – defined by a set of grammatical rules based on the sequences of natural AMPs – was proposed in the development of short synthetic antibacterial peptides [88]. Recently, α-helical peptides were rationally designed based upon principles governing the folding of natural α-helical AMPs including: 1) stabilisation of the helical coil by repetitive hydrogen bonding between the carbonyl oxygen of each amino acid and the amide hydrogen four residues ahead [89], 2) maximisation of hydrophobic moment with periodic distributions of hydrophobic and cationic amino acids having repeat periods corresponding to that of the α-helix of 3.6 residues [90, 91], and 3) the incorporation of amino acids possessing helix-forming rather than helix-breaking tendencies [92]. Natural α-helical AMPs tend to unfold in solution and adopt their secondary conformation upon contacting bacterial membranes. Thus, same-charge amino acids were placed at (i + 2)th and (i + 3)th positions so that cationic repulsive forces would ensure peptides remained

unfolded in solution. Therefore, the recurring sequence comprising four amino acids $(XXYY)_n$ – where X is a hydrophobic amino acid, Y is a cationic amino acid, and n is the number of repeat units – was devised to preserve the α-helical periodicity while ensuring a balance between hydrophobic and charged residues. The designed peptides were effective against Gram-positive bacteria and yeast, with $(LLKK)_3$ exhibiting the highest selectivity for microbial over mammalian cells [93]. A follow-on study, aimed at capitalising on the presence of free sulfhydryl (thiol) groups in natural AMPs, which has been shown to augment antibacterial killing [94], demonstrated that incorporating L-Cys residues at the end-terminals of peptides extended the spectrum of activity to Gram-negative bacteria [95]. Following this strategy, this thesis expounds the applicability of short synthetic AMPs, mimicking the α-helical folding of naturally occurring peptides, as a novel class of TB therapeutics.

Another similar strategy for the design of α-helical AMPs was proposed by Javadpour *et al.*, based on the repetitive heptad sequence: $[(PNN)(PNN)P]_n$ and $[(PNN)P(PNN)]_n$ (P= polar residue, N = nonpolar residue, and n = 1, 2, 3) [96]. An increase in the heptad repeats not only showed an increase in helical content, but also antimicrobial activity, with the 7-mers failing to adopt helical structures in membrane mimetic environments, thus rendering them inactive. While the longer 14- and 21-mers were more potent, a corresponding increase in cytotoxic and haemolytic activity was also observed. Recently, β-sheet forming peptides were generated using the short recurring sequence $(X_1Y_1X_2Y_2)_n$-NH$_2$ (X_1 and X_2= hydrophobic residue, Y_1 and Y_2 = cationic residue, and n = 1, 2, 3) [97]. This design principle was successfully

implemented in the development of broad-spectrum synthetic AMPs, capable of eradicating biofilms and inhibiting LPS-stimulated NO production. Furthermore, the most selective peptides possessed more desirable lethal dose, 50% values (LD50) of 35.2 mg kg^{-1} in comparison to gramicidin (1.5 mg kg^{-1}) and polymyxin B (5.4 mg kg^{-1}) [97].

Short β-hairpin structured peptides have also been developed using various sequence-based approaches [98-100]. Peptides comprising the simplified sequence (WRXxRW)$_n$, where Xx represents the turn sequence and n = 1, 2, 3 or 4, retained antimicrobial activities even in the presence of salts at physiological concentrations and demonstrated synergistic interactions with ciprofloxacin and chloramphenicol against *S. aureus* and *E. coli* respectively [100]. Similarly, the generic sequence Ac-C-HBHB(P)HBH-GSG-HBHB(P)HBH-C-NH$_2$, where Ac is an acetyl moiety, H is a hydrophobic residue, P is a polar residue and B is a cationic residue, served as a framework to design cyclic β-hairpin peptides with LPS and lipid A binding properties [101]. Besides being anti-endotoxic, these synthetic AMPs were highly selective for microbes over mammalian cells.

1.5.7. Critical comparison of design strategies

The various design strategies to develop synthetic AMPs, as discussed in the previous sections, each present with their own set of advantages and drawbacks. In general, synthetic AMPs are produced with the intention of enhancing the clinical utility of natural HDPs, by improving stability, reducing toxicity, and enhancing the antimicrobial efficacy of these compounds. In

addition, peptide conjugates and hybrid peptides have the added advantage of producing multifunctional peptides endowed with improved biological properties. For example, combining an AMPs with an immunomodulating peptide or ligand can create conjugates or hybrids with dual functions. In other instances, such combinations can produce synthetic conjugates and hybrids which are resistant to high salt concentrations found in biological fluids or those that possess lower cytotoxicity than the parent peptides. Having said that however, these approaches fail to account for the structural folding or refolding as a consequence of combining the two separate domains, resulting in unpredictable outcomes [102]. In line with this, one study investigating the activity of SMAP28 with a targeting domain for *P. gingivalis* did not find any significant increase in activity or specificity against the bacteria [103]. Similarly, peptide congeners produced by modifications to template sequences derived from natural HDPs present similar challenges in that the interactions between amino acids, which regulate the three-dimensional peptide structure, are not accounted for [102]. Furthermore, the influence of specific amino acid substitutions is often context-dependent, and varies according to the initial template sequences being studied [102]. This in turn limits the generalisability of the findings from one study to another.

Despite the abovementioned limitations of hybrid peptides, peptide conjugates and congeners, a far greater concern is the implications associated with antimicrobial resistance development against these compounds. Should bacteria evolve resistance mechanisms against synthetic AMPs, which bear close structural similarities to natural HDPs, it would most certainly

compromise our innate immune responses during infections [104]. Therefore, alternative strategies including the design of synthetic AMPs using *de novo* approaches and the development of peptoids which comprise of non-peptidic monomers, could help allay these concerns. A significant draw of peptoids or peptidomimetics, over conventional peptides, lies in their ability to resist proteolytic degradation due the absence of the α-polyamide backbone [26]. This enhances *in vivo* stability and in turn, prolongs the half-life of these compounds. While *de novo* generated peptides containing L-amino acids are typically rendered inactive due to proteases, this limitation can easily be overcome by incorporating D-amino acids into the sequence instead [26]. In addition, the *de novo* approach enables the rational design of short synthetic peptides while majority of the other approaches are largely empirical and often require multiple steps and several substitutions for optimisation of activity. Overall, the *de novo* approach provides a simple and straightforward means of producing short synthetic AMPs, allowing for greater flexibility in the design process, and the delineation of the effect of various physicochemical properties on biological activities.

1.6. Summary and concluding remarks

As discussed in this chapter, the escalating threat of AMR has increased pressure to develop novel therapeutic strategies to tackle drug-resistant infections. AMPs have gathered considerable interest as a new source of antibiotics due to their broad-spectrum and rapid bactericidal activities, in addition to their ability to synergise with conventional antibiotics against drug-resistant pathogens [105]. Even three decades after their discovery,

researchers are still drawing inspiration from naturally occurring peptides, including defensins, cathelicidins, magainins, melittins and cecropins, in their quest to develop novel peptide therapeutics [24]. However, natural AMPs are increasingly recognised as poor therapeutic candidates due to their long sequences, which inadvertently induce significant systemic toxicities and translate into higher manufacturing costs [22]. To enhance their clinical utility, short synthetic analogues have been designed by fine-tuning their selectivity to preferentially interact with microbial over mammalian cells. However, the strategies employed by the majority of these studies have remained largely empirical, often utilising natural AMPs as templates, or helical wheel projections to perform modifications by replacing, deleting or scrambling amino acid sequences [26]. Rational design strategies based upon an appreciation of the structural intricacies surrounding protein secondary structures have been successfully implemented in the *de novo* design of short synthetic α-helical [96], β-sheet [97, 106], and β-hairpin peptides [98-100], which bear minimal resemblance to natural HDPs. However, such rational approaches have yet to be applied to the *de novo* design of short synthetic anti-mycobacterial peptides. As such, this thesis first explores the feasibility of rationally designed synthetic α-helical AMPs as anti-tubercular agents and subsequently, a new sequence-based approach for the design of multifunctional α-helical peptides with idealised facial amphiphilicity, is proposed. In doing so, we demonstrate that the adoption of such systematic design principles, in the optimisation of short synthetic AMPs, could facilitate the development of safe and effective novel peptide therapeutics for application in infectious and inflammatory human diseases.

CHAPTER 2: Hypothesis and aims

The rapid emergence of AMR, coupled with shrinking antibiotic pipelines, has increased demands for antimicrobials with novel mechanisms of action. HDPs have been proposed as blueprints for the development of new antimicrobials to combat drug-resistant infections. Given their nonspecific membrane-lytic mechanisms, AMPs possess broad-spectrum activities, are rapidly bactericidal and consequently, more resilient to antibiotic resistance development as compared to conventional antimicrobials [24]. These inherent advantages have firmly placed the limelight on AMPs over the past decade as an alternative class of therapeutics. As discussed in Chapter 1, the clinical application of HDPs has been limited thus far, due to a combination of high manufacturing costs, toxicity issues, poor *in vivo* stability and reduced efficacy in comparison to existing treatment options [56, 107]. The synthetic approach has been adopted in the development of HDPs analogues with shorter sequence lengths to reduce production costs, while achieving equal, if not greater effectiveness and stability under physiological conditions [26, 108]. In addition, various structural modifications aimed at improving cell selectivity by minimising toxicity to host cells while enhancing antimicrobial potency have been proposed [109]. Amongst the different synthetic design strategies, hybrid peptides, peptide conjugates, and a template-based approach to generate peptide congeners, are most commonly employed. However, these approaches are mainly empirical and synthetic peptides derived from natural HDPs possess high sequence similarity, which may promote cross-resistance when applied as therapeutic agents [55]. Adopting a *de novo* approach enables the

rational design of short synthetic AMPs, whilst mitigating concerns of resistance development to naturally occurring innate immune peptides.

Thus, the overall aim of this thesis is to rationally design novel short synthetic cationic AMPs using a *de novo* approach and evaluate their efficacy and safety in anti-infective applications. We hypothesised that rationally designed synthetic AMPs, comprising of repeated sequences corresponding to the hydrophobic periodicity of natural α-helical peptides, can be safely and effectively applied in TB mono- and combination therapy, and in the treatment and prevention of drug-resistant biofilms and endotoxemia.

To test our hypothesis, we explored four specific aims:

(1) Rationally design and evaluate short cationic α-helical AMPs for their cytotoxicity, and anti-mycobacterial activity alone and in combination with first line anti-tubercular drugs.

(2) Investigate the influence of hydrophobicity and helicity of α-helical AMPs on the anti-mycobacterial mechanisms of action and synergistic interactions in combination therapy.

(3) Examine the impact of various unnatural amino acid substitutions on the stability and anti-mycobacterial selectivity of synthetic α-helical AMPs.

(4) Assess the effect of sequence pattern and length on the biological activity of multifunctional α-helical peptides with idealised facial amphiphilicity.

The work undertaken to address each of the specific aims is outlined as follows: in Chapter 4, short synthetic amphipathic α-helical peptides, with various N- and C-terminal modifications, were evaluated for synergism with rifampicin against mycobacteria, and whether such combination therapy was effective in delaying the emergence of rifampicin resistance (Specific aim 1). In Chapter 5, systematic evaluation of the anti-mycobacterial and cytotoxic activities of six α-helical peptides, with varied hydrophobicity and helical characters, was performed to determine the optimal composition for enhanced mycobacterial selectivity. The modulating effect of hydrophobicity and α-helicity on the anti-mycobacterial mechanisms of synthetic AMPs, and their synergism with rifampicin, was reported for the first time (Specific aim 2). In Chapter 6, several unnatural amino acid-modified peptides were assessed for their resistance to protease degradation, in addition to their *in vitro* and intracellular activity against *M. tuberculosis*. Mechanistic studies were also undertaken to elucidate the site of action of the most selective peptide (Specific aim 3). In Chapter 7, the *de novo* design of α-helical peptides with idealised facial amphiphilicity, based on an understanding of the pertinent features of protein secondary structures, is presented. The α-helical amphiphiles were evaluated for broad-spectrum antimicrobial activities against clinical isolates of drug-susceptible and MDR bacteria, their ability to suppress biofilm growth and disrupt mature biofilms, and also their potential to neutralise bacterial endotoxins (Specific aim 4). Finally, in Chapter 8, we provide conclusions based on the pertinent findings in this thesis and explore potential future directions for the development of synthetic peptides as therapeutics.

The successful completion of this thesis has provided insights into the design of synthetic peptide amphiphiles with improved cell selectivity, enhanced synergistic interactions and superior anti-biofilm and anti-endotoxin activities. Overall, the findings presented in this thesis underscore the applicability of *de novo* strategies employed here for the rational design of synthetic α-helical AMPs against drug-susceptible and drug-resistant biofilms and infections, including MDR-TB.

CHAPTER 3: Materials and methods

3.1. Materials

Synthetic peptides, including the N-terminal fluorescein isothiocyanate (FITC)-labelled II-D, were synthesised by GL Biochem (Shanghai, China) and their purity was confirmed to be more than 95% by reversed-phase high-performance liquid chromatography (RP-HPLC) carried out by the manufacturer. Acetonitrile (HPLC grade) and agar-agar technical for microbiology were purchased from Merck (Darmstadt, Germany). Dimethyl sulfoxide (DMSO, synthesis grade, 99.9%), Dulbecco's Modified Eagle's medium (DMEM), Dulbecco's phosphate-buffered saline (PBS) solution, Tween 80, glycerol, rifampicin, ethambutol, moxifloxacin, trifluoroacetic acid (TFA), propidium iodide (PI), carbenicillin, crystal violet (CV), HPLC grade water, Triton X-100, LPS from *E. coli* 0111:B4 and 150 kDa dextran-FITC were acquired from Sigma-Aldrich (St Louis, MO, USA). Hygromycin B was from Roche Diagnostics (Indianapolis, IN, USA). Nutrient broth (Acumedia No. 7146) and bacteriological agar (Acumedia No. 7176) were purchased from Neogen Corporation (Michigan, USA). Difco Middlebrook 7H9 broth, Difco Middlebrook 7H11 agar, BBL Middlebrook oleic acid-albumin-dextrose-catalase (OADC), BBL Middlebrook ADC supplement and Bacto Brain Heart Infusion (BHI) were purchased from BD (Sparks, MD, USA). Fetal bovine serum (FBS) was obtained from Thermo Scientific Hyclone (Logan, UT, USA). 3-(4,5-Dimethylthiazol-yl)-diphenyl tetrazolium bromide (MTT) was acquired from Duchefa Biochemie (Haarlem, Netherlands). 3',3'-dipropylthiadicarbocyanine (diS-C_3-5) dye was purchased from AnaSpec Inc (Fremont, CA, USA). Adenosine triphosphate (ATP) bioluminescence kit was

obtained from Molecular Probes Inc (OR, USA). Dry powders of the phospholipids 1,2-dioleoyl-sn-glycero-3-phospho-(1'-rac-glycerol) (DOPG) and 1,2-dioleoyl-sn-glycero-3-phosphoethanolamine (DOPE) were obtained Avanti Polar Lipids, Inc (Alabaster, AL, USA). The membrane dye FM4-64FX was from Molecular Probes, Inc (Eugene, OR, USA). N-tosyl-L-phenylalanyl chloromethyl ketone (TPCK)-treated trypsin was from AB Sciex (Framingham, MA, USA). The mouse TNF-α enzyme-linked immune sorbent assay (ELISA) Ready-SET-Go kit was from eBioscience (San Diego, CA, USA) and Griess Reagent System from Promega (Madison, WI, USA). The Limulus Amebocyte Lysate (LAL) Chromogenic Endotoxin Quantitation Kit was from Pierce Biotechnology (Rockford, IL, USA).

3.2. Peptide characterisation

3.2.1 Matrix-assisted laser desorption/ionisation time-of-flight mass spectroscopy (MALDI-TOF MS)

MALDI-TOF MS (Model 4800, Applied Biosystems, USA), using α-cyano-4-hydroxycinnamic acid (CHCA) as matrix, was performed in Chapters 4 and 5 to confirm peptide molecular weights and ensure that the peptides were synthesised to desired specifications. An equal volume of peptide solution (0.5 mg mL^{-1} in deionised water) and CHCA solution (saturated in acetonitrile/water mixture at 1:1 volume ratio) was spotted onto the MALDI ground-steel target plate for molecular weight determination.

3.2.2. Surface-enhanced laser desorption/ionisation-TOF MS (SELDI-TOF MS)

SELDI-TOF MS was performed in Chapters 6 and 7 by Dr Melissa Shea Hamilton (Department of Medicine, Imperial College London) to confirm the molecular weights of the synthetic peptides. ProteinChip® NP20 arrays (Bio-Rad Laboratories) were primed with 5 µL of HPLC grade water, and 5 µL of each peptide (0.5 mg mL^{-1}) was applied to the array surface and allowed to air-dry for 1 h at room temperature. The arrays were washed twice with 5 µL of HPLC grade water and allowed to air-dry for a further 15 min at room temperature. 20% CHCA was applied twice (2 × 0.7 µL) to each spot on the arrays, allowing the matrix to air-dry between each application. Time-of-flight spectra were generated using a PCS 4000 SELDI-TOF MS instrument (Bio-Rad Laboratories). Spectra from the peptide pools were obtained at a laser energy of 800 nJ, using a focus mass based on the theoretical molecular weight of each individual peptide and with the matrix attenuated to 500 Da. Ten shots were obtained per position and a total of 500 shots kept per array. Mass accuracy was calibrated externally using All-in-One Peptide (Bio-Rad Laboratories).

3.2.3. Circular dichroism (CD) spectroscopy

The secondary structures of the synthetic peptides were evaluated using CD spectroscopy. The peptides were first dissolved in 25 mM sodium dodecyl sulphate (SDS) surfactant to a final concentration of 0.5 mg mL^{-1}. Peptide solutions were then transferred to a quartz cell with a path length of 1.0 mm and the CD spectra were measured at room temperature with a Jasco J-810 CD

spectrometer (Jasco, Tokyo, Japan) at the National University of Singapore, and the Chirascan™ CD spectrometer (Applied Photophysics, Surrey, UK) at Imperial College London. CD spectra were recorded from a wavelength of 190 to 240 nm, at a scanning speed of 50 nm min^{-1} and averaged from two to three runs per peptide. The acquired spectra were converted to mean residue ellipticity using the following equation:

$$\theta_M = \frac{\theta_{obs}}{10} \cdot \frac{M_{RW}}{c \cdot l}$$

where θ_M is the mean residue ellipticity (deg cm^2 dmol^{-1}), θ_{obs} is the observed ellipticity corrected for the blank at a given wavelength (mdeg), M_{RW} is residue molecular weight (M_W / number of amino acids), c is peptide concentration (mg mL^{-1}), and l is the path length (cm).

3.2.4. Peptide hydrophobicity analysis

The molecular hydrophobicity of the synthetic peptides in Chapter 5 was analysed by RP-HPLC on a Shimadzu Prominence UFLC™ system (Shimadzu Corporation, Kyoto, Japan) equipped with a CBM-20A communications bus module, a SPD-20AV UV/Vis detector, a SIL-20A HT autosampler, LC-20AD pumps, a DGU-20A 5 vacuum degasser and a CTO-20A column oven. Runs were performed using an Agilent Poroshell 120 EC-C18 Threaded column (4.6 × 50 mm, particle size 2.7 μm) monitored at 220 nm, with an injection volume of 50 μL and a flow rate of 1 mL min^{-1}. The mobile phase consisted of solvent A (0.1% TFA in water) and solvent B (0.1% TFA in acetonitrile). The gradient profile applied was a 30 min linear gradient

from 5 to 50% of solvent B followed by 1 min linear gradient of 5% solvent B and 9 min at 5% solvent B for a total time of 40 min.

3.3. Bacterial and cell cultures

3.3.1. Mycobacterial strains and growth conditions

M. smegmatis (ATCC 14468) and *M. tuberculosis* H37Rv (H37Rv) were purchased from ATCC (USA). *M. smegmatis* was cultured in nutrient broth containing 0.05% Tween 80 and colonies were grown on bacteriological agar. *M. bovis* BCG *lux* (BCG), Montreal strain, transformed with the reporter plasmid construct pSMT1 as previously described [110], was a gift from Professor Douglas Young (Imperial College London). mCherry-expressing BCG (BCG-mCherry) was produced by transforming *M. bovis* BCG Danish strain 1331 (Statens Serum Institut) with pCherry3 (Addgene plasmid #24659 encoding mCherry and conferring hygromycin resistance) [111], which was a kind gift from Dr Tanya Parish (University of Washington), using established protocols for mycobacteria [112]. Transformation of BCG-mCherry was performed by Dr. Iria Uhia (Department of Medicine, Imperial College London). *M. tuberculosis* CSU87 (CSU87) is a MDR clinical isolate that was a gift from Dr Diane Ordway (Colorado State University) and is resistant to rifampicin, isoniazid, ethambutol, streptomycin and kanamycin. Three other clinical isolates, provided by Dr Guy Thwaites and the Oxford University Clinical Research Unit (OUCRU), were *M. tuberculosis* 173 (Mtb 173) from the Euro-American lineage and, *M. tuberculosis* 212 (Mtb 212) and *M. tuberculosis* 411 (Mtb 411), both from the East Asian/Beijing lineage. Liquid cultures of all mycobacterial strains were grown in Middlebrook 7H9 broth

supplemented with 0.05% Tween 80, 0.2% glycerol and 10% ADC supplement. Mycobacterial colonies were grown on solid media consisting of Middlebrook 7H11 agar supplemented with 0.5% glycerol and 10% OADC supplement. BCG and BCG-mCherry were grown in 7H9 broth or 7H11 agar in the presence of 50 μg mL^{-1} hygromycin. Bacterial stocks were frozen at -80 ^{o}C in 15% glycerol and a fresh vial was defrosted, inoculated into media and grown at 37 ^{o}C in a shaking incubator until mid-log phase.

3.3.2. Gram-positive and Gram-negative bacterial strains and growth conditions

The *P. aeruginosa* reference strain (PAO1), laboratory strains of *E. coli* (K-12 MG1655) and methicillin-sensitive *S. aureus* (MSSA 8325-4), and the clinical isolate of *Klebsiella pneumoniae* (MIDG1643) were evaluated in this study. Drug-resistant strains included the hospital-acquired MRSA (MRSA 252), and MDR *P. aeruginosa* wound isolates (PA-W1, PA-W14 and PA-W25). We would like to thank Dr John Tregoning (Imperial College London) for providing the MSSA and MRSA strains, Professor Paul Williams (University of Nottingham) for the *P. aeruginosa* wound isolates and Dr Martin Goldberg (University of Birmingham) for the *E. coli* strain. All liquid bacterial strains were grown in BHI broth at 37 ^{o}C in a shaking incubator until mid-log phase, while colonies were grown on BHI agar.

3.3.3. Cell culture

Mouse macrophage cell line RAW 264.7 was maintained in DMEM supplemented with 10% FBS, and cultured in a humidified atmosphere at 37 $^{\circ}$C and 5% CO_2.

3.4. Antimicrobial activity

3.4.1. MIC measurements

The MIC of the peptides and drugs against the six mycobacterial strains, and Gram-positive and Gram-negative bacteria, was determined by the broth microdilution method as described previously [93, 113, 114]. Peptide stock solutions were prepared in sterile water for all experiments before performing a series of two-fold serial dilutions in broth. Solutions were vortexed for 10 to 15 seconds each time to ensure thorough mixing, prior to removing half for dilution. The peptides were serially diluted with the appropriate broth (7H9 for mycobacteria and BHI for all other strains), and 100 μL was added to each well of the 96-well plate. Bacterial cultures were grown up to mid-log phase and diluted to an initial inoculum of 10^6 CFU mL^{-1} before seeding an equal volume into each well. The plates were incubated at 37 $^{\circ}$C and read after 18 h for Gram-positive and Gram-negative bacteria, 72 h for *M. smegmatis*, and 7 days for BCG, H37Rv, CSU87, Mtb 173, Mtb 212 and Mtb 411. The MIC was defined as the concentration at which no microbial growth was observed visually or spectrophotometrically by OD$_{600}$ readings taken by Tecan Infinite 200 Pro (TECAN, Switzerland). Growth media containing only microbial cells was used as the negative control. Each test was carried out in at least three replicates and repeated two to three times.

46

3.4.2. In vitro killing efficiency

The antimicrobial peptides displaying the highest selectivity for bacterial over mammalian cells were tested for their ability to kill mycobacteria, and Gram-positive and Gram-negative bacteria. Peptides were serially diluted with the appropriate broth (7H9 for mycobacteria and BHI for all other strains) to give solutions with final concentrations ranging from 0.5x to 8x MIC. Bacterial cultures were diluted to a cell density of 10^6 CFU mL^{-1} and 100 µL was added to an equal volume of peptide solution. The plates were incubated at 37 $^{\circ}$C for 18 h for Gram-positive and Gram-negative bacteria, 72 h for *M. smegmatis* and 7 days for all other mycobacterial strains, after which they were serially diluted in broth for determination of viable counts. Diluted samples (100 µL) were plated in triplicate onto agar plates and total bacterial counts were determined after incubation at 37 $^{\circ}$C for 24h for Gram-positive and Gram-negative bacteria, 72 h for *M. smegmatis*, 14 days for BCG and 14 days in the presence of 5% CO_2 for all other mycobacterial strains. The results are expressed as mean log (CFU mL^{-1}) ± standard deviation (S.D.).

3.4.3. Time-kill curve

Flasks containing 10 mL of nutrient broth with antimicrobial agents at concentrations corresponding to 1x, 4x and 8x MIC were inoculated with *M. smegmatis* at a density of approximately 10^5 CFU mL^{-1} and incubated in a shaking incubator at 37 $^{\circ}$C. A flask without any drug served as a growth control. Aliquots were removed at time 0, 8, 24, 48 and 72 h post-inoculation and serially diluted in nutrient broth for the determination of viable counts. Diluted samples (100 µL) were plated in triplicate onto agar plates and total

bacterial counts determined after incubation at 37 $^{\circ}$C for 72 h. The results are expressed as mean log (CFU mL^{-1}) ± S.D.

3.4.4. Chequerboard assay

Antimicrobial interactions between peptides and rifampicin in Chapters 4 and 5 were evaluated *via* the chequerboard assay as described elsewhere [115]. Briefly, two-fold serial dilutions of rifampicin and each peptide were prepared and added in a 1:1 volume ratio to the wells of a 96-well plate. An equal volume of bacterial solution (100 μL) at approximately 10^5 CFU mL^{-1} was then seeded into each well. The plates were incubated in a shaking incubator at 37 $^{\circ}$C and 200 rpm and read after 72 h for *M. smegmatis*, and 7 days for BCG and H37Rv. Bacterial growth was assessed visually or spectrophotometrically *via* OD$_{600}$ readings taken by Tecan Infinite 200 Pro (TECAN, Switzerland). Each assay was performed in triplicate and repeated two to three times. The fractional inhibitory concentration index (FICI) for each drug combination was calculated using the following equation:

$$FICI = \frac{MIC\ of\ peptide\ in\ combination}{MIC\ of\ peptide\ alone} + \frac{MIC\ of\ rifampicin\ in\ combination}{MIC\ of\ rifampicin\ alone}$$

An FICI of ≤ 0.5 was interpreted as synergy, 0.5 < FICI ≤ 1.0 as additive, 1.0 < FICI ≤ 4.0 as indifferent, and an FICI > 4.0 as antagonism [116, 117].

3.4.5. Drug resistance stimulation study

In Chapter 4, drug resistance was induced in *M. smegmatis* by repeated treatment with sub-inhibitory concentrations of antimicrobial agents. The MICs of the peptide M(LLKK)$_2$M and rifampicin were tested for up to 10 passages against *M. smegmatis* using the same broth microdilution method.

For each antimicrobial agent, bacterial cells exposed to sub-MIC (⅛ of MIC at that particular passage) were re-grown to the log phase and reused for the following passage's MIC measurement. To explore if the combination of rifampicin and peptides could suppress resistance development in *M. smegmatis*, a fixed concentration of M(LLKK)$_2$M (equivalent to ¼ of MIC) was added to two-fold increasing concentrations of rifampicin. Bacterial cells from the highest drug combination showing growth were re-grown to the log phase before measuring the MIC of rifampicin and treating them with the drug combination again. Changes in the MIC were depicted by normalising the MIC at passage *n* to that of the first passage.

3.4.6. Intracellular anti-mycobacterial activity

The intracellular activity of the antimicrobial peptide II-D in Chapter 6 was assessed against *M. tuberculosis* clinical isolates Mtb 411 and CSU87 as described previously [118]. Briefly, RAW 264.7 cells were plated at a final concentration of 4×10^4 per well in 96-well plates and incubated for 24 h to allow adherence. Prior to infection, mid-log phase bacterial cultures were washed twice with PBS, resuspended in DMEM, and added at a final concentration of 4×10^5 CFU per well to achieve a multiplicity of infection (MOI) of 10:1. Plates were incubated at 37 $^{\circ}$C and 5% CO_2 for 4 h to allow uptake of bacteria by macrophages. Subsequently, cells were washed thrice with prewarmed DMEM to remove extracellular bacteria before adding 200 µL of DMEM, with or without drugs, to each well. II-D was tested at concentrations corresponding to 0.5x, 1x, 2x and 4x MIC, while rifampicin and moxifloxacin were evaluated at 1x, 2x, 4x and 8x MIC. Each

concentration was tested in triplicate. For determination of bacterial viability at various time points, macrophages were lysed with 200 μL of sterile water for 30 min, serially diluted with PBS and 10 μL was plated out in duplicate on 7H11 agar. Following incubation at 37 °C for 14 days, bacterial colonies were enumerated and data are expressed as mean log (CFU mL^{-1}) ± S.D.

3.5. Toxicity and stability

3.5.1. Haemolytic activity test

The safety of the peptides against mammalian cells was assessed by evaluating their haemolytic activity using freshly drawn RBCs as reported previously [93, 113, 114]. Rat RBCs used in this study were obtained from the Animal Handling Units of the Biomedical Research Centre (AHU, BRC, Singapore) while whole blood was obtained from healthy adult donors at Imperial College London. Prior to commencement, ethics approval was granted by Imperial College London NHS Healthcare Tissue Biobank (sub-collection reference number: Pae-SN-15-001) and written informed consent was obtained from all participants. Briefly, the RBCs were diluted 25 times with PBS to obtain a 4% (v/v) suspension for subsequent testing. Two-fold serial dilutions of the peptides were prepared in PBS to give solutions with final concentrations ranging from 0 up to 1000 mg L^{-1} or 2000 μM. Three hundred μL of the blood suspension was then mixed with an equal volume of the peptide solution and incubated at 37 °C for 2 h. Following incubation, the mixtures were centrifuged at 1700 g for 5 min and 100 μL of the supernatant was transferred to each well of the 96-well plate. Haemoglobin release was quantified spectrophotometrically by absorbance measurements at 576 nm by Tecan

Infinite 200 Pro (TECAN, Switzerland). Data are expressed as mean ± S.D. for two independent experiments performed in at least four replicates. RBCs treated with 1% Triton X-100 served as the positive control while untreated RBCs served as the negative control. The extent of haemolysis was calculated using the following equation:

$$Haemolysis\ (\%) = \frac{(OD_{576nm}\ of\ treated\ sample - OD_{576nm}\ of\ negative\ control)}{(OD_{576nm}\ of\ positive\ control - OD_{576nm}\ of\ negative\ control)} \times 100\%$$

3.5.2. Cytotoxicity testing

Peptides were evaluated for their cytotoxicity against the mouse macrophage RAW 264.7 cell line using the MTT assay. The cells were seeded into 96-well plates at a density of 1×10^4 cells per well and incubated overnight at 37 $^{\circ}$C and 5% CO_2. Peptides, serially diluted in DMEM to give final concentrations ranging from 1.95 to 250 mg L^{-1}, were added and the plates further incubated for 24 h. Cells without peptides served as controls. Following treatment, the media was replaced with 200 µL fresh growth media and 40 µL MTT solution (5 mg mL^{-1}) and incubated for an additional 4 h at 37 $^{\circ}$C. Next, 150 µL of DMSO was added to each well to dissolve the resultant formazan crystals and absorbance at 595 nm was measured using Tecan Infinite 200 Pro (TECAN, Switzerland) or a VersaMax Tunable microplate reader (Molecular Devices, Sunnyvale, CA, USA). Cell viability was expressed as $\frac{(A_{595nm}\ of\ treated\ sample)}{A_{595nm}\ of\ control} \times 100\%$. Experiments were performed in triplicate per concentration.

3.5.3. Protease stability assay

The proteolytic stability of the synthetic peptides in Chapter 6 was assessed by measuring their antimicrobial activity against BCG after pretreatment with the serum protease, trypsin, in accordance with methods described previously [119]. Briefly, peptide solutions at a fixed concentration of 4x MIC were incubated with trypsin at an enzyme to peptide ratio of 1:100. Following incubation at 37 °C for 6 h, the solutions were heat-treated at 80 °C for 10 min to inactivate the enzyme. One hundred µL of the treated peptide solution was then added to an equal volume of bacterial culture (10^6 CFU mL^{-1}) and incubated at 37 °C in a shaking incubator for 7 days. Inhibition of bacterial growth was determined by spectrophotometric measurements at OD$_{595}$. Data are expressed as mean ± S.D. for two independent experiments performed in triplicate.

3.6. Anti-biofilm activity

3.6.1. Inhibition of biofilm formation

The ability of L12 to prevent biofilm formation was studied in Chapter 7 in 96-well plates using the CV staining assay as described previously [120]. Briefly, bacterial cultures were grown to mid-log phase before diluting to give an inoculum of 10^6 CFU mL^{-1}. Fifty µL of the bacterial suspension was seeded into each well together with an equal volume of peptide solution. The anti-biofilm activity of the L12 was assessed at concentrations corresponding to 0.06x 0.125x, 0.25x, 0.5x, 1x and 2x MIC. Following overnight incubation at 37 °C to facilitate biofilm formation, the culture media was aspirated and wells washed with deionised water to remove planktonic cells. Adherent biofilms

were stained with 0.1% (w/v) CV solution (125 μL) for 10 min at room temperature and subsequently washed with deionised water to remove the excess dye. Two hundred μL of 70% ethanol was transferred to each well to solubilise the dye and the biomass of biofilms was quantified by absorbance measurements at 595 nm taken with the VersaMax Tunable microplate reader (Molecular Devices, Sunnyvale, CA, USA). Data are expressed as mean ± S.E.M. for three independent experiments performed in triplicate.

3.6.2. Disruption of pre-formed biofilms

The viability of pre-formed biofilms following peptide treatment was assessed in Chapter 7 according to previously established protocols [121]. Mid-log phase cultures of PA-W25 and MRSA 252 were diluted to 10^6 CFU mL^{-1} and 100 μL was added to each well. After incubation for 18 h at 37 ^{o}C to allow biofilm formation, wells were washed with deionised water and 100 μL of peptide solution was added at concentrations equivalent to 2x, 4x, 8x and 16x MIC. After 2 h exposure to L12, wells were washed with deionised water before determination of biofilm viability using the MTT assay as described in Section 3.5.2. Data are expressed as mean ± S.E.M. for three independent experiments performed in triplicate.

3.6.3. Bioluminescence imaging of biofilms

To complement the microbiological biofilm assays, bioluminescence imaging studies were performed in Chapter 7 to visualise the extent of peptide-mediated biofilm eradication and growth suppression. Bioluminescent *P. aeruginosa* (ATCC 9027), transformed using a recombinant plasmid

containing the *luxCDABE* gene cassette of *Photorhabdus luminescens* excised from pAKlux1.1, which was a kind gift from Attilia Karsi (Mississippi State University), and cloned into the PUCP19 vector backbone by electroporation, was employed in the screening of anti-biofilm activity of the synthetic peptides [122]. Transformed *P. aeruginosa* was maintained in LB broth containing carbenicillin (300 μg mL^{-1}). Preparation of bacterial inoculums and treatment of biofilms were conducted according to protocols reported in the previous sections. Inhibition of biofilm growth was assessed after 18 h treatment with L12 up to 4x MIC while pre-formed biofilms were evaluated following 2 h exposure to L12 up to 64x MIC. The IVIS imaging system was utilised for imaging of bioluminescent biofilms and acquired with Living Image software. Bioluminescence signals are expressed as photons per second per centimetre squared per steradian (p/s/cm^2/sr) and presented as an intensity map. Biofilm imaging was performed by Ms. Sybil Obuobi (Department of Pharmacy, National University of Singapore).

3.7. Antimicrobial mechanisms

3.7.1. Membrane permeability studies

3.7.1.1. Flow cytometry

Mycobacterial membrane integrity of *M. smegmatis*, H37Rv and CSU87 following peptide treatment was evaluated in Chapters 5 and 6 using flow cytometry. Briefly, mid-log phase bacterial cultures were washed twice with PBS and re-suspended to give ~10^8 CFU mL^{-1} in the same buffer. *M. smegmatis* was treated with peptides at different concentrations (62.5, 125 and 250 mg L^{-1}) for 2 h, while cells treated with rifampicin and ethambutol (1x, 2x

and 4x MIC) served as negative controls. H37Rv and CSU87 were treated with peptides at 4x MIC for 3 h, while cells treated with rifampicin and moxifloxacin at 4x MIC served as negative controls for H37Rv and CSU87, respectively. Next, treated cells were incubated with 20 μg mL^{-1} PI for 30 min, followed by washing and re-suspension in PBS to remove any unbound dye. Cells were then fixed overnight with 4% formaldehyde solution. The fixed samples were washed twice with PBS before performing flow cytometric analysis using LSR II and FACSDiva software (Becton Dickinson, San Jose, CA) at the St Mary's FACS Facility, Imperial College London or using CyAn™ ADP Analyser (Becton Dickinson, San Jose, CA) at the Flow Cytometry Laboratory, National University Health System, Singapore.

3.7.1.2. Cytoplasmic membrane depolarisation assay

The ability of the peptides to disrupt the mycobacterial membrane potential was assessed in Chapter 5 using the membrane potential sensitive dye diS-C$_3$-5. An overnight *M. smegmatis* culture was first washed with 5 mM HEPES buffer containing 20 mM glucose and 0.1 M KCl (pH 7.2) and re-suspended to an OD$_{600}$ of 0.4 in the same buffer. The cells were then incubated with 10 μM of diS-C$_3$-5 for 1 h at 37 °C after which 600 μL was transferred to a stirred quartz cuvette. Change in fluorescence intensity following the addition of peptides at 1x, 4x and 8x MIC was monitored using a Quanta Master spectrofluorometer (Photon Technology International, NJ, USA) with an excitation and emission wavelength of 622 and 670 nm respectively.

3.7.1.3. ATP bioluminescence assay

Extracellular ATP levels following treatment of *M. smegmatis* with peptides were measured in Chapter 5 as described previously [123]. Briefly, an overnight *M. smegmatis* culture was first washed and re-suspended in 10 mM phosphate buffer to an OD_{600} of 0.4. Peptides serially diluted with the same buffer to give final concentrations from 15.6 to 500 mg L^{-1} were added to an equal volume of bacterial suspension (300 μL) and incubated at 37 $^{\circ}$C for 2 h. Next, samples were centrifuged at 5000 g for 5 min and 50 μL of the supernatant was added to 450 μL of boiling TE buffer (50 mM Tris, 2 mM EDTA, pH 7.8). The mixture was boiled for an additional 2 min and stored on ice until assayed. One hundred μL of cooled mixture was added to 100 μL of luciferin-luciferase assay mixture and luminescence was recorded using Tecan Infinite 200 Pro (TECAN, Switzerland). Extracellular ATP concentrations were determined from ATP standard curves using ATP assay kit according to the manufacturer's instructions. Data are expressed as mean ± S.E.M. for three independent experiments performed in duplicate.

3.7.1.4. Calcein leakage assay

The calcein leakage assay was performed in Chapter 5 by Dr. Ke Xi Yu (IBN, Singapore). Large unilamellar vesicles (LUVs) loaded with calcein dye were prepared according to methods described previously [124]. Calcein dye was dissolved to a final concentration of 40 mM in 10 mM Na_2HPO_4 in H_2O (pH 7.0). 476 μL PE and 127 μL PG dissolved in 25 mg mL^{-1} $CHCl_3$ were mixed in a round bottom flask. Solvent removal by rotatory evaporator left behind a thin lipid film which was then hydrated using 1 mL calcein solution. The

mixture was stirred for an additional hour on the rotary evaporator at atmospheric pressure before being subjected to ten freeze-thaw cycles (dry ice/acetone to freeze and warm water to thaw). Extrusion of the suspension was then carried out twenty times through a polycarbonate membrane with 400 nm pore diameter. Removal of excess dye was performed using a Sephadex G-50 column, with a buffer consisting of 10 mM Na_2HPO_4 and 90 mM NaCl as the eluent. Dye-filled LUVs were then diluted 2000 times using the same buffer to achieve a final lipid concentration of approximately 5.0 mM. The calcein fluorescence emission intensity I_t (λ_{em} = 515nm, λ_{ex} = 490nm) was measured following treatment of LUVs with peptides at various concentrations (125, 250 and 500 mg L^{-1}) for 1 h and 2 h. Fluorescence emission following addition of 50 μL Triton X-100 (20% in DMSO) (I_x) was taken as 100% leakage while the baseline (I_0) was measured without peptide addition. Treatment with pure DMSO did not produce any leakage. Data are expressed as mean ± S.D. for two independent experiments performed in triplicate. The percentage of calcein leakage was calculated as follows:

$$Leakage\ (\%) = (I_t - I_0)/(I_x - I_0) \times 100\%$$

3.7.2. Microscopy studies

3.7.2.1. Membrane integrity study using confocal laser scanning microscopy (CLSM)

The loss of membrane integrity after exposure of *M. smegmatis* to peptides in Chapter 4 was studied using CLSM. *M. smegmatis* was incubated overnight in a Lab-Tek 8-well-chambered coverglass (Nalge Nunc International, Rochester, NY, U.S.A.) at 37 °C at 200 rpm to allow for adherence of bacterial cells to the chamber surface. After the removal of the bacterial solution from

the chamber, the adhered bacterial cells were treated with $M(LLKK)_2M$ at its MIC for 10, 30 and 60 min, in the presence of FITC-labelled dextran probe. Following treatment, the peptide solution was removed and the bacterial cells washed thoroughly with PBS thrice to ensure that no free probe remained. Imaging was carried out using the Zeiss LSM 510 inverted confocal microscope (Carl Zeiss, Inc.) Bacterial cells treated with PBS in the presence of FITC-labelled probe served as a control for this study.

3.7.2.2. Peptide localisation study using CLSM

The site of action of II-D in BCG was studied in Chapter 6 using CLSM. BCG and BCG-mCherry cultures were grown to mid-log phase, centrifuged at 2000 g for 10 min, washed, and resuspended in PBS at a cell density of 10^8 CFU mL^{-1}. Following treatment with 500 mg L^{-1} FITC-labelled II-D for 2 h, bacterial cells were centrifuged at 2000 g for 10 min and washed three times with PBS. To stain bacterial membranes, BCG cells were resuspended in PBS with 2 µg mL^{-1} FM4-64 for 10 min at 37 ^{o}C with shaking. Cells were then pelleted, washed twice with PBS to remove any unbound dye, and fixed overnight with 4% formaldehyde solution at 4 ^{o}C. Following fixation, cells were pelleted, resuspended in PBS and allowed to air dry on microscope slides for 20 min. Samples were mounted with Mowiol mounting medium and imaged with a 100x oil-immersion objective lens using a Zeiss LSM 510 inverted confocal microscope (Carl Zeiss, Inc.). FITC was excited with a 488 nm laser and detected with a 505-530 nm band-pass filter while mCherry and FM4-64 were both excited with a 543 nm laser and detected with a 615 nm and 650 nm long-pass filters, respectively.

3.7.2.3. Field emission scanning electron microscopy (FE-SEM)

Mycobacterial membrane damage following peptide treatment in Chapter 4 was visualised using FE-SEM. *M. smegmatis* suspension at ~10^8 CFU mL^{-1} was treated with an equal volume of peptide at lethal doses of 250 mg L^{-1} (4x MIC) or PBS for 2 h. Five replicates were pooled together, centrifuged at 2700 g for 10 min and washed twice with PBS. The samples were then fixed with 4% formaldehyde for 30 min before rinsing with deionised water. A series of ethanol solutions (35%, 50%, 75%, 90%, 95%, and 100%) was used to perform sample dehydration, after which they were mounted on copper tapes and allowed to air-dry for 2 days. Samples were finally sputter coated with platinum before imaging under a FE-SEM (JEOL JSM-7400F, Japan) at IBN, Singapore.

3.7.2.4. Microfluidic live-cell imaging with time-lapse fluorescence microscopy

Live-cell imaging was performed in Chapters 6 and 7 using the automated CellASIC ONIX Microfluidic Platform with the CellASIC ONIX B04A-03 Microfluidic Bacteria Plates (EMD Millipore Corporation, Hayward, CA, USA). Mid-log phase bacterial cultures were first diluted in the appropriate broths (7H9 for BCG and BHI for *E. coli* and *S. aureus*) to a final density of 10^7 CFU mL^{-1}, before adding 100 μL to each of the cell loading wells. To evaluate the antimicrobial mechanisms of action, the most selective peptides II-D and L12, were serially diluted in broth to give final concentrations corresponding to 4x and 8x MIC. Peptide solutions were then added to the inlet wells together with the membrane-impermeable dye, PI (10 μg mL^{-1}), in

a total volume of 350 μL. Next, the microfluidic plate was vacuum-sealed to the F84 manifold and the CellASIC ONIX FG Software initiated. Loading and subsequent washing of un-trapped bacterial cells was carried out according to the manufacturer's protocol [125]. Peptide solutions were perfused into culture chambers at the recommended pressure of 2 psi for up to 4 h. The temperature was maintained at 37 °C and bacterial cells treated with medium and PI alone served as negative controls. Phase contrast and fluorescent images of bacterial cells were captured with a 63x oil-immersion objective lens every 10 min using the Zeiss Axiovert 200M inverted microscope (Carl Zeiss, Inc.). Microscopy was performed in the Facility for Imaging by Light Microscopy (FILM) at Imperial College London.

3.7.2.5. Image and statistical analysis

The Huygens Deconvolution software (Scientific Volume Image) was used to perform deconvolution of confocal images. Fluorescence intensity profiles along the bacterial cell length were obtained with the segmented line and multi-channel intensity line profile plot tools in the ImageJ software. Processing and compiling of phase and fluorescent images into movies at two frames per second, were carried out using the ImageJ software. All statistical analysis in this study was performed with GraphPad Prism 6 software (GraphPad Software Inc., CA, USA) using either one-way analysis of variance (ANOVA), with Bonferroni's post hoc test for multiple comparisons or a non-parametric Kruskal Wallis multiple comparisons test with Dunn's post-test. Significant differences between groups were indicated as follows: * $p \leq 0.05$, ** $p \leq 0.01$, *** $p \leq 0.001$, **** $p \leq 0.0001$.

3.8. Immune-modulating activity

3.8.1. NO production by peptide-treated macrophages

The ability of II-D to active macrophages in Chapter 6 was determined by measuring NO production following peptide treatment. RAW 264.7 cells were seeded in 96-well plates at a density of 4 x 10^4 per well, followed by incubation at 37 ^{o}C and 5% CO_2 for 24 h. The medium was removed and cells were treated with peptide solutions ranging from 7.81 to 250 mg L^{-1} for an additional 24 h. NO production was estimated by measuring nitrite concentrations in supernatants using the Griess reagent (0.1% N-1-napthylethylenediamine dihydrochloride, 1% sulfanilamide and 5% phosphoric acid) according to the manufacturer's protocols. The absorbance was measured at 540 nm and nitrite concentrations were determined using standard curves generated with $NaNO_2$ solutions. Macrophages stimulated with 100 ng mL^{-1} LPS served as positive controls while unstimulated macrophages served as negative controls. Data are expressed as mean ± S.D. for two independent experiments performed in triplicate.

3.8.2. TNF-α production by peptide-treated macrophages

The ability of II-D to active macrophages in Chapter 6 was also determined by measuring TNF-α production following peptide treatment. RAW 264.7 cells were seeded in 96-well plates at a density of 4 x 10^4 per well, followed by incubation at 37 ^{o}C and 5% CO_2 for 24 h. The medium was removed and cells were treated with peptides solutions ranging from 7.81 to 250 mg L^{-1} for an additional 24 h. TNF-α concentration in supernatants was determined using the mouse TNF-α ELISA kit as per the manufacturer's instructions.

Absorbance readings were measured at 450 nm. Unstimulated macrophages served as negative controls, and positive controls were stimulated with 100 ng mL^{-1} LPS. Data are expressed as mean ± S.D. for two independent experiments performed in triplicate. The degree of TNF-α production was calculated as follows:

$$TNF - \alpha \; production \; (\%) \frac{(OD_{450nm} \; of \; treated \; sample - OD_{450nm} \; of \; negative \; control)}{(OD_{450nm} \; of \; positive \; control - OD_{450nm} \; of \; negative \; control)} \times 100\%$$

3.8.3. NO production by LPS-stimulated macrophages

The *de novo* designed peptides were evaluated for their anti-endotoxic activity in Chapter 7 by determining the reduction in NO production in macrophages stimulated with LPS. RAW 264.7 cells were seeded at a density of 4 x 10^4 cells per well in 96-well plates and incubated for 24 hours at 37 $^{\circ}$C and 5% CO_2. Following medium removal, cells were stimulated with LPS (100 ng mL^{-1}), either in the presence or absence of peptides for an additional 24 hours. NO formation was determined by measuring nitrite concentrations in supernatants using the Griess reagent (0.1% N-1-napthylethylenediamine dihydrochloride, 1% sulfanilamide and 5% phosphoric acid) according to the manufacturer's protocols. Absorbance readings were taken at 540 nm by the VersaMax Tunable microplate reader (Molecular Devices, Sunnyvale, CA, USA) and standard curves generated with $NaNO_2$ solutions were used to quantify nitrite levels. Untreated cells and those stimulated with LPS alone served as negative and positive controls, respectively. Data are expressed as mean ± S.E.M. for three independent experiments performed in triplicate.

3.8.4. Neutralisation of endotoxins

The *de novo* designed peptides were evaluated for their LPS-binding activity in Chapter 7 using the LAL chromogenic assay in accordance with the manufacturer's protocols. Peptides were serially diluted in endotoxin-free water and added to an equal volume of LPS (0.5 EU mL^{-1}) in 96-well plates in a final volume of 50 μL. The plates were incubated for 30 min at 37 $^{\circ}$C to facilitate interactions between the peptides and LPS, following which, 50 μL of LAL was added to each well. After additional 10 min incubation at 37 $^{\circ}$C, 100 μL of the chromogenic substrate solution (Ac-Ile-Glu-Ala-Arg-p-nitroalanine) was added to each well. Next, the plates were incubated for a further 6 min at 37 $^{\circ}$C before adding 50 μL of 25% acetic acid to terminate the reaction. The extent of LPS binding was quantified relative to untreated controls by absorbance measurements at 405 nm taken with the VersaMax Tunable microplate reader (Molecular Devices, Sunnyvale, CA, USA). Data are expressed as mean ± S.D. for three independent experiments.

CHAPTER 4: Anti-mycobacterial activities of synthetic cationic α-helical peptides and their synergism with rifampicin

4.1. Introduction

Inspired by nature, many AMPs are currently under clinical development for treating various bacterial infections [56]. There is a huge diversity in sequences, although their common cationic and amphiphilic nature is apparent [22]. With their overall positive charges, AMPs contact bacterial cell surfaces by associating with acidic polymers and other negatively charged molecules, after which they insert themselves into the membrane and disrupt its physical integrity *via* membrane thinning, transient pore formation and/or disruption of the barrier function [126-128]. Some studies have also shown that they kill bacteria by translocating across the membrane and acting on internal targets [21]. This membrane-targeted mechanism of action is responsible for their activity against a wide range of pathogens. While natural AMPs have demonstrated potent activity against Gram-positive and Gram-negative bacteria, their efficacy tends to be diminished against *M. tuberculosis*. In the context of tuberculosis, even though the composition of the mycobacterial cell wall is inherently different with a higher proportion of lipids such as mycolic acids, natural AMPs, including the human cathelicidin LL-37, hBDs and HNPs, have been documented to kill *M. tuberculosis* albeit at rather high concentrations. LL-37 has been found to be inactive *in vitro* against H37Rv and MDR *M. tuberculosis* at concentrations of 50 mg L^{-1} [30]. hBD-2 and hBD-3 demonstrated superior *in vitro* activities in comparison to LL-37, with MICs against H37Rv of 12 and 24 mg L^{-1}, respectively [129]. hBD-1, however, exhibited poor *in vitro* killing of H37Rv and MDR *M. tuberculosis*

even up to concentrations of 128 mg L^{-1} [130]. Amongst the HDPs, HNP-1 emerged as the most potent inhibitor of H37Rv *in vitro* with a relatively low MIC of 2.5 mg L^{-1} [35].

It is, however, widely recognised that natural AMPs do not make good drug candidates mainly due to their large sizes that translate to higher production cost and significant toxicity [22, 26]. As such, synthetic variants have been developed *via* several design approaches (described in Section 1.5) in attempts to enhance the biological activities of natural HDPs against mycobacteria, while minimising undesirable toxic side effects. Sonawane *et al*. prepared a truncated LL-37 congener with threefold greater potency than the native peptide [31], while a 15-amino acid analogue of LL-37 possessed a fourfold lower MIC against *M. smegmatis* and a 5.6-fold reduction in cytotoxicity [131]. The recombinant hBD-2 and hBD-3 hybrid also displayed the best activity against MDR *M. tuberculosis* in comparison to either of the peptides alone [129]. Unsurprisingly, the empirical nature of majority of these strategies implies that failure, to some extent, is unavoidable. For example, congeners based on truncations of granulysin proved unsuccessful in producing synthetic analogues with superior killing efficacy against *M. tuberculosis*, with the full-length granulysin exhibiting the most potent antimicrobial effect [132]. Additionally, it has been argued that widespread clinical use of AMPs bearing close resemblance to host innate immunity peptides will inevitably select for drug-resistant bacteria, thereby posing an immense threat to human health [104].

To mitigate concerns of antimicrobial resistance development to host peptides, and to overcome their inherent drawbacks, the rational approach *via de novo* design is thus being adopted to produce counterparts endowed with superior properties. To the best of our knowledge, there are no studies assessing rationally designed *de novo* synthetic AMPs for their antimicrobial activity against *M. tuberculosis*. As discussed in Section 1.5.6, the recurring sequence comprising four amino acids $(XXYY)_n$ – where X is a hydrophobic amino acid, Y is a cationic amino acid, and n is the number of repeat units – was successfully implemented in the design of α-helical AMPs [93]. $C(LLKK)_2C$ was shown to be the most selective peptide against Gram-positive and Gram-negative bacteria, and yeast [95]. The inclusion of arginine instead of lysine as the cationic residue was found to produce peptides with greater haemolytic activities, while incorporating alanine or phenylalanine instead of leucine as the hydrophobic amino acid resulted in peptides with reduced helical propensity [95]. Thus, based on this information, $(LLKK)_2$ was used as a starting point in this study, to elucidate the influence of various structural modifications on anti-mycobacterial activity of the synthetic α-helical AMPs.

The synthetic α-helical AMPs comprising the backbone sequence $(XXYY)_n$ were systematically evaluated against several mycobacterial strains including clinically isolated MDR *M. tuberculosis*. Additionally, the approach of combination therapy of conventional antibiotics and AMPs was evaluated with the objective of preventing or delaying the development of antibiotic resistance in TB. Such combination has not been reported in the literature and if successful, synergism is expected to reduce treatment costs and minimise

peptide toxicity for the application of AMPs in TB treatment. Initially, characterisation of peptide secondary structures was performed, followed by the evaluation of their anti-mycobacterial properties by MIC measurements against *M. smegmatis,* BCG*,* H37Rv and the MDR strain, CSU87. The antimicrobial mechanism of the peptides was evaluated using CLSM, while haemolytic toxicity against mammalian cells was assessed using rat RBCs. Drug resistance was stimulated *in vitro* by repeatedly exposing *M. smegmatis* to sub-inhibitory concentrations of rifampicin and the peptides. Lastly, synergistic interactions were determined by co-treatment of the mycobacterial strains with rifampicin and AMPs *via* the chequerboard assay.

4.2. Results and Discussion

4.2.1. Peptide design and characterisation

Peptides were designed on the basis of evaluating if two different structural modifications of the primary peptide, (LLKK)$_2$, could potentially modulate its anti-mycobacterial activity. The first was to evaluate if the presence of free sulfhydryl (thiol) groups in L-Cys residues could enhance the anti-mycobacterial activity of these synthetic α-helical peptides. The second was to assess if positional hydrophobicity was an important determinant of anti-mycobacterial activity of these synthetic α-helical peptides. To do so, L-Cys was substituted to either or both the N- and C-terminals of the peptides to obtain the following peptides: C(LLKK)$_2$, (LLKK)$_2$C and C(LLKK)$_2$C. To verify the influence of free sulfhydryl groups on antimicrobial activity, control peptides were included by substituting methionine (Met) on either or both terminals to obtain the following peptides: M(LLKK)$_2$, (LLKK)$_2$M and M(LLKK)$_2$M. It should be noted that the peptides (LLKK)$_2$C, C(LLKK)$_2$C and M(LLKK)$_2$M have been previously evaluated against yeast and Gram-positive and Gram negative bacteria, although the influence of positional hydrophobicity on antimicrobial activity was not studied [95]. The primary peptide without any additional amino acid residues, (LLKK)$_2$, also served as a control. C-terminal amidation of peptides was performed to augment anti-mycobacterial activity *via* enhancement of net positive charge [133, 134]. MALDI-TOF MS analysis showed that there was close agreement between the measured and theoretical molecular weights of the peptides (Table 4.1), confirming that peptide synthesis had been performed to the desired specifications.

Table 4.1. α-helical peptide sequences and their molecular weights. The close agreement between the theoretical and measured molecular weights (M_w) confirmed the fidelity of peptide synthesis.

AMP	Peptide sequence	Theoretical M_w	Measured M_w[a]
(LLKK)₂	LLKKLLKK-NH₂	982.37	983.02
C(LLKK)₂	CLLKKLLKK-NH₂	1085.51	1086.01
(LLKK)₂C	LLKKLLKKC-NH₂	1085.51	1085.76
C(LLKK)₂C	CLLKKLLKKC-NH₂	1188.66	1188.76
M(LLKK)₂	MLLKKLLKK-NH₂	1113.57	1113.79
(LLKK)₂M	LLKKLLKKM-NH₂	1113.57	1114.08
M(LLKK)₂M	MLLKKLLKKM-NH₂	1244.76	1247.07

[a] Measured by MALDI-TOF MS, apparent Mw = $[Mw + H]^+$.

4.2.2. CD spectroscopic study

The peptides adopted a random conformation in aqueous solution (data not shown) but folded into α-helical structures once a membrane-like environment was provided with the addition of SDS surfactant. Figure 4.1 summarises the CD spectra of the peptides with Met and Cys terminal residues. The addition of Cys and Met residues resulted in greater α-helical folding as characterised by the presence of double minima at 208 nm and 222 nm. These additional amino acids increased the peptide length and hydrophobicity, which in turn enhanced hydrogen bonding between the ith and $(i+4)$[th] amino acid in the peptide backbone [135]. As a result, there was stabilisation of the α-helix and increased peptide helicity. Thus, peptides with amino acid substitutions on both faces had the greatest helicity as determined by a more negative mean residue ellipticity value (θ_M). By comparing the θ_M values of the peptides at these wavelengths, it can be ascertained that the peptides C(LLKK)₂ and (LLKK)₂M had a higher propensity for α-helical folding as compared to peptides (LLKK)₂C and M(LLKK)₂, respectively. A plausible explanation is

that the substitution of a hydrophobic Met residue onto the non-polar peptide face increased peptide amphiphilicity, which in turn stabilised the α-helical conformation of $(LLKK)_2M$. Cys, on the other hand, is a polar uncharged residue and exerted similar influence only when it was substituted onto the polar peptide face in $C(LLKK)_2$ and not the non-polar face as in $(LLKK)_2C$. These results are in agreement with previous findings that showed that hydrophobicity of the non-polar region is important for conserving the α-helical configuration of peptides and that addition of polar residues onto the non-polar peptide region could potentially destabilise its helical structure [136].
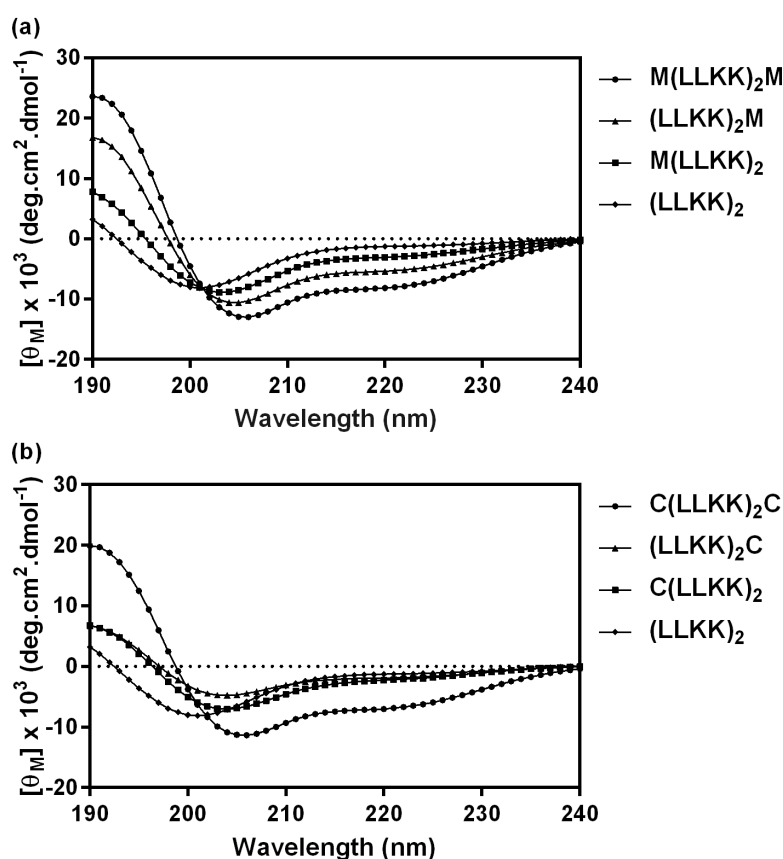
Figure 4.1. CD spectra of α-helical peptides with (a) Met and (b) Cys residues. The presence of the double minima at 208 nm and 222 nm confirmed the α-helical secondary structures of the synthetic peptides. Data are expressed as the mean of two runs per peptide.

4.2.3. In vitro anti-mycobacterial activity

The antimicrobial activities of the peptides were determined by the standard broth microdilution method with the corresponding MICs against *M. smegmatis* summarised in Table 4.2. The peptides efficiently inhibited bacterial growth at varying MICs, with the primary $(LLKK)_2$ peptide having a MIC of 125 mg L^{-1}. Generally, the addition of one or more amino acids either increased or preserved the inhibitory activity of the peptides, except for $C(LLKK)_2C$ which displayed a decline in inhibitory activity as reflected by a MIC of 250 mg L^{-1}. The addition of L-Cys to the N-terminus served to enhance the potency of the primary peptide with $C(LLKK)_2$ having the lowest MIC of 62.5 mg L^{-1}, while its incorporation at the C-terminus did not render the parent peptide any more active against *M. smegmatis*. However for $C(LLKK)_2C$, a reduction in efficacy may partly be due to its sparingly soluble nature at high concentrations as seen from its high solution turbidity. As for the peptides with Met substitutions, $(LLKK)_2M$ and $M(LLKK)_2M$ recorded the lowest MIC of 62.5 mg L^{-1}, while there was no improvement in activity for $M(LLKK)_2$ as compared to the primary peptide. It is likely that the increase in hydrophobicity/α-helicity enhanced the membrane permeabilisation and antimicrobial potency of these peptides. These findings are consistent with those reported previously by Chen *et al*. who found that increasing the hydrophobicity of α-helical peptides consequently improved their antimicrobial activity against both Gram-positive and Gram-negative bacteria [136, 137]. The lack of improvement in activity of $M(LLKK)_2$ and $(LLKK)_2C$ could be in part due to the influence of positional hydrophobicity, whereby the substitution of a hydrophobic Met residue onto the polar peptide face, and a

polar Cys residue onto the non-polar peptide face, decreased facial amphiphilicity, in turn reducing antimicrobial activity [138]. Notably, the antimicrobial potency of the three most effective peptides (MIC of 62.5 mg L^{-1}) was preserved in rifampicin-resistant *M. smegmatis* (Table 4.2). This confirmed that the synthetic peptides functioned *via* a different mechanism of action as compared to rifampicin, which hinders transcription by inhibiting DNA-dependent RNA polymerase.

Table 4.2. MICs of synthetic α-helical peptides against *M. smegmatis* and their 50% haemolysis concentration (HC$_{50}$). Addition of Cys and Met residues enhanced the antimicrobial activity of the primary peptide, (LLKK)$_2$, as reflected by lower MIC values.

Antimicrobial agent	MIC (mg L^{-1})		HC$_{50}$ (mg L^{-1})
	Susceptible strain	Resistant strain	
Rifampicin	7.8	500	ND
(LLKK)$_2$	125	ND[a]	>1000
(LLKK)$_2$M	62.5	62.5	>1000
M(LLKK)$_2$	125	ND	>1000
M(LLKK)$_2$M	62.5	62.5	>1000
(LLKK)$_2$C	125	ND	>1000
C(LLKK)$_2$	62.5	62.5	>1000
C(LLKK)$_2$C	250	ND	>1000

[a] ND, not determined

The antimicrobial activities of the three most effective peptides against *M. smegmatis* were further evaluated in BCG, H37Rv and CSU87 and the results are summarised in Table 4.3. Of the three peptides, the most hydrophobic analogue M(LLKK)$_2$M proved to be the most effective against all three mycobacterial strains. It had the lowest MIC of 15.6 mg L^{-1} against BCG and was the only peptide active against H37Rv with an MIC of 125 mg L^{-1}. Against CSU87, the MIC of M(LLKK)$_2$M was reduced to 62.5 mg L^{-1}. It is likely that the enhancement of peptide hydrophobicity resulted in an increase in anti-mycobacterial activity, in line with observations from previous studies [139, 140]. Despite being ineffective against H37Rv, (LLKK)$_2$M had an MIC

of 125 mg L^{-1} against CSU87. Since alterations of the membrane barrier is one way in which resistance develops [141], it is plausible that the CSU87 strain studied may have undergone cell wall modifications that enhanced the permeabilisation of more hydrophobic AMPs. As such, the addition of one or two hydrophobic Met residues to the parent (LLKK)$_2$ peptide resulted in an increased antimicrobial potency against CSU87 as compared to H37Rv for both (LLKK)$_2$M and M(LLKK)$_2$M. Although the inclusion of L-Cys on the N-terminus of (LLKK)$_2$ corresponded with a twofold reduction in MIC against BCG, this modification proved ineffective in augmenting anti-mycobacterial activity against both H37Rv and CSU87.

Table 4.3. MICs of synthetic α-helical peptides against BCG, H37Rv and CSU87. M(LLKK)$_2$M was the most effective peptide against all three mycobacterial strains.

Antimicrobial agent	MIC (mg L^{-1})		
	BCG	H37Rv	CSU87
(LLKK)$_2$	500	>500	>500
(LLKK)$_2$M	500	>500	125
M(LLKK)$_2$M	15.6	125	62.5
C(LLKK)$_2$	250	>500	>500
Rifampicin	0.001	0.008	>32
Moxifloxacin[a]	ND	ND	0.06

[a] Moxifloxacin served as a positive control

4.2.4. Killing efficiency and time-kill curve

The antimicrobial potency of the most effective peptide, M(LLKK)$_2$M, was further studied by measuring its killing efficiency against *M. smegmatis*, BCG and H37Rv. As shown in Figure 4.2, M(LLKK)$_2$M had a killing efficiency of ≥ 99.9 % at MIC and 2x MIC levels against both *M. smegmatis* and BCG. The killing efficiency against H37Rv was found to be ≥ 99 % and ≥ 99.9 % at MIC and 2x MIC respectively.
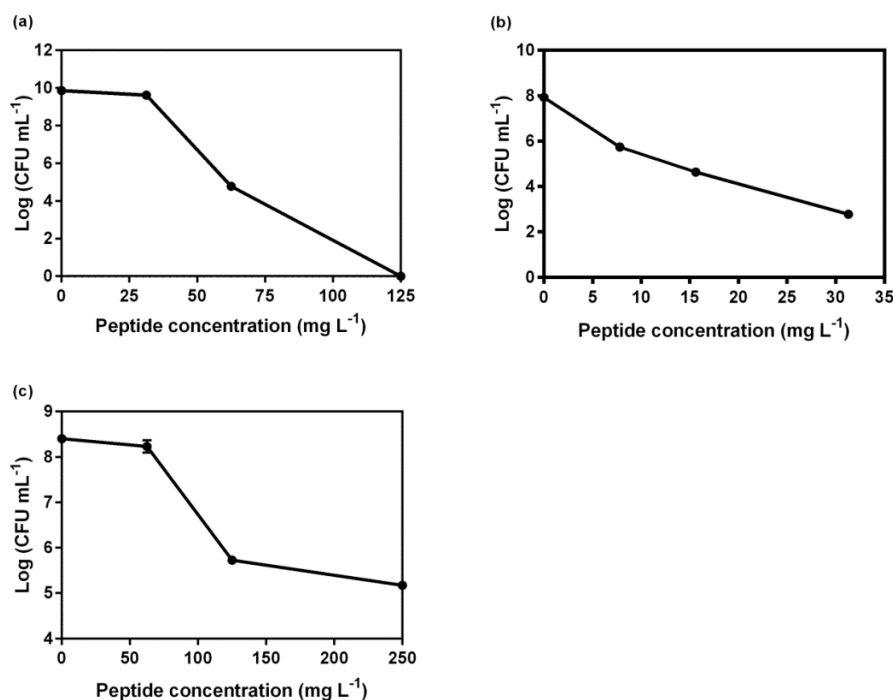
Figure 4.2. Plot of viable CFUs after treatment of (a) *M. smegmatis*, (b) BCG and (c) H37Rv with M(LLKK)$_2$M at concentrations corresponding to 0, 0.5x, 1x and 2x MIC. M(LLKK)$_2$M reduced bacterial burden by $\geq$ 99.9% against *M. smegmatis* and BCG, and $\geq$ 99 % against H37Rv, at the respective MICs. Data expressed as mean $\pm$ S.D. and are representative of two independent experiments.

The bactericidal properties of M(LLKK)$_2$M were further evaluated by time-kill assay against *M. smegmatis* and the results were compared to that of rifampicin. As shown in Figure 4.3, the peptide exhibited dose-dependent bactericidal effects, defined as a $\geq$ 3 log decrease in the initial inoculum [142]. The peptide was rapidly bactericidal within 8 h of exposure at 8x MIC and within 24 h of exposure at MIC and 4x MIC. Furthermore, at 8x MIC, there was complete eradication of all bacteria by 24 h. The bactericidal effect of the peptide was much stronger than that of the first-line anti-TB drug, rifampicin. Rifampicin was only bacteriostatic at MIC and 4x MIC and bactericidal activity was achieved only at 8x MIC after 48 h. This rapid killing kinetics is commonly observed for AMPs due to their membrane-lytic mechanisms of

action, which results in pore formation, and leakage of cellular contents [38, 143].
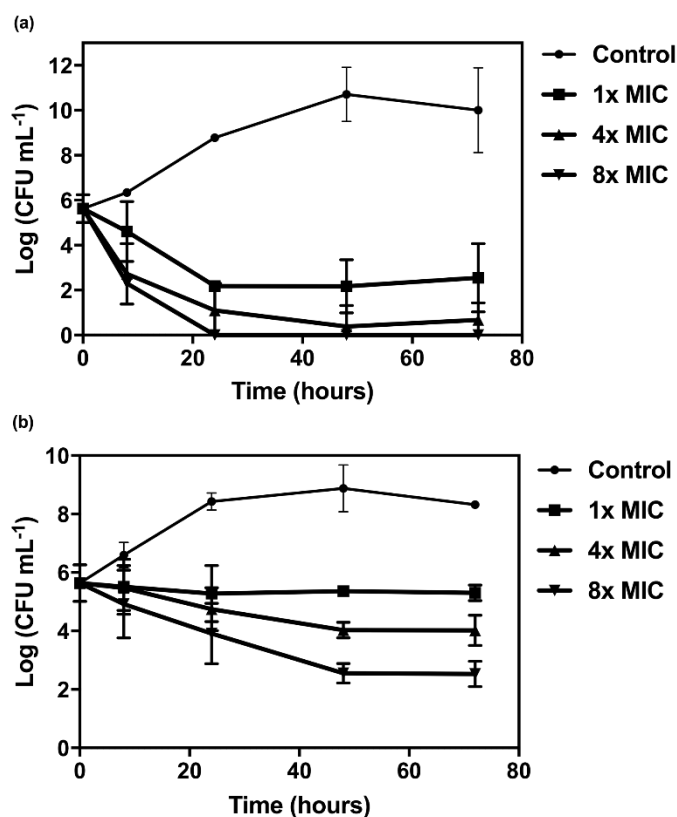
Figure 4.3. Killing curves of *M. smegmatis* following exposure to (a) M(LLKK)$_2$M and (b) rifampicin over 72 h at 1x, 4x and 8x MIC. M(LLKK)$_2$M was rapidly bactericidal at MIC within 24 h while rifampicin remained bacteriostatic at MIC even after 72 h. Data expressed as mean ± S.D. for two independent experiments.

4.2.5. Haemolytic activity

The potential of the synthetic peptides to cause haemolysis was assessed to provide an indication of their cytotoxicity. The 50% haemolysis concentration of the peptides (HC$_{50}$) against rat RBCs is summarised in Table 4.2 and Figure 4.4. Generally, the synthetic peptides, including the most potent peptide M(LLKK)$_2$M, exhibited low haemolytic activity even up to concentrations of 1000 mg L^{-1}. Importantly, the peptides displayed very low haemolytic activity at their respective MICs (< 1% haemolysis). The peptides M(LLKK)$_2$M and

C(LLKK)$_2$C induced the highest haemolysis of 1.1% and 12.9% respectively at 1000 mg L^{-1}. It is likely that both of these peptides possessed higher membrane disrupting abilities due to an increase in peptide hydrophobicity, thus resulting in greater haemolysis of mammalian RBCs, similar to observations in other studies [136, 137].
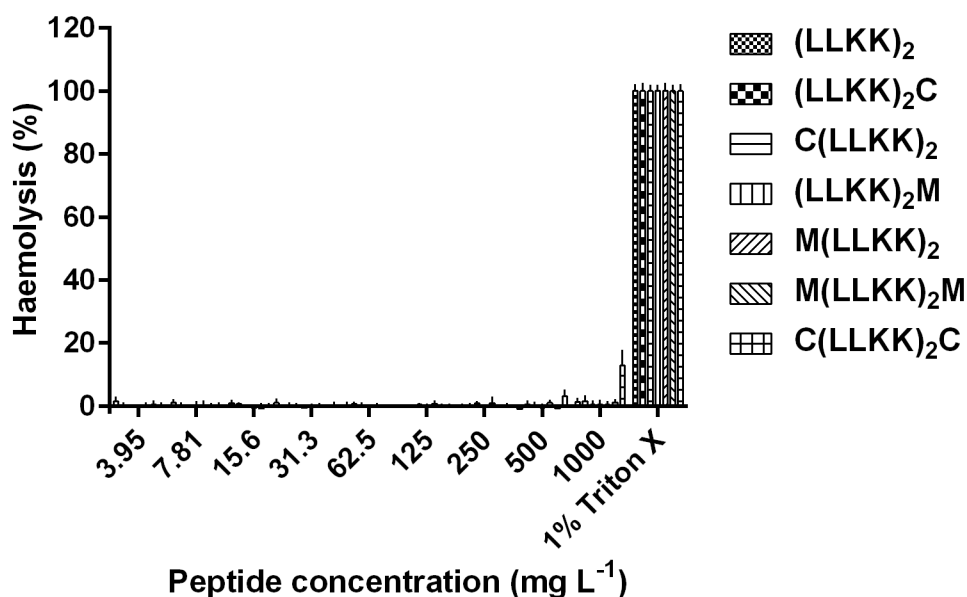
Figure 4.4. Haemolytic activity of α-helical AMPs following treatment with two-fold increasing peptide concentrations. All peptides possessed desirable cytotoxicity profiles with < 1% haemolysis at their respective MIC. Data expressed as mean ± S.D. for two independent experiments.

4.2.6. Antimicrobial mechanisms

M. smegmatis was treated with M(LLKK)$_2$M for 10, 30 and 60 min in the presence of FITC-labelled dextran probe so as to elucidate the antimicrobial mechanisms of the α-helical peptides. AMPs are membrane active agents which compromise the cell membrane integrity and result in pore formation. As such, exposure of bacterial cells to the peptides would induce pore formation and result in the passive diffusion of the fluorescent dye into the cells. It can be seen in Figure 4.5a that treatment with PBS alone did not result

76

in the uptake of FITC-dextran, supported by the absence of any green fluorescence signal. Treatment with M(LLKK)$_2$M, however, induced a significant increase in the uptake of the fluorescence probe. Furthermore, increasing the duration of exposure to this peptide resulted in a greater uptake of FITC-dextran, evidenced by the greater proportion of fluorescently stained cells at the three different time points (Figures 4.5b to d). This progressive increase in the fraction of fluorescent bacterial cells imaged from 10 to 60 min implies that longer treatment potentially resulted in greater destruction and pore formation in the bacterial membrane. Together, these findings lend support to the membrane-permeabilising mechanisms of the synthetic AMPs presented here.
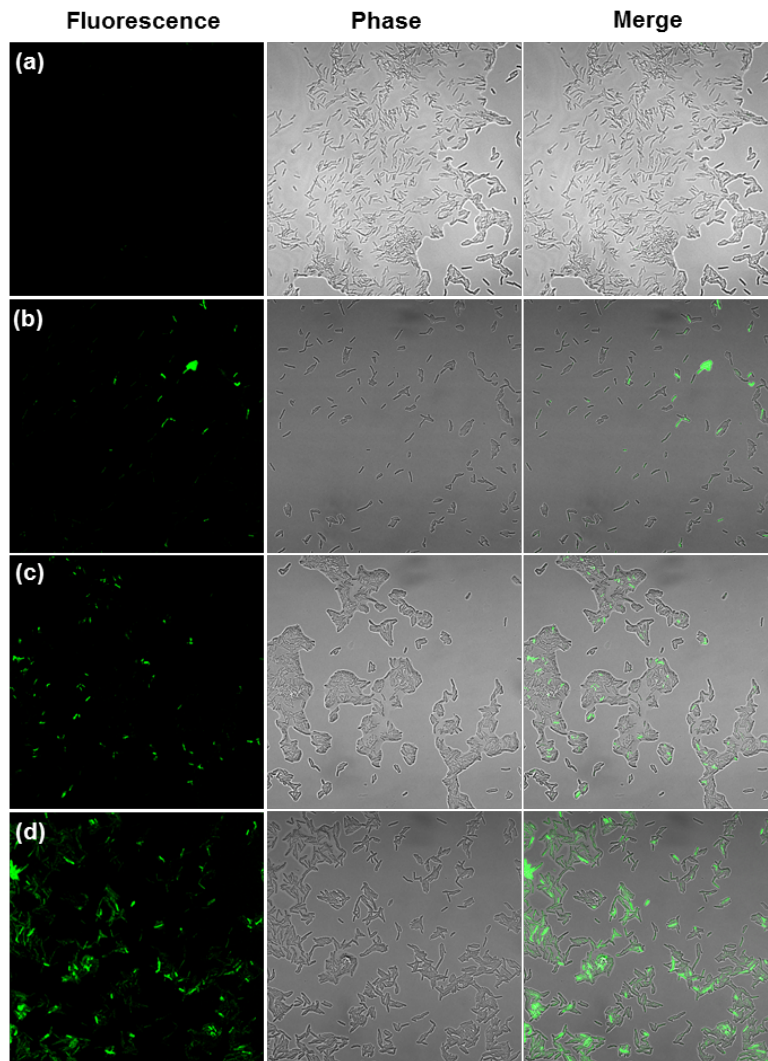
Figure 4.5. Confocal microscopic images of *M. smegmatis* after treatment with (a) PBS, and M(LLKK)$_2$M at its MIC for (b) 10 min, (c) 30 min and (d) 60 min in the presence of 150 kDa FITC-dextran. Increasing fluorescence intensity from 10 to 60 min after peptide treatment is indicative of progressive membrane damage and pore formation, allowing for greater uptake of the fluorescent probe.

4.2.7. Development of drug resistance

The problem of drug resistance mainly stems from inappropriate drug use, often associated with poor adherence to regimens or inappropriate dosing. To simulate these conditions *in vitro*, *M. smegmatis* cells were exposed to sub-therapeutic doses of rifampicin and M(LLKK)$_2$M over 10 passages. As shown in Figure 4.6, there was rapid onset of rifampicin resistance as early as passage

two and a 16-fold increase in MIC was observed by passage four. After 10

passages, the MIC had increased by 32-fold, demonstrating that resistance to

rifampicin can indeed develop rapidly with sub-therapeutic doses. In contrast,

resistance did not readily develop with $M(LLKK)_2M$ treatment as shown by

the consistent MIC obtained over 10 passages. Furthermore, the occurrence of

rifampicin resistance could be delayed with the addition of a fixed

concentration of $M(LLKK)_2M$ (15.6 mg L^{-1}) to rifampicin treatment. This was

shown by a twofold increase in MIC after five passages and a MIC that was

four times lower in combination as compared to treatment with rifampicin

alone after 10 passages. These findings underline the potential benefits that

using the synthetic α-helical peptide $M(LLKK)_2M$ alone or in combination

with first-line anti-TB drugs can have in preventing the emergence of drug-

resistant bacteria.
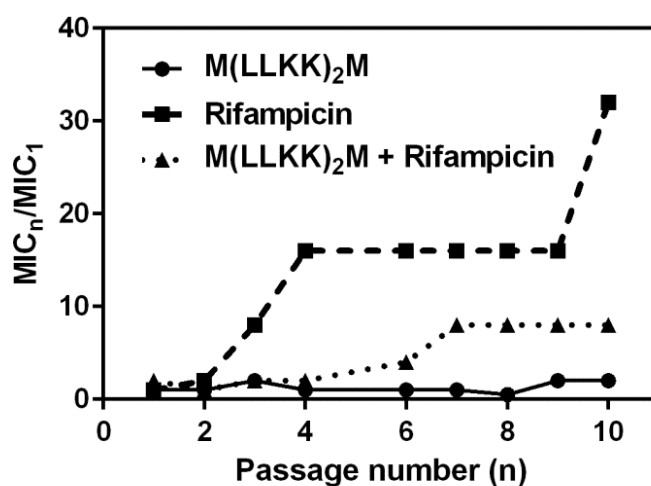
Figure 4.6. Changes in MIC of $M(LLKK)_2M$ and rifampicin alone, and in combination, after exposure of *M. smegmatis* to sub-lethal doses over 10 passages. Resistance against rifampicin developed rapidly when administered alone but was delayed when a fixed concentration of $M(LLKK)_2M$ was added.

4.2.8. Synergistic antimicrobial interactions

The antibacterial interactions between the M(LLKK)$_2$M and rifampicin were analysed *via* the chequerboard assay. As shown in Table 4.4, M(LLKK)$_2$M displayed synergism with rifampicin with an FICI value of 0.5 against rifampicin-susceptible *M. smegmatis*. Subsequent testing against rifampicin-resistant *M. smegmatis* (MIC = 250 mg L^{-1}) and BCG produced similar results, whereas the peptide-drug combination had an additive effect against H37Rv with an FICI of 0.56. Notably, a low peptide concentration equivalent to 1/16th its MIC, halved the amount of rifampicin required to inhibit H37Rv growth. It is likely that peptide-mediated destruction of membrane integrity facilitated the entry of rifampicin to cytoplasmic targets and was responsible for the synergism observed. Synergistic interactions between rifampicin and natural AMPs have been reported previously and this effect has also been attributed to the enhanced intracellular access of the drug aided by these membrane-permeabilising peptides [144-146]. It is thus likely that peptides with stronger membrane-permeabilising properties would potentially display stronger synergistic interactions. This may be the reason why C(LLKK)$_2$ did not exhibit synergism with rifampicin (Table 4.4), in part due to its lower α-helicity (Figure 4.1) and reduced membrane permeabilisation in comparison to M(LLKK)$_2$M and (LLKK)$_2$M, both of which demonstrated synergism with rifampicin against rifampicin-susceptible *M. smegmatis*.

Table 4.4. Chequerboard assay of rifampicin and synthetic peptides against four different mycobacterial strains. Synergism was observed for the M(LLKK)$_2$M and rifampicin combination against rifampicin-susceptible and –resistant *M. smegmatis* and BCG while additivity was observed against H37Rv.

Mycobacterial strain	Drug combination	MIC (mg L^{-1})		FIC	FICI[a]
		Alone	Combination		
M. smegmatis	Rifampicin	7.81	1.95	0.25	-
	M(LLKK)$_2$M	62.5	15.6	0.25	0.50 (S)
	(LLKK)$_2$M	62.5	15.6	0.25	0.50 (S)
	C(LLKK)$_2$	62.5	31.3	0.50	0.75 (A)
Rifampicin-resistant *M. smegmatis*	Rifampicin	250	62.5	0.25	-
	M(LLKK)$_2$M	62.5	15.6	0.25	0.50 (S)
BCG	Rifampicin	0.001	0.00025	0.25	-
	M(LLKK)$_2$M	15.6	3.91	0.25	0.50 (S)
H37Rv	Rifampicin	0.008	0.004	0.50	-
	M(LLKK)$_2$M	125	7.81	0.06	0.56 (A)

[a] Antimicrobial interactions were classified as additive (A) or synergistic (S).

4.3. Conclusions

In this study, a series of synthetic α-helical peptides modified with L-Cys or L-Met residues on either or both the N- and C-terminals have been evaluated for their anti-mycobacterial activities and cytotoxicity towards mammalian cells. The peptide (LLKK)$_2$ modified with two Met residues (i.e. M(LLKK)$_2$M) was effective against both drug-susceptible (H37Rv) and MDR (CSU87) *M. tuberculosis* without causing any cytotoxicity at concentrations eightfold greater than its highest MIC. The peptide eradicated mycobacteria based on membrane-lytic mechanism, and displayed synergistic interactions with rifampicin against both *M. smegmatis* and BCG, and an additive effect against H37Rv. Moreover, resistance against M(LLKK)$_2$M did not develop readily, and when used in combination with rifampicin, the peptide was shown to delay the emergence of rifampicin resistance. These findings underscore the potential applicability of M(LLKK)$_2$M to fight drug-resistant mycobacterial infections and could eventually lead to its incorporation into multi-drug

regimens as a cost-effective and non-toxic alternative in overcoming MDR-

TB.

CHAPTER 5: Designing α-helical peptides with enhanced synergism and selectivity against *Mycobacterium smegmatis* – Discerning the role of hydrophobicity and helicity

5.1. Introduction

TB is a preventable and curable infectious disease caused by *M. tuberculosis*, a pathogen which possesses marked biological and genomic differences as compared to both Gram-positive and Gram-negative bacterium [147]. One major distinction is that the composition of the mycobacterial cell wall, which unlike its Gram-positive counterparts, is highly complex and consists of an outer membrane with mycolic acids covalently linked to the peptidoglycan-arabinogalactan polymer (Figure 5.1) [148, 149]. Mycolic acids are high molecular weight branched fatty acids containing about 70-90 carbon atoms, which accounts for up to 60% of the dry weight of mycobacterial cells [150]. This lipid-rich cell envelope forms a formidable barrier to prevent the entry of noxious substances and therapeutic agents alike, thereby posing an immense challenge to the design of new anti-tubercular drugs which must first penetrate this layer to exert their action at the target site [151].
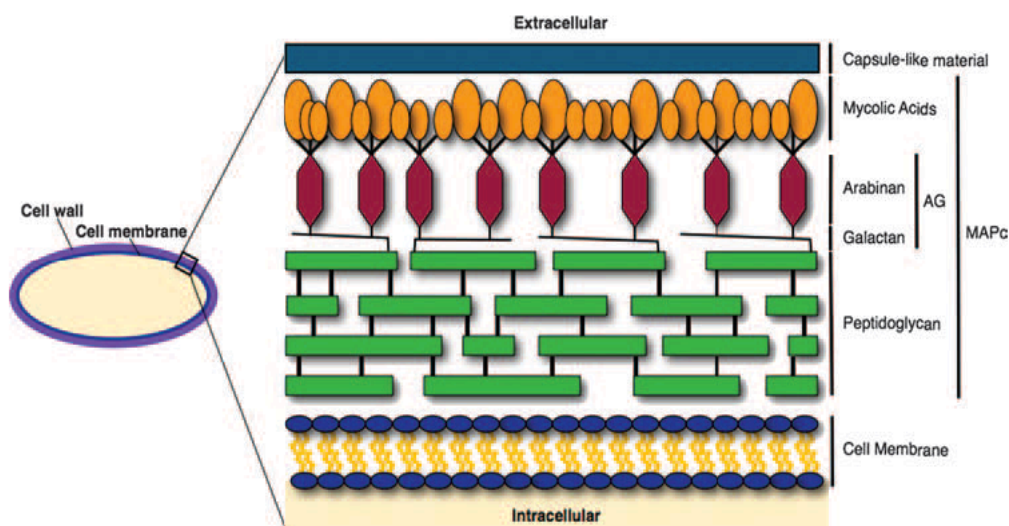
Figure 5.1. Diagram illustrating the basic component of the mycobacterial cell wall consisting of MAPc (mycolic acid-arabinogalactan-peptidoglycan complex). Reproduced with permission from [149]. Copyright (2008) American Society for Microbiology.

The permeation of hydrophilic solutes across the mycobacterial cell wall mainly occurs through porin channels while lipophilic solutes are able to traverse the lipid-rich outer membrane [152]. As such, it has been suggested that in principle, more lipophilic compounds are expected to exhibit improved activity against mycobacteria due to enhanced intracellular drug uptake [148]. Yajko *et al*. demonstrated that the more hydrophobic fluoroquinolone, sparfloxacin, displayed superior killing effect against the MAC as compared to ciprofloxacin [153]. Haemers *et al*. found that increasing hydrophobicity by adding N-alkyl substituents to ciprofloxacin served to enhance *M. tuberculosis* and *M. avium* inhibition [154]. The enhancement of hydrophobicity of the hydrophilic isoniazid by the addition of palmitoyl substituent improved activity against the MAC as reported by Rastogi *et al*. [155]. Hence, structural modifications aimed at enhancing the hydrophobicity of compounds could

serve as an effective strategy when designing new anti-tubercular drugs with enhanced anti-mycobacterial activity.

With respect to AMPs, such a strategy has been used to optimise the activity against Gram-positive and Gram-negative bacteria. Lee *et al.* showed that increasing the hydrophobicity of the antimicrobial peptide HP (2-20) by specific amino acid substitution brought about a considerable increase in antimicrobial activity against both Gram-positive and Gram-negative bacteria [139]. Meng and Kumar found that the increased hydrophobicity of peptides modified with fluorinated amino acids also yielded greater activity against both Gram-positive and Gram-negative bacteria [156]. Radzishevsky *et al.* studied the effect of hydrophobicity by conjugating various acyl moieties to AMPs and observed that the potency of the parent peptide against Gram-positive and Gram-negative bacteria was enhanced [157]. To the best of our knowledge, the only study employing this strategy to systematically design and evaluate AMPs for their activity against mycobacteria met with limited success [158]. In fact, enhancements in peptide hydrophobicity decreased antimicrobial efficacy against *M. tuberculosis*, and this was accompanied by dramatic increments in haemolytic activity of up to 120-fold, resulting in reduced selectivity indices [158]. These findings highlight the long-standing impediment to the clinical application of AMPs: their high systemic toxicity. Hence, the challenge thus far has been to develop compounds with improved microbial selectivity, especially against the genus *Mycobacterium*.

In Chapter 4, we reported on a series of short amphipathic α-helical peptides, comprising the backbone sequence (LLKK)$_2$, with the ability to kill drug-susceptible and drug-resistant *M. tuberculosis*. The addition of free sulfhydryl (thiol) groups by incorporating Cys residues in the AMPs did not improve anti-mycobacterial activity against drug-susceptible and drug-resistant *M. tuberculosis*, while the enhancement of peptide hydrophobicity by incorporation of Met residues increased the efficacy of the primary peptide against all mycobacterial strains tested, including clinically isolated MDR *M. tuberculosis*. The peptide with the optimal composition M(LLKK)$_2$M was bactericidal, and eradicated mycobacteria *via* a membrane-lytic mechanism. Furthermore, a reduction in α-helical character for C(LLKK)$_2$ was found to unfavourably impact peptide-drug synergistic interactions. These preliminary findings suggest that several key physicochemical parameters, namely hydrophobicity and α-helicity, are critical determinants of anti-mycobacterial activity, thus warranting further investigation.

In this chapter, we set out to systematically evaluate the importance of both hydrophobicity and α-helicity in potentiating the anti-mycobacterial mechanism of action of AMPs against the mycobacterial cell wall, as well as their synergistic activity in combination with rifampicin. A series of six synthetic α-helical peptides, designed from the parent peptide (LLKK)$_2$ over a range of hydrophobicities, were evaluated for their activity against *M. smegmatis* and eukaryotic cells, with the primary objective of developing synthetic analogues with enhanced selectivity. Herein, we provide the first report on the modulating effect of hydrophobicity and α-helicity on the

antimicrobial mechanisms of synthetic AMPs and their synergism with first-line antibiotics against mycobacteria. Peptide hydrophobicity was experimentally determined using RP-HPLC and changes in secondary conformation were assessed by CD spectroscopy. *In vitro* antimicrobial efficacy was evaluated by MIC and synergy chequerboard assays followed by cytotoxicity studies against rat RBCs and the murine macrophage RAW 264.7 cell line. The anti-mycobacterial mechanisms were investigated by membrane depolarisation, flow cytometry and FE-SEM. Membrane destruction triggering the leakage of cytoplasmic content was examined by dye leakage and ATP bioluminescence assays.

5.2. Results and discussion

5.2.1. Peptide design and characterisation

The interactions between peptides and bacterial membranes are modulated by various physicochemical properties including peptide hydrophobicity, charge, secondary structure, and amphiphilicity [102, 159]. In order to elucidate the influence of hydrophobicity on their antimicrobial activity, synthetic peptides were designed with minimal sequence modification to maintain their charges and amphiphilicity fairly unaltered. To achieve this, $(LLKK)_2$ was used as a framework to systematically modify peptide hydrophobicity by substituting amino acids to both the N- and C- terminals to obtain peptides with the backbone sequence $X(LLKK)_2X$, where X is a hydrophobic amino acid. Five amino acids, Met, Cys, proline (Pro), isoleucine (Ile) and Trp were selected to obtain the following peptides: $M(LLKK)_2M$, $C(LLKK)_2C$, $P(LLKK)_2P$, $I(LLKK)_2I$ and $W(LLKK)_2W$, which will henceforth be referred to as per their abbreviated denotations listed in Table 5.1. The C-terminal of all six analogues was amidated to improve antimicrobial activity by conferring peptides with an extra net positive charge [133, 134]. The fidelity of peptide synthesis was confirmed *via* MALDI-TOF MS and the results are summarised in Table 5.1. The close agreement between the measured and theoretical molecular weights of the peptides indicates that the compounds were synthesised to the desired specifications. The overall hydrophobicity of the peptides was measured by their retention time (t_R) using RP-HPLC and ranged from 15.68 to 24.40 min (Table 5.1). The parent peptide LK without any additional amino acid residues recorded the lowest t_R of 15.68 min while WW, with two extra Trp residues, displayed the greatest hydrophobicity with a

corresponding t_R of 24.40 min. The ranking of the peptides in terms of increasing overall hydrophobicity is as follows: LK < PP < CC < II < MM < WW.

Table 5.1. Amino acid sequence of synthetic cationic α-helical peptide analogues and their physiochemical parameters including charge, hydrophobic moment, hydrophobicity and helicity.

Amino acid sequence	AMP	Theoretical M_w	Measured $M_w{}^a$	Net charge	μH^b	$t_R{}^c$ (min)	% Helicity $_d$
LLKKLLKK-NH₂	LK	982.37	983.02	+4	3.69	15.68	9.3
PLLKKLLKKP-NH₂	PP	1176.60	1177.02	+4	3.69	17.80	9.7
CLLKKLLKKC-NH₂	CC	1188.66	1187.51^e	+4	3.69	20.76	29.3
ILLKKLLKKI-NH₂	II	1208.69	1209.14	+4	3.69	21.63	38.1
MLLKKLLKKM-NH₂	MM	1244.76	1245.18	+4	3.69	21.69	35.4
WLLKKLLKKW-NH₂	WW	1354.79	1355.15	+4	3.69	24.40	25.1

^{a} Measured by MALDI-TOF MS, apparent $M_w = [M_w + H]^+$.
^{b} The hydrophobic moment (μH) was determined by the Totaliser module of Membrane Protein Explorer (MPEx) which uses the experimentally based interfacial Wimley-White hydrophobicity scales and is available online at http://blanco.biomol.uci.edu/mpex.
^{c} Retention time as determined by RP-HPLC.
^{d} % helicity was calculated from ratio of $[\theta]_{222}/[\theta]_{max}$ using a modified Baldwin equation as described in section 4.3.2.
^{e} An additional dimer peak was observed at m/z 2374.78 for CC.

5.2.2. CD spectroscopic study

The secondary structure of the synthetic peptides in a membrane-like environment was studied using CD spectroscopy and the results are summarised in Figure 5.2. The peptides adopted α-helical structures in 25 mM SDS solution as confirmed by the presence of the double minima at ~208 and 222 nm. Generally, the addition of amino acids to both the N- and C-terminals resulted in greater α-helical conformation as determined by a more negative mean residue ellipticity value at 222 nm (θ_{222}). Although, the value at θ_{222} is commonly used to determine the degree of helicity of peptides, these estimates tend to be less accurate for short helices [160]. Hence, the percentage α-helicity of synthetic peptides was calculated using an equation

described by Baldwin and subsequently modified by Fairlie, given by the ratio of $\theta_{222}/\theta_{max}$, and θ_{max} is calculated using the following equation:

$$\theta_{max} = (-44000 + 250\text{T})\left(1 - \frac{k}{n}\right),$$ where T is the temperature in $^{\circ}$C, k is the finite length correction and n is the number of peptide residues [161, 162]. The θ_{max} for 8 and 10 residue helices is -19500 and -23400 respectively when $k = 4$ and $T = 20\,^{\circ}$C. The percentage helicity of the peptides is summarised in Table 5.1. Of the six, LK and PP were found to possess the lowest α-helical contents of about 9%, while the α-helicity of the other four peptides was three to fourfold greater. These findings suggest that increasing peptide hydrophobicity results in an increase in α-helical structure, and is consistent with reports by other research groups [137, 163]. Only PP did not conform to this trend as its enhanced hydrophobicity as compared to LK did not improve its propensity for α-helical folding. This finding implies that factors other than hydrophobicity may be modulating the helical propensity of the Pro substituted analogue. One possibility could be that steric hindrance induced by the bulky pyrrolidine ring present in Pro residues, gives rise to conformational distortion in the preceding helical turn, thus hindering the formation of stable α-helices [164, 165]. In addition, the inclusion of Pro in the middle of helices or near the C-terminal also causes breakage of adjacent hydrogen bonds and premature termination of the helix [166, 167]. Both of these factors could have in turn mitigated the effects of increasing hydrophobicity on α-helicity, resulting in similar α-helical contents as seen for both LK and PP.
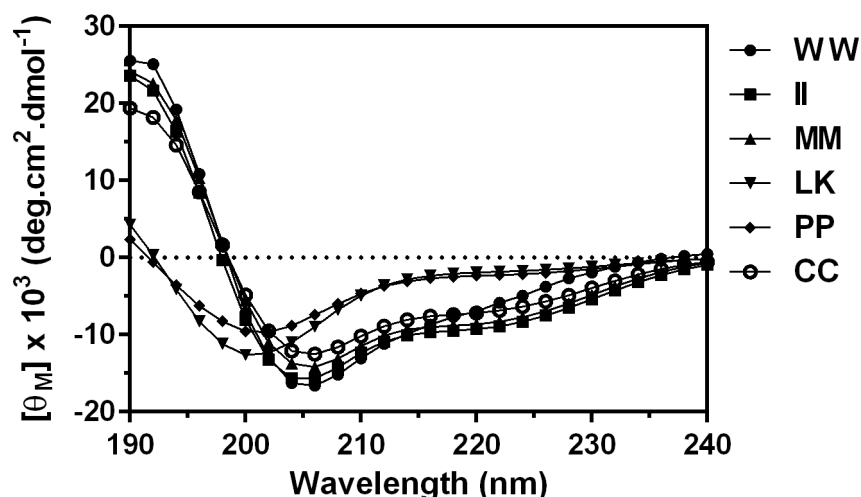
Figure 5.2. CD spectra of synthetic peptide analogues displaying characteristic double minima at ~208 and 222 nm, confirming their α-helical secondary conformations. Data are expressed as the mean of two runs per peptide.

5.2.3. In vitro anti-mycobacterial activity

The antimicrobial activities of the synthetic peptides and rifampicin against *M. smegmatis* determined by the broth microdilution method are summarised in Table 5.2. The peptide analogues displayed varying efficacy against *M. smegmatis* with MICs ranging from 62.5 to 250 mg L^{-1}. Overall, hydrophobic modifications to LK produced three analogues with improved antimicrobial activity while the other two inhibited bacterial growth less effectively. The addition of Trp, Met and Ile residues to both the N- and C- terminals enhanced the potency of LK, reflected by the decrease in MIC from 125 to 62.5 mg L^{-1} for WW, MM and II. While enhancing the hydrophobicity of α-helical peptides has been shown to improve antimicrobial activity, high peptide hydrophobicity is associated with stronger peptide self-association resulting in the formation of dimers/oligomers [136, 137]. Peptide self-association in turn correlates with weaker antimicrobial activity since peptide dimers/oligomers

are prevented from readily passing through the bacterial cell wall in order to reach their target plasma membrane. Therefore, a lack of improvement in the MIC of the most hydrophobic peptide, WW, against *M. smegmatis* could possibly be attributed to stronger self-association as compared to the less hydrophobic analogues, MM and II. Surprisingly, despite its increased hydrophobicity and α-helicity, CC demonstrated poorer anti-mycobacterial activity as compared to LK. Since CC is less hydrophobic than MM, II and WW, any peptide self-association resulting in dimer/oligomer formation should not significantly compromise its activity as compared to the three most hydrophobic analogues. Yet it was found to be the least potent analogue, which implies that another factor unique to this peptide alone might be responsible for this observation. Further discussions on the diminished activity of CC will be carried out in Section 5.2.6 together with the flow cytometric analysis. As for PP, it is likely that the reduced propensity for helical formation observed (Figure 5.2) was responsible for the decrease in antimicrobial potency as compared to WW, MM and II. A decrease in α-helicity by introducing Pro residues into helices has been shown to greatly reduce the antimicrobial efficacy and activity spectrum of α-helical peptides [168]. Hence, peptide helicity is another important parameter which should be given due consideration when looking to design more potent peptides. Even though our findings highlight that flanking of both the N- and C-terminals with Pro can produce detrimental effects on antimicrobial potency, the incorporation of Pro residues in peptides should not be dismissed entirely as an ineffective strategy in designing more selective analogues. A recent study

found that the careful substitution of Pro residues into peptide sequences can reduce cytotoxicity and improve antibacterial selectivity [169].

Table 5.2. MIC, FICI, and SI values of synthetic peptides against *M. smegmatis*

Antimicrobial agent	MIC (mg L^{-1})		FIC	FICI^a	HC$_{50}$ (mg L^{-1})	SI^b
	Alone	Combination				
LK	125	62.5	0.5	0.75 (A)	>500	8
PP	250	125	0.5	0.75 (A)	>500	4
CC	250	250	1.0	1.25 (I)	>500	4
II	62.5	15.6	0.25	0.50 (S)	>500	16
MM	62.5	15.6	0.25	0.50 (S)	>500	16
WW	62.5	15.6	0.25	0.50 (S)	363	5.8
Rifampicin	3.90	0.98	0.25	-	-	-

^{a} Antimicrobial interactions were classified as additive (A), indifferent (I) or synergistic (S).
^{b} SI is determined as follows: (HC$_{50}$/MIC). When no detectable haemolysis was observed at the highest tested concentration of 500 mg L^{-1}, a value of 1000 mg L^{-1} was used for SI calculations.

5.2.4. Haemolytic activity and cell selectivity

The haemolytic activities of the synthetic peptides were evaluated using 4% (v/v) rat blood as a measure of their toxicity against mammalian cells, and the results are summarised in Figure 5.3. The HC$_{50}$ values, defined as the peptide concentration producing 50% haemolysis of rat RBCs, are shown in Table 5.2. Except for WW, all the other five peptides exhibited very low haemolysis ($\leq$ 3%) even up to concentrations of 500 mg L^{-1}. Notably, all six peptide analogues induced minimal haemolysis ($\leq$ 3%) at their respective MICs. The most hydrophobic peptide, WW, displayed the strongest haemolytic activity of ~19% and 69% at 250 and 500 mg L^{-1}, respectively. This corresponded to a far lower HC$_{50}$ value of 363 mg L^{-1} for WW as compared to the other peptides (> 500 mg L^{-1}). While the modulating effect of hydrophobicity on the haemolytic activity of the peptides was evident, the contribution of α-helicity was far less apparent. The two most helical peptides, MM and II, were minimally

haemolytic even at 500 mg L^{-1}, suggesting that hydrophobicity, rather than helicity, was more likely the driving force behind the enhanced haemolytic activity observed for WW. Previous studies examining the membrane permeability of electrically neutral POPC vesicles treated with peptide analogues of varying hydrophobicity have also shown that increasing hydrophobicity produced a greater degree of haemolysis [140, 170]. This phenomenon was attributed to the zwitterionic nature of eukaryotic membranes, which facilitates deeper penetration of more hydrophobic peptides thus inducing greater pore formation and consequently, stronger haemolysis.
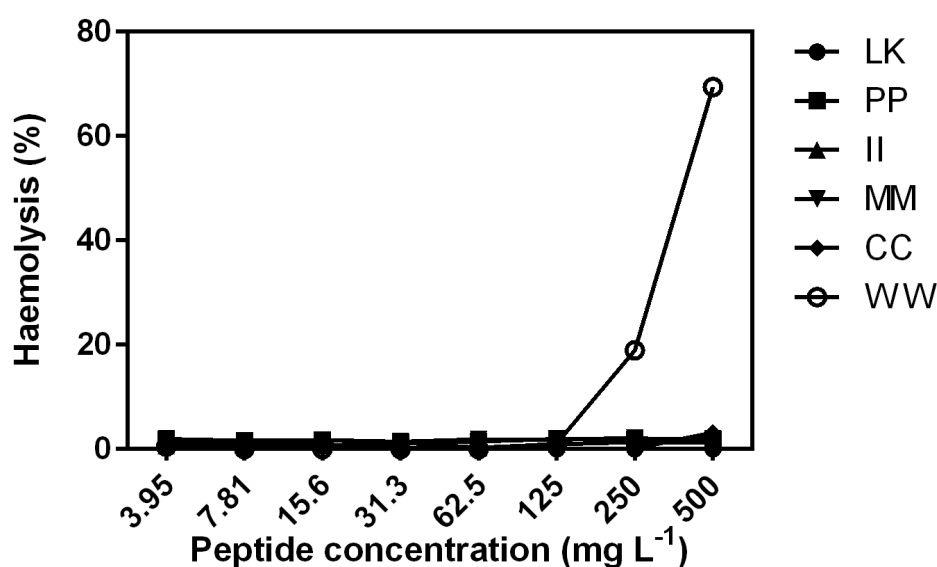
Figure 5.3. Haemolytic activity of synthetic α-helical peptides against rat RBCs following 2 h treatment. All peptides except WW induced minimal haemolysis up to 500 mg L^{-1}. Data expressed as mean ± S.D. for two independent experiments.

The selectivity indices (SIs) shown in Table 5.2, defined as the ratio of HC$_{50}$ to MIC values, serve as a measure of antibacterial selectivity, with larger SI values indicative of greater selectivity towards microbial over mammalian

membranes. MM and II proved to be the best analogues (SI = 16), while the most hydrophobic analogue, WW, had a lower selectivity index as compared to LK. Previous studies have also shown that increasing peptide hydrophobicity may decrease antimicrobial selectivity of α-helical peptides [158, 171]. However, the findings presented in this study suggest that a moderate increase in peptide hydrophobicity can translate into better selectivity, as seen for MM and II, but further increments could produce deleterious effects on peptide selectivity, as observed for WW.

5.2.5. Cytotoxic effect of peptides on macrophages

The cytotoxicity of the peptides against mammalian cells was further evaluated against RAW 264.7 macrophage cells and the results are shown in Figure 5.4. LK, PP and II were found to be the least cytotoxic analogues with cell viabilities in excess of 85% even up to concentrations of 250 mg L^{-1}. The most hydrophobic analogue, WW, was also the most cytotoxic, recording the greatest reduction in cell viability from 92.3 to 13.2% with an increase in concentration from 3.95 to 250 mg L^{-1}. At MIC levels (62.5 mg L^{-1}), approximately 50% of the cells treated with WW remained viable, whereas for MM and II, which also had similar MICs, cell viabilities were higher at 77.9% and 98.5%, respectively. Similar to the trends observed with regards to their haemolytic activities, hydrophobicity was found to be a more significant contributor towards cytotoxicity than the α-helical character of the peptides. This observation is in line with previous findings reported by Jacob *et al.* who also found that increasing the hydrophobicity of α-helical peptides induced greater cytotoxicity against RAW 264.7 cells [172]. Interestingly, despite its superior hydrophobicity and helicity, the Ile substituted analogue II possessed

a comparable cytotoxicity profile to LK even up to 250 mg L^{-1}. Though the hydrophobic and helical characters of MM and CC were comparable to II, both were found to be more toxic towards mammalian cells with 80% cell viabilities even at 15.6 mg L^{-1}. Given that macrophages are potentially major reservoirs for mycobacteria during pulmonary TB infection, the incorporation of Ile as compared to other hydrophobic amino acids such as Met, Cys and Trp, may be a more suitable when designing potent peptides with reduced cytotoxicity against mammalian cells.
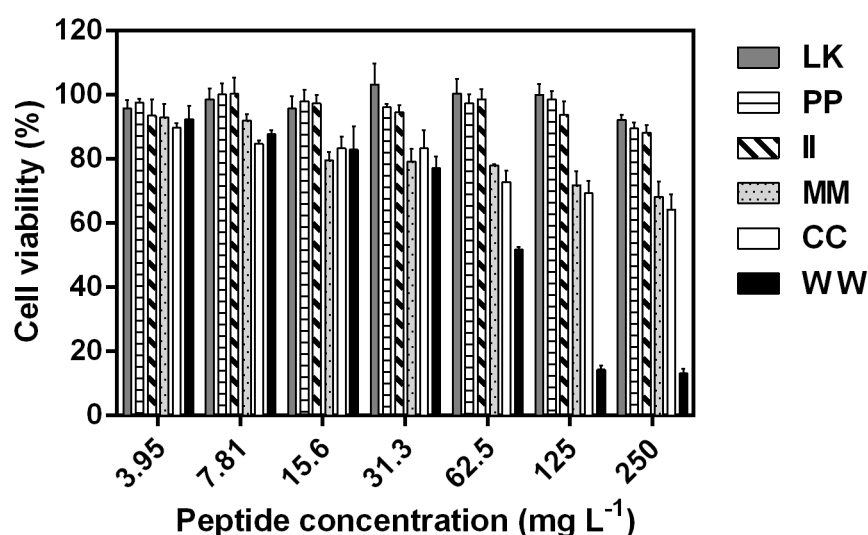
Figure 5.4. Cytotoxicity profiles of the synthetic α-helical peptides against the mouse macrophage cell line RAW 264.7 after exposure for 24 h treatment. WW was found to be the most toxic analogue of all six peptides tested. Data expressed as mean ± S.E.M. for three independent experiments.

5.2.6. Flow cytometry

To investigate the extent of membrane disruption induced by the peptide analogues, *M. smegmatis* was treated with all six peptides in the presence of the DNA intercalating agent PI. Peptide-mediated destruction of the bacterial membrane is expected to facilitate the intracellular diffusion of PI and the proportion of bacterial cells fluorescently stained by PI following incubation

with peptides at various concentrations (62.5, 125 and 250 mg L^{-1}) is summarised in Figure 5.5. First-line anti-tubercular agents, rifampicin and ethambutol, served as negative controls given that they target DNA-dependent RNA polymerases and arabinosyl transferases, respectively, rather than the mycobacterial membrane directly. Both drugs resulted in staining of approximately 1% of bacterial cells at 1x, 2x and 4x MIC implying that mycobacterial membrane integrity remained largely uncompromised (Figure 5.5b). Notably, > 99% of cells treated with LK and PP did not present any fluorescent signal even up to concentrations of 250 mg L^{-1}, indicative of intact bacterial cell membranes. This implies that the anti-mycobacterial mechanism of action of both these peptides could be different from that of the other peptides. In contrast, treatment with the three most hydrophobic peptides, WW, MM and II resulted in a significant concentration dependent increase in proportion of bacterial cells taking up the fluorescence dye. At concentrations equivalent to MIC, 63.8%, 88.3% and 84.0% of cells were stained with PI following treatment with WW, MM and II, respectively. The stronger membrane-permeabilising capacity of these peptide analogues could be attributed to their higher hydrophobic and α-helical character as compared to LK and PP. Additionally, we found that helicity was more closely correlated to PI uptake as compared to hydrophobicity (Figure 5.5c). This suggests that the folding of the synthetic peptides into amphipathic structures was necessary for the penetration of peptides into the hydrophobic core and subsequent disruption of the lipid bilayer in bacterial cell membranes.
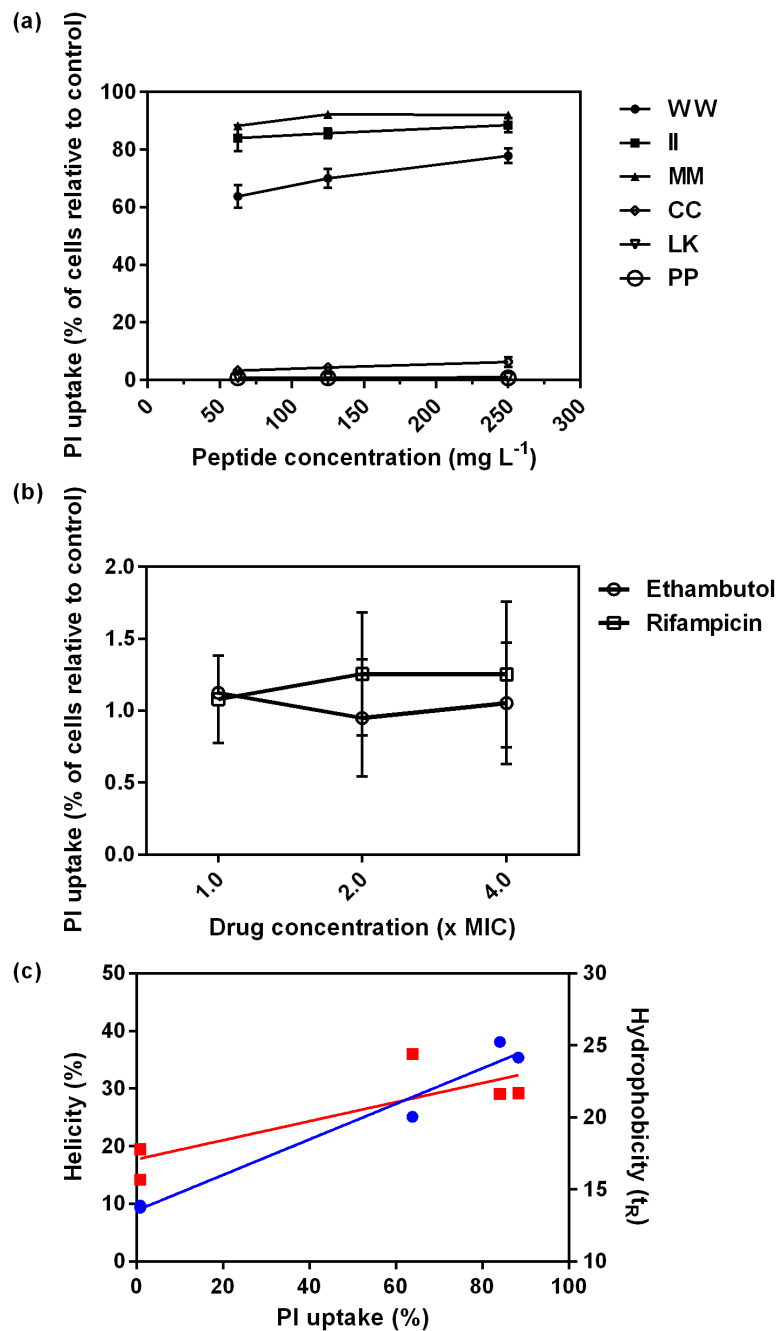
Figure 5.5. Flow cytometric analysis of the mycobacterial cell membrane-permeabilising properties of (a) synthetic α-helical peptides (b) first-line drugs ethambutol and rifampicin. WW, MM and II induced significant membrane damage as shown by the greater uptake of PI into bacterial cells as compared to CC, PP and LK. Negligible PI uptake into bacterial cells after treatment with ethambutol and rifampicin confirmed the absence of rapid membrane-targeted mechanism of action. MIC of ethambutol and rifampicin was 0.5 and 3.90 mg L^{-1} respectively. Data expressed as mean ± S.D for three independent experiments. (c) Correlation of PI uptake and peptide hydrophobicity (■) or helicity (●) with R^2 values of 0.6945 and 0.9683 respectively. CC was excluded from the analysis due to the formation of dimers.

As for CC, only 6% of cells were stained with PI even up to concentrations of 250 mg L^{-1}. A plausible explanation for this observation could be the dimerisation/oligomerisation of CC monomers, driven not by self-association, but by the oxidation of reactive sulfhydryl groups present in Cys residues. MALDI-TOF MS analysis covering up to 10,000 Da confirmed the formation of dimers as a distinct peak was observed at m/z 2374.78 (Figure 5.6), however no oligomer formation was observed. It is likely that these CC dimers are prevented from readily penetrating the mycobacterial cell wall to reach the target cytoplasmic membrane, thus reducing its antimicrobial efficacy.
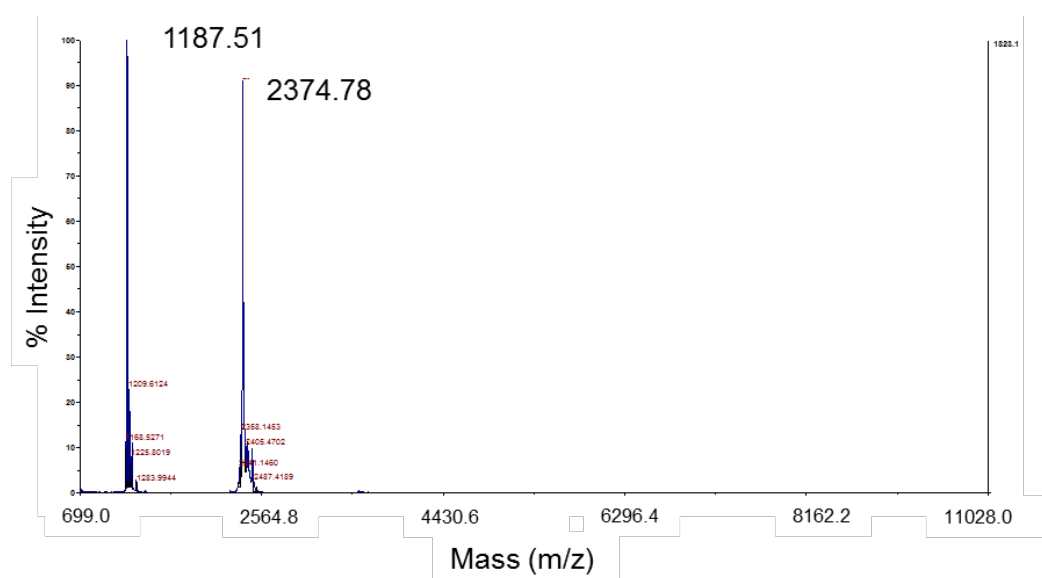
Figure 5.6. MADLI-TOF mass spectra of CC displaying a distinct peak at m/z 2374.78, indicating possible dimerisation of CC monomers due to the presence of reactive sulfhydryl groups.

5.2.7. Synergistic antimicrobial interactions

Given that combinatorial drug regimens are the cornerstone of successful anti-tubercular chemotherapy, the potential for synergistic interactions between the peptides and rifampicin was assessed by the chequerboard assay. As shown in Table 5.2, none of the six synthetic peptides demonstrated antagonistic

activity when treated in combination with rifampicin. The three most effective peptides WW, MM and II exhibited synergism with a FICI of 0.5 against *M. smegmatis* while LK and PP both displayed an additive effect with rifampicin (FICI of 0.75). The combination of CC and rifampicin was interpreted as indifferent with a FICI value greater than 1. The mechanism behind this observed synergism could be attributed to the membrane-permeabilising activity of peptides that compromises membrane integrity. This in turn allows for the increased uptake of rifampicin into the cells and enhances its accessibility to intracellular targets [145, 146]. As such, peptides with superior membrane-disrupting properties would be expected to better facilitate the cytoplasmic entry of rifampicin and consequently demonstrate stronger synergistic interactions. The flow cytometric analysis revealed that LK and PP possessed poor membrane-permeabilising activity (Figure 5.5a), which lends support as to why they were additive with rifampicin while WW, MM and II, synergistic. Due to their lower hydrophobic and α-helical propensity, LK and PP possessed weaker membrane disrupting properties and hence, a higher concentration of these two peptides was required to inhibit bacterial growth as compared to WW, MM and II (62.5 and 125 versus 15.6 mg L^{-1}) when co-administered with the same amount rifampicin (0.98 mg L^{-1}).

5.2.8. Antimicrobial mechanisms

The ability of the peptides to perturb the phospholipid bilayer was investigated by determining the dye leakage from calcein-loaded LUVs composed of PE/PG lipids (4:1). As shown in Figure 5.7, II induced calcein release from the bacterial membrane-mimicking vesicles in a concentration- and time-

dependent manner. As compared to LK, ≥ 4 fold increment in dye leakage was observed for II at all concentrations tested. The more hydrophobic and helical nature of II, in comparison to LK, is likely responsible for its stronger membrane-permeabilising properties. This in turn translated into improved anti-mycobacterial efficiency, evident from the lower MIC and FICI values seen for II (Table 5.2). These results are supported by previous findings that compounds inherently more injurious to membranes, as ascertained by dye leakage assays, also tend to possess enhanced antimicrobial activities [173].
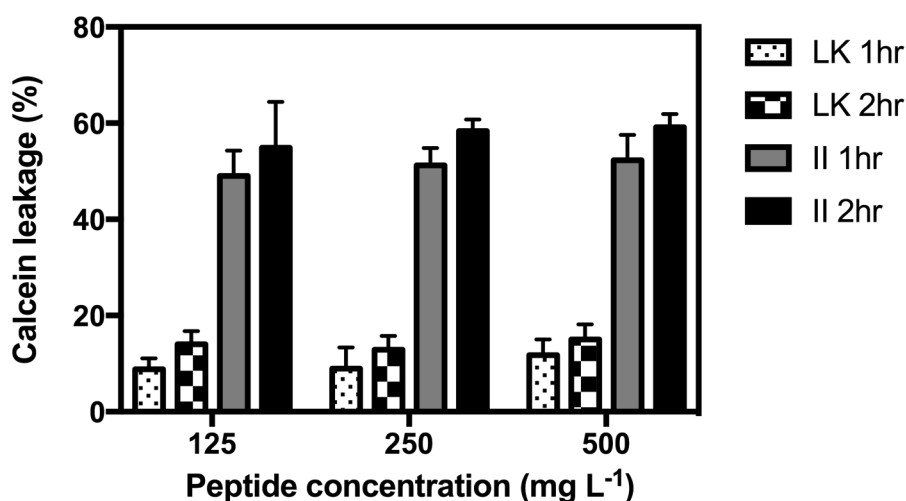
Figure 5.7. Concentration- and time-dependent dye leakage from PE/PG vesicles following antimicrobial peptide treatment. II induced greater leakage as compared to LK, representative of its superior membrane-disrupting properties. Data are expressed as mean ± S.D. for two independent experiments.

Based on the MIC, FICI, and SI values, and cytotoxicity profiles of the synthetic peptide analogues, II possessed the greatest potential for practical applications and hence, was selected for further evaluation of its antimicrobial mechanisms of action against *M. smegmatis*. The surface morphology of *M. smegmatis* was visualised by scanning electron microscopy following incubation with II at 4x MIC for 2 h, and compared to controls treated with

PBS. The untreated bacterial cells had regular, smooth surfaces and remained visibly intact without any extracellular debris (Figures 5.8a and b). Cells treated with II however, had suffered significant structural changes. Compared to the control, cells exposed to II possessed extensively rough, corrugated surfaces covered with irregular debris (Figures 5.8c and d). The significant cell surface damage induced by lethal doses of II provides evidence of the membrane-targeted mechanism of action of this peptide.
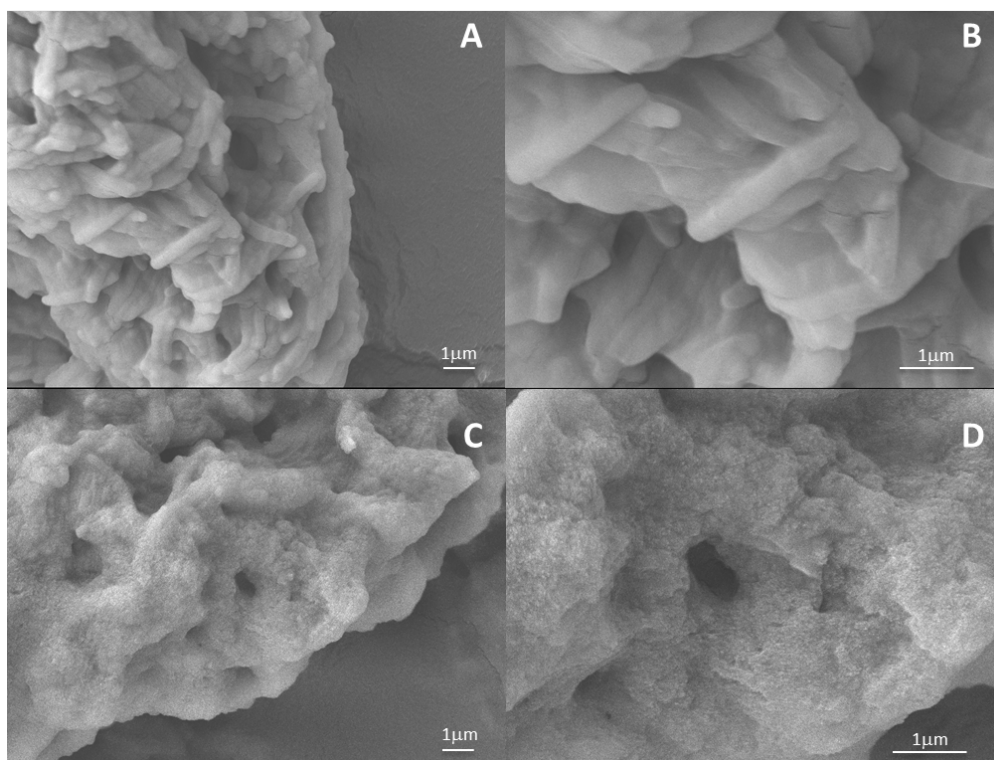
Figure 5.8. SEM micrographs of *M. smegmatis* treated with PBS for 2 h, imaged at magnifications of (a) 7500× and (b) 18000×. Cells were incubated with II at 4x MIC for 2 h and similarly image at magnifications of (c) 7500× and (d) 18000×. Untreated cells presented with smooth surfaces while peptide treatment induced damage to the cell surface.

This proposed mechanism was further investigated by examining the ability of II to depolarise the cytoplasmic membrane of *M. smegmatis* using the membrane potential sensitive dye diS-C$_3$-5. As diS-C$_3$-5 partitions into the cytoplasmic membrane, its fluorescence is self-quenched due to the polarised

membrane surface. Subsequent exposure to pore-forming or membrane-disrupting peptides will dissipate the membrane potential, resulting in the release of diS-C_3-5 into the medium [174]. Fluorescence recovery is then measured by spectrofluorometry and is indicative of the extent of membrane potential reduction. As seen in Figure 5.9, there was a rapid, concentration-dependent surge in fluorescence intensity upon the addition of II to *M. smegmatis*. Cells exposed to II at 4x and 8x MIC produced an instantaneous increase in fluorescence signals while those treated with II at 1x MIC showed gradual dissipation of membrane potential instead.
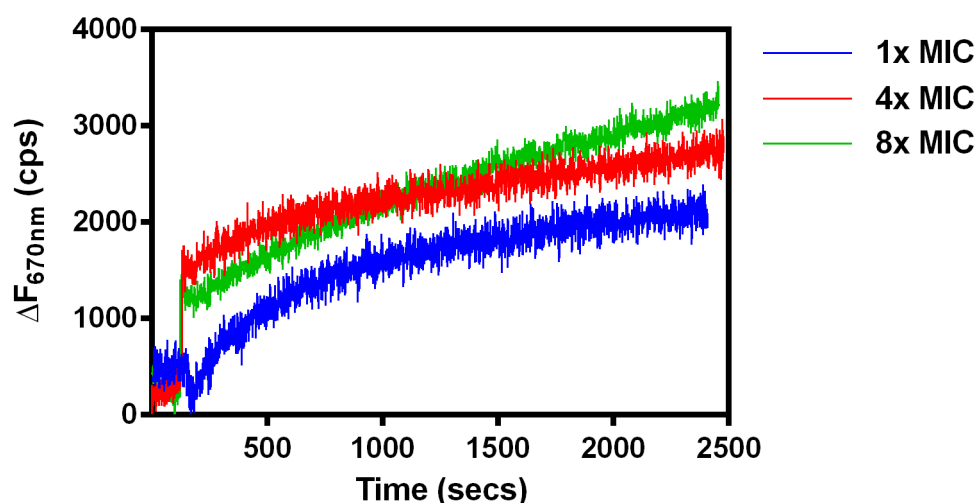
Figure 5.9. Dissipation of cytoplasmic membrane potential following treatment of *M. smegmatis* with II at 1x, 4x and 8x MIC. Membrane depolarisation, monitored by fluorescence recovery of diS-C_3-5, was immediate at 4x and 8x MIC.

Membrane destruction leading to loss of barrier function would result in the depletion of intracellular stores of critical components. As such, extracellular ATP levels following exposure of *M. smegmatis* to supra and sub-inhibitory concentrations of II were assessed and the findings are summarised in Figure 5.10. The peptide induced concentration-dependent release of ATP from

bacterial cells after 2 h, with no detectable ATP at concentrations below 15.6 mg L^{-1}. At 4x and 8x MIC, the amount of ATP released was 106 and 132 nM respectively, an increase of approximately three to fourfold as compared to ATP concentrations at MIC (33 nM).
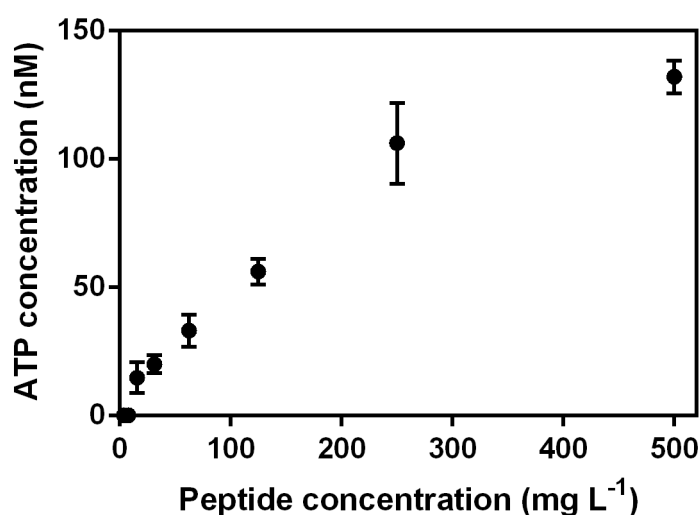
Figure 5.10. Extracellular ATP release in a concentration-dependent manner after exposure of *M. smegmatis* to II for 2 h. Peptide-induced membrane damage is accompanied by leakage of intracellular content due to compromised membrane integrity. Data expressed as mean ± S.E.M. for three independent experiments.

To determine if the bactericidal activity of the peptides is associated with ATP release and membrane depolarisation, killing efficiency assays were performed for II at the relevant concentrations. As shown in Figure 5.11, 100% reduction in bacterial load was observed at 2x, 4x and 8x MIC while in contrast, II was only bacteriostatic at its MIC, with < 1 log reduction in final CFU counts as compared to the initial inoculum. These findings suggest that the bactericidal activity of II is possibly mediated through disruption of the mycobacterial cytoplasmic membrane, with high levels of ATP release and dissipation of membrane potential, in a concentration-dependent manner.
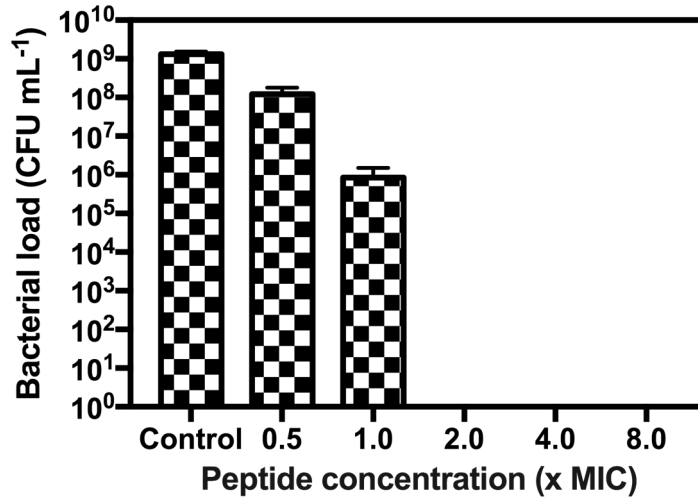
Figure 5.11. Plot of viable CFU after treatment of *M. smegmatis* with various concentrations of II. 100% reduction in bacterial burden was observed at 2x, 4x and 8x MIC, suggestive of a bactericidal mechanism of action at these concentrations. Data expressed as mean ± S.E.M. for three independent experiments.

Taken together, our results highlight that the bacterial membrane is the main target site of the synthetic cationic α-helical peptide, II. Flow cytometric analysis revealed that the formation of helical structures is crucial for rapid pore or channel formation, in agreement with previously published works [159]. Though active against mycobacteria, LK and PP did not induce significant membrane permeabilisation, suggesting that they may either act *via* non-membrane lytic mechanisms or that the duration of drug exposure was insufficient to cause appreciable membrane damage. WW, MM and II, however, rapidly permeabilised the mycobacterial membrane, enabling the free diffusion of PI into the cytoplasm. Concomitantly, peptides induced immediate dissipation of the cytoplasmic membrane potential, accompanied by leakage of intracellular components as quantified by the ATP bioluminescence assay, eventually leading to cell death. Furthermore, SEM analysis revealed that the peptides possessed strong membrane-disrupting

properties while calcein leakage from LUVs was reflective of their ability to permeabilise the lipid bilayer, resulting in the loss of intracellular contents.

5.3. Conclusions

In this study, six synthetic peptide analogues with varying hydrophobicity and helical propensities were assessed for their potency against *M. smegmatis,* and toxicities towards eukaryotic cells. Hydrophobic modifications produced three analogues, WW, MM and II with improved anti-mycobacterial activity. Increasing peptide hydrophobicity/helicity induced greater membrane perturbation as shown by the significant PI uptake as compared to controls during flow cytometry assays. Furthermore, the three most hydrophobic peptides were found to interact synergistically with rifampicin, potentially mediated by enhanced intracellular access of the drug. Amongst the six, II (the Ile substituted peptide) was selected for elucidation of anti-mycobacterial mechanisms, given its superior selectivity index and safer toxicity profile against macrophage cells. This peptide was shown to primarily target the plasma membrane, acting rapidly in a concentration-dependent manner, and exhibiting bactericidal activity at $\geq$ 2x MIC. II induced instantaneous membrane depolarisation, damaged structural integrity of the membrane and caused the leakage of cellular contents within 2 h. These findings serve to deepen our understanding of the modulating effect of hydrophobicity/helicity on the anti-mycobacterial mechanisms of action and demonstrate the applicability of strategies employed here for the rational design of AMPs with the aim of improving cell selectivity and synergistic interactions when co-

administered with first line antibiotics in the fight against drug-resistant tuberculosis.

CHAPTER 6: Unnatural amino acid analogues of membrane-active helical peptides with enhanced anti-mycobacterial selectivity and improved stability

6.1. Introduction

Various virulence strategies have been implicated in the persistence and survival of microbes during chronic infections, including the secretion of proteinases to facilitate tissue invasion, evade host defences and modulate host immune responses [175]. Natural HDPs are essential components of the innate immune response, and contribute towards the first line of defence against invading pathogens [176]. Therefore, unsurprisingly, the inactivation of antimicrobial proteins and peptides by microbial proteases could serve as crucial means of overcoming host defence mechanisms. This is supported by evidence that the human cathelicidin LL-37 was rapidly degraded by proteinases of *P. aeruginosa*, *E. faecalis*, *Proteus mirabilis* and *Streptococcus pyogenes*, which resulted in loss of antibacterial activity [177]. LL-37 was also found to be inactivated by staphylococcal aureolysin, leading to diminished anti-staphylococcal activity [178]. Thus, the production of extracellular proteases can contribute towards bacterial resistance against HDPs.

AMPs have gained prominence over the past few decades as a promising class of therapeutics due to their potent broad activity spectrum encompassing both drug-susceptible and drug-resistant pathogens [24]. However, the transition of AMPs from bench to bedside has largely been hindered by their susceptibility to enzymes in biological fluids and degradation by bacterial proteases, resulting in short half-lives and loss of antimicrobial properties [26]. Several

strategies have been employed to enhance AMP stability including the incorporation of unnatural amino acids, N- and/or C-terminal modifications, cyclisation, inclusion of non-peptidic backbones (peptidomimetics), and multimerisation of AMP monomers to form dimers, oligomers and dendrimers [26]. Previously, D-enantiomers were studied to determine the influence of peptide chirality on function, and the importance of stereospecific interactions with enzymes, receptors or lipids in membranes [179, 180]. While both L- and D-enantiomers of peptides emerged equally active, suggesting a lack of specific peptide-receptor interactions, the latter were more resistant to trypsin degradation [181]. This in turn translated into longer half-lives *in vivo*, reinforcing their potential as therapeutic candidates.

Increasing evidence suggests that incorporation of D-amino acids not only confers protection against proteolysis by trypsin, but also enhances stability against bacterial proteases, thus rendering peptides more active. While the all L-amino acid analogue of M33 underwent proteolysis by staphylococcal aureolysin within 1 h, the D-amino acid analogue remained unchanged even after 24 h of treatment, which in turn translated into superior *in vitro* and *in vivo* activity for the D-isomer against *S. aureus* [182]. Similarly, specific D-amino acid substitutions were also found to enhance stability towards *P. aeruginosa* elastase, staphylococcal V8 protease and aureolysin [183]. Recently, the D-enantiomer of a lactoferricin-derived peptide demonstrated better inhibitory activity against *M. avium* in comparison to the L form, likely due to higher resistance to proteases [184].

M. tuberculosis is also known to secrete enzymes such as proteases, lipases, esterases, and dehydrogenases, which contribute towards its pathogenicity and persistence in the host [185]. As such, the above mentioned strategy of incorporating unnatural amino acids into peptide sequences could potentially be exploited to develop more selective anti-mycobacterial peptides. One study in particular demonstrated that D-enantiomeric forms of AMPs, including the all D-analogue of LL-37, were found to inhibit growth of H37Rv to a greater extent than the L-enantiomers [158]. However, there are limited reports systematically evaluating the impact of various stability-enhancing modifications on the anti-mycobacterial activity of synthetic AMPs.

In Chapter 5, N- and C-terminal capping of short amphipathic α-helical anti-mycobacterial peptides evaluated in Chapter 4, with hydrophobic residues revealed the importance of both hydrophobicity and helicity on the anti-mycobacterial activity, with I(LLKK)$_2$I emerging as the most selective peptide. These synthetic α-helical peptides primarily targeted the mycobacterial membrane, inducing rapid membrane permeabilisation and depolarisation, resulting in leakage of intracellular contents. In this chapter, the effect of various unnatural amino acid substitutions on the anti-mycobacterial properties and stability of the peptide, I(LLKK)$_2$I, were investigated. Peptide secondary structures were assessed by CD spectroscopy, while cytotoxicity was evaluated against human RBCs and the murine macrophage RAW 264.7 cell line. Antimicrobial activities were studied against a panel of six mycobacterial strains using the broth microdilution method. The stability of the modified peptides was also evaluated against the

serine protease trypsin. Since *M. tuberculosis* is a major intracellular pathogen, the ability of peptides to activate macrophages and eliminate intracellular mycobacteria was also examined. Finally, the *in vitro* anti-mycobacterial mechanisms were studied using CLSM and time-lapse fluorescence microscopy.

6.2. Results and discussion

6.2.1. Peptide design and characterisation

In this study, systematic substitutions with unnatural or D-amino acids were performed in an attempt to design synthetic analogues with improved stability and selectivity indices. The Ile substituted analogue, I(LLKK)$_2$I or II, which emerged as one of the most selective peptides against mycobacteria in Chapter 5, served as a framework for these structural modifications. To maintain sequence identity and structural integrity of the optimised lead peptide, the two main modifications involved (a) swapping all L-amino acid with D-amino acid residues and (b) substitution of Lys residues with Lys analogues possessing shorter side-chains including ornithine (Orn), 2,4-diaminobutyric acid (Dab) or 2,3-diaminopropionic acid (Dap). The C-terminal of all synthetic analogues was amidated to improve anti-mycobacterial activity by increasing net positive charge [133, 134]. The sequences and abbreviated names of the five synthetic peptides evaluated in this study are listed in Table 6.1. In order to verify that the peptides were successfully synthesised according to the desired specifications, SELDI-TOF MS was performed for molecular weight determination. As shown in Table 6.1, the close agreement between the theoretical and measured molecular weights of the peptides served as confirmation of the fidelity of peptide synthesis.

Table 6.1. Design of α-helical peptides modified with unnatural amino acids and their molecular weights.

AMP	Peptide sequence[a]	Theoretical M_W	Measured M_W[b]	$[\theta]_{222}$[c]	Relative helicity[d]
II	I(LLKK)$_2$I-NH$_2$	1208.67	1209	11290	1.00
II-D	i(llkk)$_2$i-NH$_2$	1208.67	1209	10033	0.89
II-Orn	I(LL-Orn-Orn)$_2$I-NH$_2$	1152.56	1153	11432	1.01
II-Dab	I(LL-Dab-Dab)$_2$I-NH$_2$	1096.70	1097	11081	0.98
II-Dap	I(LL-Dap-Dap)$_2$I-NH$_2$	1040.35	1041	11765	1.04

[a] D-amino acids are represented by lower case letters. Ornithine, 2,4-diaminobutyric acid and 2,3-diaminopropionic acid are abbreviated as Orn, Dab and Dap respectively.
[b] M_w determined by SELDI-TOF MS.
[c] The mean residue ellipticity values at 222 nm (θ_{222}) were measured in 25 mM SDS solution by CD spectroscopy.
[d] The helical content of modified peptides relative to the mean residue ellipticity values at 222 nm of II.

6.2.2. CD spectroscopic study

The influence of unnatural or D-amino acid substitutions on the secondary conformation of the synthetic peptides was investigated in a membrane-like environment consisting of 25 mM SDS micelle solution, and studied using CD spectroscopy. The CD spectra of the synthetic peptides are summarised in Figure 6.1. The presence of the characteristic absorption bands at ~208 and 222 nm suggests that all five synthetic peptides adopted α-helical structures in 25 mM SDS. The replacement of Lys residues with Orn, Dab or Dap, did not compromise the helical structure of peptides, evident from the comparable relative helicities and mean residue ellipticity values at 222 nm (θ_{222}) as shown in Table 6.1. As expected, II-D exhibited a CD spectrum of opposite sign to that of II, though not an exact mirror image. II-D recorded a lower absolute θ_{222} value than II (10033 versus 11290), indicative of a slight reduction in α-helical conformation. Since, D-allo-Ile was utilised during peptide synthesis, the observed differences in CD ellipticity at 222 nm could be attributed to II and II-D being diastereomers, rather than enantiomers of

each other [186].
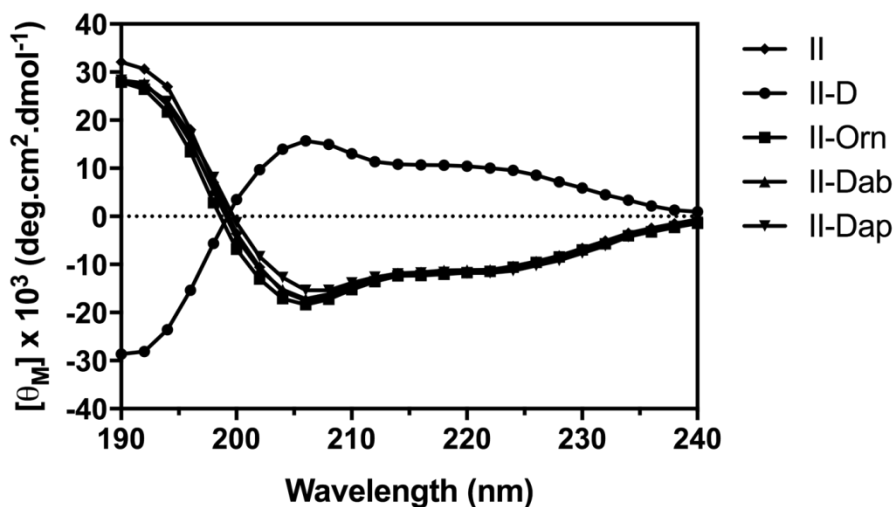
Figure 6.1. CD spectra demonstrating α-helical secondary conformations of II and its synthetic analogues with unnatural amino acid substitutions in 25 mM SDS micelle solution. Data are expressed as the mean of three runs per peptide.

6.2.3. In vitro anti-mycobacterial activity

The antimicrobial activities of the synthetic helical peptides were evaluated by the broth microdilution method against a panel of six mycobacterial strains and the results are summarised in Table 6.2. Overall, structural modifications with unnatural or D-amino acids were effective in producing analogues with improved anti-mycobacterial activities. A two to fourfold reduction in the GM of the MICs was observed for the modified peptides as compared to II. Importantly, three of the synthetic peptides displayed a fourfold reduction in MIC in comparison to II against the MDR clinical isolate CSU87. The replacement of Lys with Orn proved least effective, with II-Orn demonstrating similar activity as II against 50% of the mycobacterial strains tested. This analogue was more active against only two of the six strains, while replacement of Lys with Dab and Dap resulted in a decrease in MICs against

114

five and four of the six strains, respectively. The all D-amino acid analogue exhibited superior efficacy as compared to II against all six mycobacterial strains, which translated into a fourfold reduction in the GM of its MICs.

Table 6.2. MICs and SIs of helical peptides against various mycobacterial strains including drug-susceptible and MDR clinical isolates of *M. tuberculosis*

AMP	MIC[a] (mg L^{-1})						GM[b] (mg L^{-1})	HC$_{50}$ (mg L^{-1})	SI[c]
	BCG	H37Rv	Mtb 173	Mtb 212	Mtb 411	CSU87			
II	125	500	>500	>500	250	250	397	>1000	5
II-D	31.3	250	125	250	62.5	62.5	99	>1000	20
II-Orn	62.5	>500	>500	500	250	250	354	>1000	6
II-Dab	31.3	>500	500	500	62.5	62.5	177	>1000	11
II-Dap	62.5	>500	> 500	500	62.5	62.5	223	>1000	9
Rifampicin	0.001	0.015	0.008	0.004	0.002	>32	0.004	-	-

[a] MIC results are representative of 2 to 3 independent experiments.
[b] The geometric mean (GM) of the MICs against the 6 mycobacterial strains. A value of 1000 mg L^{-1} was used for GM calculations when no anti-mycobacterial activity at observed at the highest tested concentration of 500 mg L^{-1}.
[c] SI is determined as follows: (HC$_{50}$/GM). When no detectable haemolysis was observed at the highest tested concentration of 1000 mg L^{-1}, a value of 2000 mg L^{-1} was used for SI calculations.

We had previously reported in Chapter 5 that both hydrophobicity and folding of peptides into amphipathic helical structures was crucial for inducing mycobacterial membrane permeability and augmenting anti-mycobacterial activity. Given that II and II-D are diastereomers of each other, their amino acid composition, charge, molecular weight, amphiphilicity and in turn hydrophobicity is expected to be similar. However, the lower relative helicity of 0.89 for II-D (Table 6.1), as compared to II, would be expected to compromise its activity, but the converse was true. The reduced hydrophobicities of II-Orn, II-Dab and II-Dap relative to that of II, also did not translate into reduced activities. This suggests that factors unrelated to the physiochemical properties of the peptides may also be responsible for the observed differences in anti-mycobacterial efficacy of the synthetic peptides. A plausible explanation is that the structural modifications employed in this

study could potentially have enhanced peptide stability to extracellular proteolytic enzymes of *M. tuberculosis*, in turn rendering them more active against the pathogen. *M. tuberculosis* culture filtrates containing proteases were found to diminish the anti-tubercular activity of the L- rather than D-enantiomer of peptides, with the latter demonstrating greater resistance to degradation, evident from the significantly higher recovery as compared to the L-enantiomer (89% versus 26%) after 7 days exposure [158]. These findings suggest that stability-enhancing modifications such as the incorporation of unnatural amino acids may be crucial to developing AMPs with superior efficacies against slowly-replicating bacilli such as *M. tuberculosis*.

6.2.4. Haemolytic activity, cytotoxicity and cell selectivity

The haemolytic activities of the synthetic peptides were evaluated using 4% (v/v) human blood from two healthy adult donors and the results are summarised in Figure 6.2a. Even at the highest tested concentration of 1000 mg L^{-1}, all five peptides displayed minimal haemolysis of approximately 2%. The HC_{50} values, defined as the lowest peptide concentration resulting in 50% haemolysis of RBCs, of all five peptides was found to be >1000 mg L^{-1} (Table 6.2). Similar observations were also made with respect to the cytotoxicity of the peptides against the murine macrophage cell line, RAW 264.7. As highlighted in Figure 6.2b, cell viabilities remained in excess of 80% even at concentrations of 250 mg L^{-1} following 24 h exposure to synthetic peptides. Importantly, none of the modifications produced analogues of II with an inferior toxicity profile against mammalian cells. The SIs highlighted in Table 6.2, defined as the ratio of HC_{50} to GM MIC values, are often utilised to

identify analogues with superior antibacterial selectivity. The D-amino acid analogue of II emerged as the most selective for mycobacterial over mammalian cells, with a SI value of 20. This was fourfold greater than that of II and approximately 1.8 and 2.2 times higher than that of II-Dab and II-Dap, respectively. Since larger SI values are deemed as more desirable, the strategies presented in this study could therefore prove useful in designing more selective AMPs to treat *M. tuberculosis* infections.
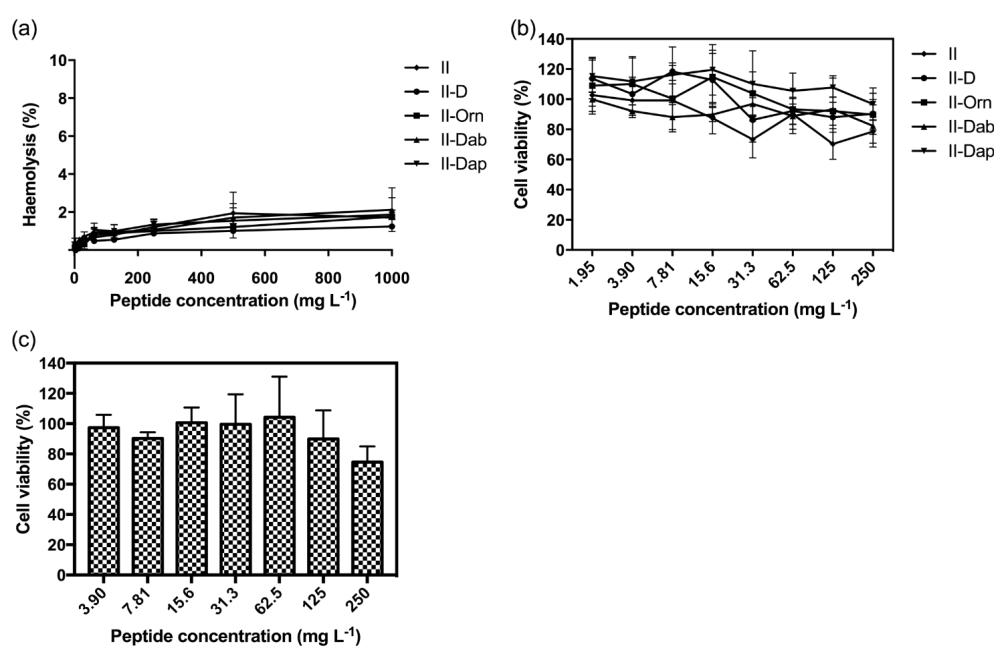
Figure 6.2. Toxicity profiles of synthetic peptides modified with unnatural amino acids against (a) human red blood cells and (b) the mouse macrophage cell line RAW 264.7. (c) Viability of RAW 264.7 cells after 4 days of treatment with II-D. Peptides displayed minimal haemolytic activity and cytotoxicity against mammalian cells at various concentrations tested. Data are expressed as mean ± S.D. for two independent experiments.

6.2.5. Resistance to protease degradation

A major barrier limiting the clinical application of AMPs is their susceptibility to protease degradation in biological fluids [26]. Trypsin specifically cleaves the C-terminal of both Lys and Arg, thus, peptides containing these cationic residues are likely to be rendered inactive. We therefore assessed the stability

of the Lys-rich II and its unnatural amino acid substituted analogues by pre-treating the peptides with trypsin before evaluating their antimicrobial activities against BCG using the standard broth microdilution method. As shown in Figure 6.3, all five peptides inhibited bacterial growth after 7 days when no prior treatment with trypsin was performed. However, following pre-treatment with trypsin, the antimicrobial activity of only II was lost while that of the other four modified peptides was preserved. The modifications to II not only produced analogues with superior mycobacterial selectivity (Table 6.2), but also conferred protection against the serine protease trypsin, enhancing their clinical utility.
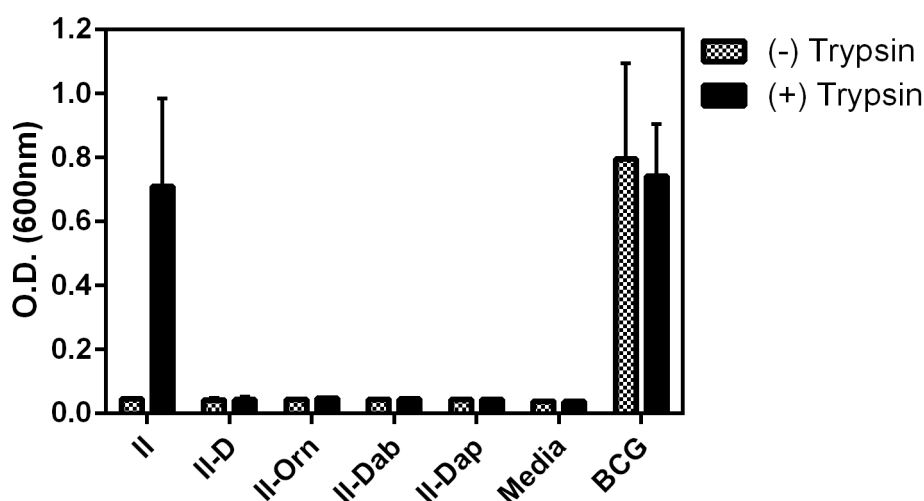
Figure 6.3. Inhibitory activity of synthetic peptides against BCG at concentrations of 4x MIC following 6 h treatment with trypsin at a ratio of 1:100. Only the unmodified peptide, II, did not inhibit bacterial growth after 7 days. Data are expressed as mean ± S.D. for two independent experiments.

6.2.6. In vitro and intracellular killing efficiency

The D-amino acid analogue of II was not only more resistant to enzymatic degradation, but also exhibited the highest SI of all peptides evaluated in this study. Hence, II-D was evaluated for its *in vitro* killing efficiency against laboratory strain H37Rv, the drug-susceptible clinical isolate Mtb 411, and the

MDR clinical isolate CSU87. II-D displayed killing efficiencies of > 90% at the respective MICs for all three strains (Figure 6.4). At 2x the respective MIC values, II-D killing efficiency was > 99% against both H37Rv and CSU87 and > 97% against Mtb 411.
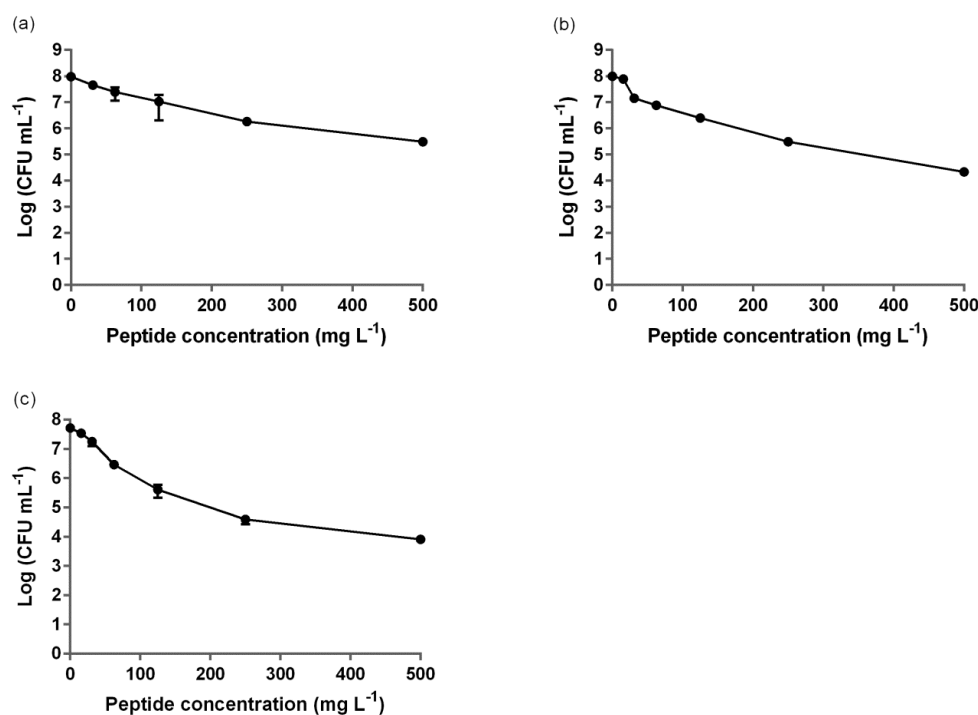
Figure 6.4. Killing efficiencies of antimicrobial peptide II-D against (a) H37Rv, (b) Mtb 411 and (c) CSU87 following treatment for 7 days at various concentrations. Data are expressed as mean ± S.D. for two independent experiments.

The intracellular activity of II-D was subsequently evaluated against both drug-susceptible and MDR clinical isolates of *M. tuberculosis* during macrophage infection, at concentrations corresponding to 0.5x, 1x, 2x and 4x MIC. The first-line anti-tubercular drug, rifampicin, and second-line fluoroquinolone, moxifloxacin, served as controls for Mtb 411 and CSU87, respectively. As shown in Figures 6.5a and b, significant reductions in intracellular Mtb 411 counts were observed in comparison to untreated controls following 4-day treatment with II-D ($p < 0.0001$) and rifampicin ($p <$

0.001) at the highest concentrations tested. Both II-D and rifampicin demonstrated concentration-dependent killing of Mtb 411, although peptide treatment was more effective in rapidly eliminating the intracellular pathogen. At their respective MICs, rifampicin and II-D reduced bacillary loads within 3 days by 36% and 84%, respectively. Furthermore, exposure to II-D at 250 mg L^{-1} (4x MIC) resulted in approximately 1 log reduction of intracellular bacterial burden by days 3 and 4 (Figure 6.5a). This effect was less pronounced with rifampicin as bacterial counts decreased by 66% and 70% on days 3 and 4, respectively, even up to concentrations corresponding to 8x MIC (0.016 mg L^{-1}). Similarly, significant reductions in intracellular CSU87 counts were observed after 4 days in comparison to untreated controls for both II-D ($p < 0.001$) and moxifloxacin ($p < 0.0001$) at the highest concentrations tested. II-D brought about a 62% decrease in bacterial load within 4 days, even at sub-MIC of 31.3 mg L^{-1} (Figure 6.5c). II-D was also more effective than moxifloxacin in clearing intracellular CSU87 at equivalent concentrations of 1x, 2x and 4x MIC (Figure 6.5d). Given that II-D demonstrated minimal toxicity towards RAW 264.7 macrophage cells after 4 days, with a cell viability of 75% even up to concentrations of 250 mg L^{-1} (Figure 6.2c), the observed reductions in intracellular mycobacterial load were a direct consequence of peptide treatment rather than cytotoxic effects on macrophages. Overall, these findings reinforce the applicability of AMPs for the treatment of intracellular pathogens such as *M. tuberculosis*.
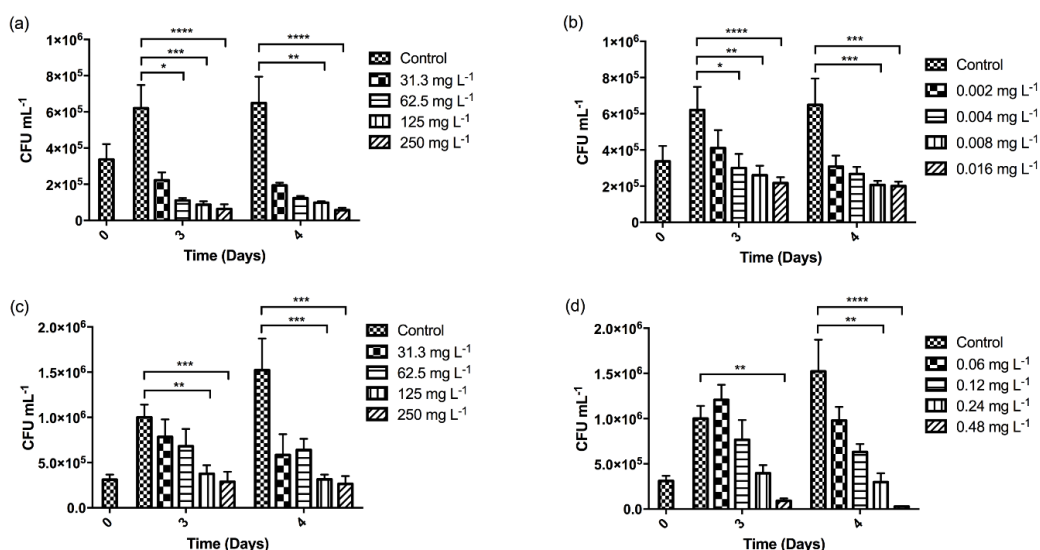
Figure 6.5. Intracellular killing of the drug-susceptible clinical isolate Mtb 411 by (a) antimicrobial peptide II-D and (b) rifampicin, and the MDR clinical isolate CSU87 by (c) antimicrobial peptide II-D and (d) moxifloxacin. Data expressed as mean ± S.D. and are representative of two independent experiments. (* $p \leq 0.05$, ** $p \leq 0.01$, *** $p \leq 0.001$, **** $p \leq 0.0001$).

6.2.7. In vitro and intracellular antimicrobial mechanisms

The bactericidal activity of AMPs is largely mediated by non-specific membrane-lytic mechanisms, which induce pore formation and/or membrane destruction, leading to membrane depolarisation and outflow of cytoplasmic contents [22]. In this study, the antimicrobial mechanisms of II-D were investigated against BCG using microfluidic live-cell imaging by employing the CellASIC™ ONIX Microfluidic Platform. Bacterial cells were treated with peptides at 4x and 8x MIC, in the presence of the DNA intercalating dye PI for up to 4 h. Exposure of BCG to II-D at 4x and 8x MIC resulted in fluorescence staining of bacterial cells within 10 min. The uptake of PI was concentration-dependent, with ~50% of bacterial cells exhibiting fluorescence after 210 min at 8x MIC of II-D (Figure 6.6b) while a much lower proportion of cells were stained over the same time period at 4x MIC of II-D (Figure 6.6a). Since we do not have facilities for live-cell imaging with Hazard Group

3 pathogens such as *M. tuberculosis*, the ability of II-D to compromise the membrane integrity of H37Rv and CSU87 was evaluated using flow cytometry of fixed cells. As shown in Figure 6.7, exposure of H37Rv to rifampicin, and CSU87 to moxifloxacin, for up to 3 h did not induce any appreciable uptake of the fluorescent probe. Treatment with II-D at 4x MIC however, resulted in the appearance of a new cell population, with PI-positive cells accounting for approximately 21% and 40% of the entire H37Rv and CSU87 cell populations, respectively (Figures 6.7c and f). Given the membrane-impermeant nature of PI, the dye is generally excluded from viable cells with intact bacterial membranes. Hence, the observed fluorescence provides evidence of the membrane-permeabilising activity of II-D, resulting in the loss of membrane integrity which in turn facilitates intracellular diffusion and binding of PI to DNA. These findings also reiterate the rapid membrane disruption induced by peptides in comparison to first-line anti-tubercular drugs. Furthermore, II-D demonstrated bactericidal activity at 4x and 8x MIC against BCG with a > 2 log reduction in RLU readings after 7 day treatment as compared to controls (Figure 6.9a). Taken together, these findings suggest that the bactericidal activity of II-D may partly be mediated by disrupting the structural integrity of the mycobacterial membrane.

(a)

	Phase	Fluorescence	Merge
0 min			
90 min			
150 min			
210 min			

Figure 6.6. Time-lapse fluorescence microscopy images of BCG following treatment with antimicrobial peptide II-D at (a) 4x MIC and (b) 8x MIC in the presence of the membrane-impermeable dye, PI. Peptide-mediated membrane disruption promoted uptake of PI into bacterial cells. Scale bar = 10 μm.

Figure 6.7. Flow cytometric analysis of the proportion of bacterial cells positively stained by the membrane-impermeable dye PI after 3 h exposure to different antimicrobials. Controls consisted of (a) H37Rv and (d) CSU87 treated with media alone. H37Rv was treated with (b) rifampicin and (c) II-D, while CSU87 with (e) moxifloxacin and (f) II-D at 4x MIC concentrations. II-D induced a significant shift in the percentage of H37Rv and CSU87 taking up PI, suggestive of membrane permeabilising mechanisms of action. The levels of PI uptake for negative controls, rifampicin and moxifloxacin, were similar to that of media. Data are representative of three independent experiments.

Increasingly, the ability of AMPs to modulate the host innate immunity has been explored as an alternative strategy for effective infection control [176]. To evaluate the capacity of II-D to modulate host immunity by activating macrophages, unstimulated RAW 264.7 cells were treated with up to 250 mg L^{-1} of the peptide for 24 h and pro-inflammatory responses were quantified by analysing NO and TNF-α production relative to that of LPS-stimulated macrophages. As shown in Figure 6.8, II-D neither induced NO nor TNF-α production, suggestive of its inability to effect macrophage activation. Thus, the observed intracellular anti-mycobacterial activity of II-D is likely due to direct bactericidal mechanisms rather than the induction of secondary pro-inflammatory responses.

Figure 6.8. The ability of antimicrobial peptide II-D to promote (a) NO and (b) TNF-α production in unstimulated RAW 264.7 mouse macrophage cells following 24 h treatment. II-D did not induce NO or TNF-α when compared to positive controls consisting of cells stimulated with 100 ng mL^{-1} LPS. Data are expressed as mean ± S.D. for two independent experiments.
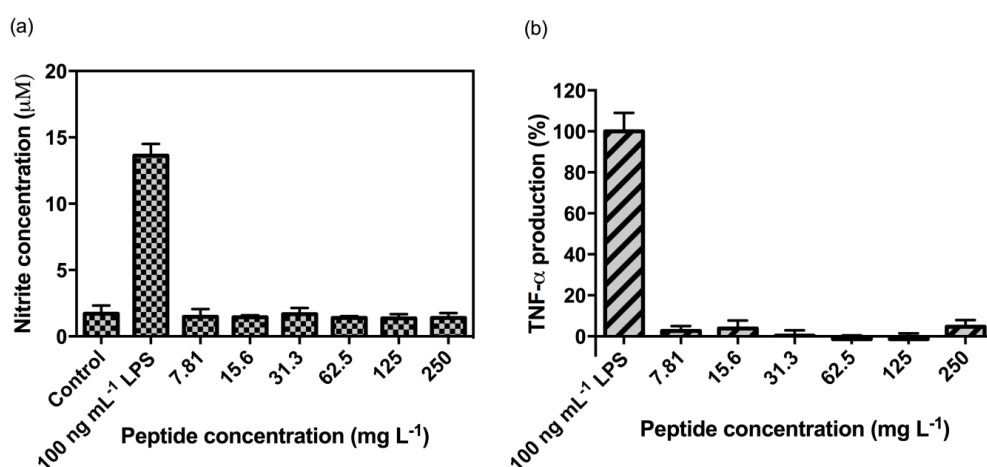
6.2.8. Cellular localisation of II-D

To ascertain the site of action of II-D, BCG was exposed to FITC-labelled II-D for 2 h using the CellASIC™ ONIX Microfluidic Platform and its localisation was visualised by fluorescence microscopy. FITC-II-D was tested at 500 mg L^{-1} as the killing efficacy against BCG was similar to that of II-D at 2x MIC (Figures 6.9a and b).
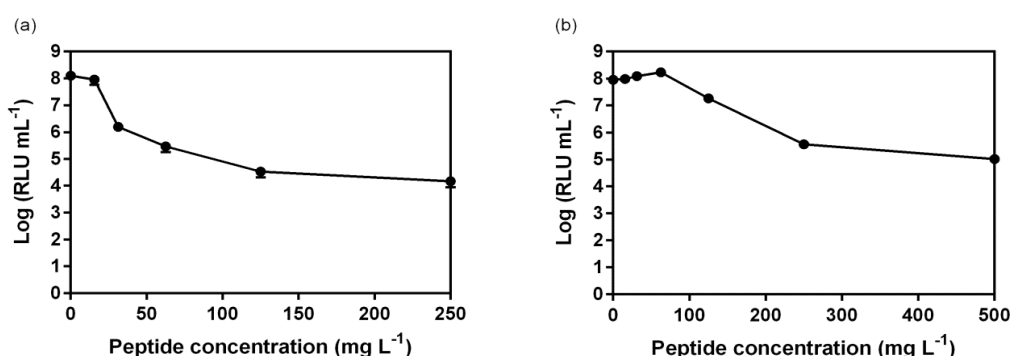
Figure 6.9. Killing efficiencies of antimicrobial peptides (a) II-D and (b) FITC-II-D against BCG following treatment for 7 days at various concentrations. II-D had killing efficiencies of > 98% and > 99% at 31.3 and 62.5 mg L^{-1}, respectively, while FITC-II-D had killing efficiencies of > 99% at both 250 and 500 mg L^{-1}. Data are expressed as mean ± S.E.M. for three independent experiments.

As shown in Figure 5.10a, treatment of BCG with 500 mg L^{-1} of FITC-II-D resulted in peptide accumulation within the cytoplasm as evidenced by the bright green fluorescence signal. This was confirmed by CLSM studies with mCherry-expressing BCG where the co-localisation of FITC-II-D with the cytosolic fluorescence protein mCherry was observed (Figure 6.10b). Bacterial cells unaffected by FITC-II-D demonstrated strong red fluorescence signal across the entire cell length without any detectable green fluorescence peptide signal (Figures 6.10b, 6.11b and c), while peptide penetration into bacterial cells resulted in a stronger green than red intracellular fluorescence intensity profile along the cell length (Figure 6.11a). This observed reduction

127

in red fluorescence mCherry signal in cells which internalised FITC-II-D was likely due to peptide-mediated membrane permeabilisation resulting in leakage of cytosolic contents.
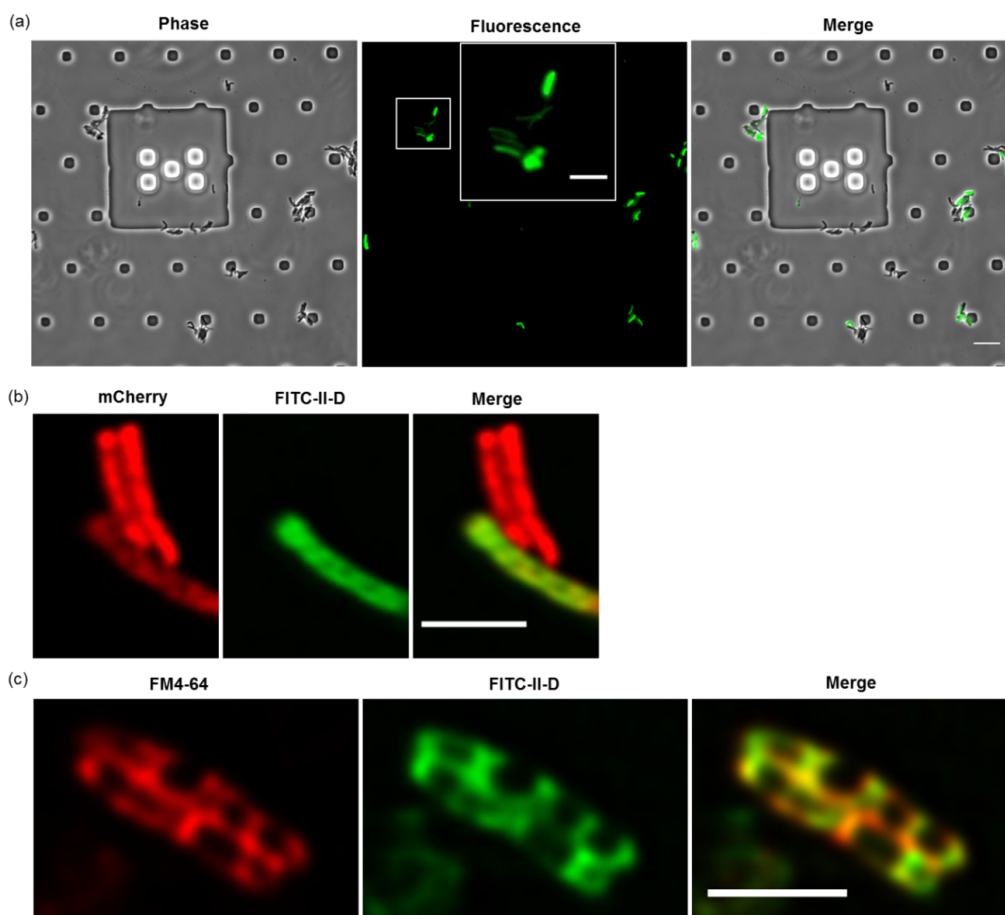
Figure 6.10. (a) Fluorescence microscopy images of BCG treated with 500 mg L^{-1} FITC-labelled II-D for 2 h using the CellASIC ONIX Microfluidic Platform. Scale bar = 10 μm (inset scale bar = 5μm). Confocal microscopy images following incubation of 500 mg L^{-1} FITC-labelled II-D for 2 h with (b) BCG-mCherry and (c) BCG in the presence of 2 μg mL^{-1} membrane dye FM4-64. Scale bar = 2 μm.

Next, co-labelling studies with the membrane-binding dye FM4-64 in BCG revealed that the red FM4-64 signal was predominantly located on the bacterial cell surface, and showed the same pattern of staining as the green fluorescence of FITC-II-D (Figure 6.10c). Moreover, the fluorescence intensity profile of FM4-64 across the cell width matched that of FITC-II-D

(Figures 6.11d and e). Previous studies have reported that the cell-penetrating peptide, buforin II, accumulates in cytoplasm without inducing the influx of PI into bacterial cells, suggestive of a non-membrane permeabilising mode of action [187]. Following internalisation, buforin II promotes cell death by inhibiting cellular functions through binding strongly to DNA and RNA [188]. In contrast, the membrane-permeabilising α-helical peptide magainin II, binds to the bacterial membrane, inducing pore formation and promoting the influx of PI [187]. In this study, fluorescence and CLSM analysis revealed that II-D permeates the mycobacterial cell membrane and accumulated in the cytoplasm (Figure 6.10). Additionally, membrane integrity studies with PI provided evidence of the membrane-lytic mechanisms of action (Figures 6.6 and 6.7). Taken together, the killing mechanisms of II-D could potentially be attributed to both pore-formation and targeting of intracellular components. Recently, non-membrane lytic, cell-penetrating synthetic AMPs (SAMPs) were reported to selectively kill *M. smegmatis* by binding bacterial DNA and consequently inhibiting DNA-dependent processes including replication and transcription [189]. Hence, the ability of the membrane-active peptide II-D to interact with intracellular targets such as bacterial DNA and RNA warrants further investigation.
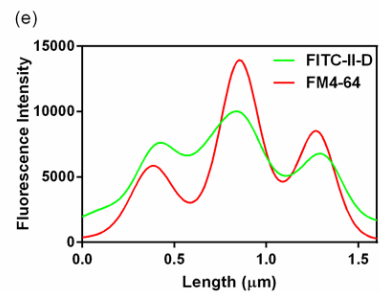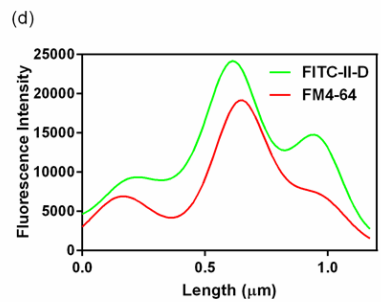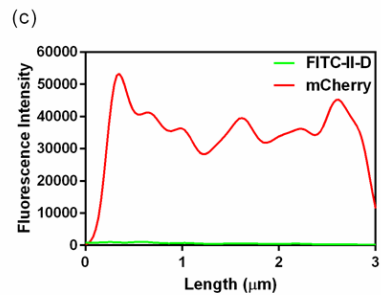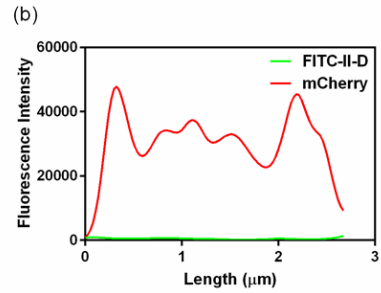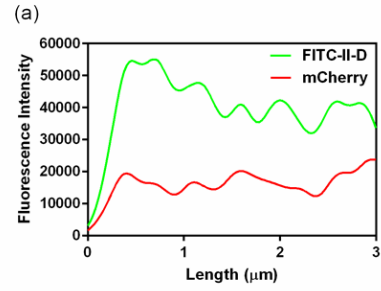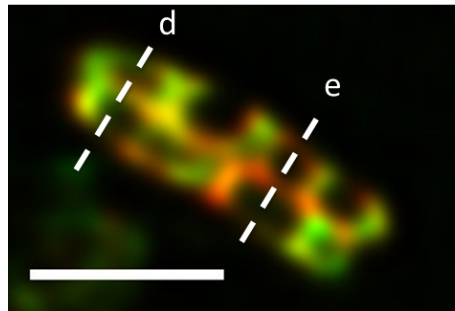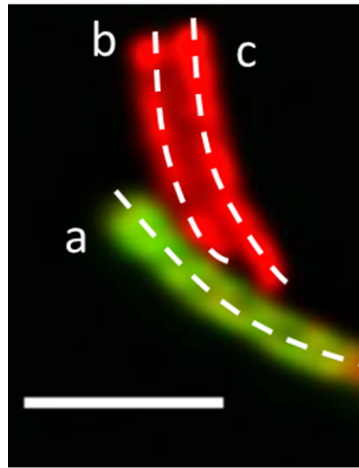
Figure 6.11. Fluorescence intensity profiles of BCG-mCherry along the cell length (dashed lines) showing (a) entry of FITC-II-D into the cytoplasm while (b) and (c) represent unaffected cells. Fluorescence intensity profiles of BCG along the cell width (dashed lines) showing presence of FITC-II-D in the bacterial membrane segments (d) and (e). Images were acquired following 2 h treatment with 500 mg L^{-1} of antimicrobial peptide FITC-II-D. Scale bar = 2 μm.

6.3. Conclusions

In summary, synthetic helical AMPs modified with unnatural amino acids demonstrated improved anti-mycobacterial activities and stability to trypsin degradation as compared to the all L-amino acid peptide, II. The incorporation of D-amino acids proved to be the most effective modification, with the diastereomer II-D exhibiting a fourfold increase in SI as compared to II, likely due to the enhanced stability to *M. tuberculosis* proteases. In addition to its *in vitro* inhibitory activity against both drug-susceptible and MDR *M. tuberculosis*, II-D was equally, if not more effective, at clearing intracellular mycobacteria than both rifampicin and moxifloxacin at MIC equivalent concentrations. Mechanistic studies revealed that the site of action of II-D may not be limited to the mycobacterial membrane, but could potentially involve intracellular targets following internalisation of the peptide. Overall, these findings reiterate the importance of unnatural amino acid substitutions towards enhancing protease stability while highlighting their applicability in designing AMPs with superior mycobacterial selectivity.

CHAPTER 7: Disruption of drug-resistant biofilms using *de novo* designed short synthetic α-helical antimicrobial peptides with idealised facial amphiphilicity

7.1. Introduction

Besides their direct antimicrobial activity, AMPs demonstrate diverse immunomodulatory properties including their ability to reduce the production of pro-inflammatory mediators in response to bacterial endotoxins [190]. Moreover, these multifunctional molecules also effectively inhibit biofilm formation and disrupt mature biofilms [191]. Biofilms are structured aggregates of microbial cells enclosed within an extracellular polymeric substance (EPS) matrix, which adhere to biological or non-biological surfaces [192]. Associated with over 65% of all infections, biofilms are involved in various device-related infections and chronic infections, including cystic fibrosis pneumonia, endocarditis, necrotising fasciitis and musculoskeletal infections [191]. These sessile bacterial communities are inherently resistant to antimicrobials due to poor drug penetration through the EPS matrix, and the existence of subpopulations of stationary phase and persister cells with drug tolerant phenotypes [193]. Despite the immense challenges of eradicating biofilm-related infections, the antimicrobials being developed are rarely evaluated for their anti-biofilm activities.

Over the past few decades, various efforts directed toward understanding the structural determinants of AMPs affecting activity, have revealed that the clustering of hydrophobic and cationic amino acids into spatially distinct

regions is fundamental to the formation of amphipathic structures [21]. Building upon these findings, investigations aimed at optimising the amphipathic α-helix as a means of enhancing antimicrobial potency uncovered that peptides with idealised facial amphiphilicities, comprising of uninterrupted hydrophobic and cationic segments, possessed superior membrane-targeting activities and in turn enhanced selectivity [172, 194]. One such study found that amongst a series of peptides presenting perfectly amphipathic helices, the peptide demonstrating optimal antibacterial selectivity, LBU2, also had the highest mean hydrophobic moment – a measure of amphiphilicity of an α-helix [195]. The otherwise continuous hydrophobic face of the LL-23 fragment of human cathelicidin is interrupted by a single hydrophilic Ser residue at position 9, creating two amphipathic domains [80]. Substitution of Ser9 with either of the hydrophobic residues Val or alanine (Ala) creating the uninterrupted hydrophobic surface found in primate cathelicidins not only resulted in higher antimicrobial activity due to enhanced membrane penetration and depolarisation, but also increased the suppression of LPS-induced pro-inflammatory mediators [80]. These findings highlight the importance of optimising the facial amphiphilicity of synthetic peptides in order to generate more selective lead compounds to be brought forward for clinical testing.

A commonality amongst majority of these studies is the adoption of a template-based approach, utilising naturally-occurring or synthetic AMPs as a starting point, generating helical wheel projections based on their amino acid sequences, and subsequently introducing point mutations to achieve idealised

facial amphiphilicity. However, these strategies remain largely empirical, often entailing multiple steps and requiring several substitutions for structural optimisation [106]. Additionally, optimised sequences derived from natural AMPs, with high sequence homology to HDPs, could inadvertently compromise innate immunity should antimicrobial resistance develop [104]. As such, implementing a rational approach in the design of short synthetic peptides presenting idealised facial amphiphilicity, and with distinct sequences from natural AMPs, could allay these concerns.

In Chapter 4, the repeating sequence $(XXYY)_n$, devised on the basis of mimicking the hydrophobic periodicity of natural α-helical AMPs, was successfully applied in the development of short synthetic amphipathic α-helical peptides. However, in order to maintain a balance between hydrophobic and charged residues, the number of repeat units is restricted to positive integers (n = 1, 2, 3, and so forth) and, moreover, this sequence approach cannot be utilised to generate peptides with idealised facial amphiphilicity for n > 2. Therefore, in this study, α-helical amphiphiles with perfectly segregated hydrophobic and cationic faces were designed using the recurring sequence comprising four amino acids $(X_1Y_1Y_2X_2)_n$ – where X_1 and X_2 are hydrophobic amino acids, Y_1 and Y_2 are cationic amino acids, and n is the number repeat units. This proposed sequence preserves the α-helical periodicity, recognised as a key driver of helical formation [196], while allowing for amphipathic peptides of intermediate lengths (n = 1.5, 2.5, 3.5, and so forth). Importantly, this sequence enables the *de novo* design of peptides with perfectly amphipathic structures for n ≤ 3.

Various amino acid substitutions were performed to understand the effect of sequence pattern and length on the biological activity of peptides with idealised facial amphiphilicities. The synthetic amphiphiles were initially characterised for their α-helical propensity in a membrane-mimicking environment, before evaluation of their therapeutic efficacy against a range of both drug-susceptible and drug-resistant bacteria. Live-cell imaging studies provided insights into the membrane-lytic antimicrobial mechanisms, while their versatility in inhibiting biofilm formation and disrupting pre-formed drug-resistant biofilms was also assessed. Finally, the anti-endotoxin activity of the designed peptides was studied to determine their potential applicability in the treatment of endotoxemia.

7.2. Results and Discussion

7.2.1. Peptide design and characterisation

In this study, short cationic helical peptides with idealised facial amphiphilicity were designed based on the recurring sequence $(X_1Y_1Y_2X_2)_n$, where the hydrophobic residues $X_1 = X_2 =$ Leu or Ile or Trp, and the cationic residues $Y_1 = Y_2 =$ Lys. The influence of size of the cationic and hydrophobic faces on the biological and haemolytic activities was assessed by comparing 8-mer, 10-mer and 12-mer peptides with varying number of repeat units ($n = 2$ or 2.5 or 3) (Figure 7.1). Besides the inclusion of residues which were helix formers rather than breakers, another key consideration was the selection of amino acids that could enhance peptide selectivity for microbial over mammalian cells. Hence, Lys was selected over Arg as the polar residue due to its high helical propensity [92], and lower cytotoxicity [93]. The hydrophobic residue Leu was also included due to its high helical propensity [92], while Trp was chosen because of its strong interaction with the lipid bilayer interface [197]. Finally, the selection of Ile was supported by evidence that Lys to Ile substitutions produced peptides with identical bactericidal activity, but markedly reduced toxicity [198]. The synthetic peptides were amidated at the C-terminus to improve antimicrobial activity by increasing net positive charge [133, 134].
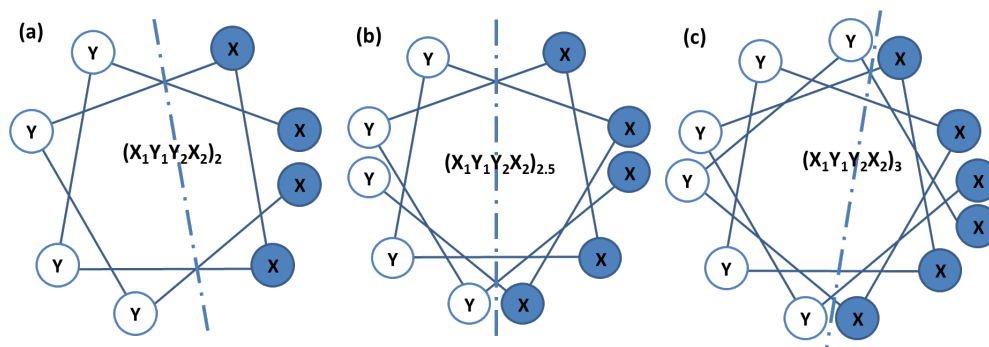
136

Figure 7.1. Helical wheel projection of α-helical peptides with idealised facial amphiphilicity, possessing the backbone sequence $(X_1Y_1Y_2X_2)_n$, where X_1 and X_2 are hydrophobic amino acids, Y_1 and Y_2 are cationic amino acids, and n is the number repeat units.

The sequences of the *de novo* peptides, their denotations and molecular weights are provided in Table 7.1. The molecular weights of the synthetic peptides were verified using SELDI-TOF MS, and agreement between the theoretical and measured molecular weights confirmed that the peptides had been synthesised to the desired specifications.

Table 7.1. Design of α-helical peptides with idealised facial amphiphilicity and their molecular weights.

AMP	No. of repeat units [n]	Repeat unit	Peptide sequence	Theoretical M_W	Measured M_W^a	Charge
L8	2		LKKLLKKL-NH$_2$	982.36	982	+4
L10	2.5	LKKL	LKKLLKKLLK-NH$_2$	1223.69	1224	+5
L12	3		LKKLLKKLLKKL-NH$_2$	1465.02	1465	+6
I8	2		IKKIIKKI-NH$_2$	982.36	982	+4
I10	2.5	IKKI	IKKIIKKIIK-NH$_2$	1223.69	1224	+5
I12	3		IKKIIKKIIKKI-NH$_2$	1465.02	1466	+6
W8	2		WKKWWKKW-NH$_2$	1274.57	1276	+4
W10	2.5	WKKW	WKKWWKKWWK-NH$_2$	1588.95	1589	+5
W12	3		WKKWWKKWWKKW-NH$_2$	1903.33	1904	+6

^{a} M_w determined by SELDI-TOF MS.

The secondary structures of the synthetic peptides were evaluated in the presence of a 25 mM SDS micelle solution to simulate a microbial membrane environment. Under these conditions, the synthetic peptides readily adopted α-helical conformations, as supported by the characteristic double minima at ~208 and 222 nm (Figure 7.2). In general, increasing the number of repeat

units enhanced the helical propensity of synthetic peptides comprising of Leu and Ile residues, evident from the lower mean residue ellipticity values at 222 nm (θ_{222}). While the shorter Trp-containing peptides W8 and W10 displayed strong helical signatures, the longer W12 exhibited a broader minima between 208 and 222 nm (Figure 7.2c), possibly due to self-aggregation of the more hydrophobic peptide [199].
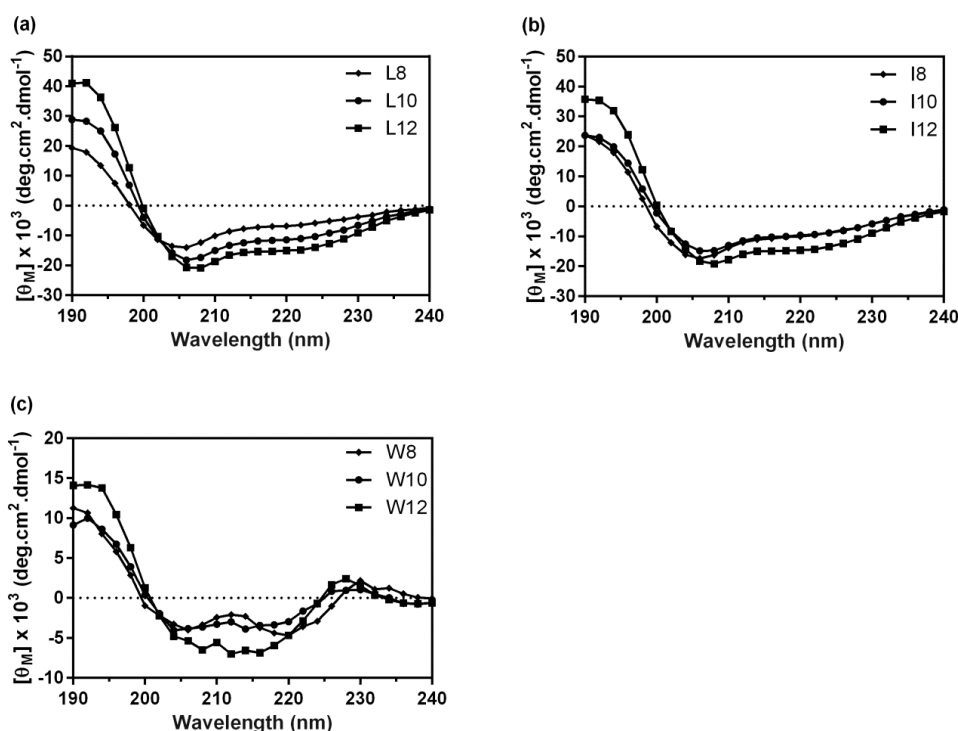
Figure 7.2. CD spectra representing α-helical propensity of peptides with the backbone sequence (a) $(LKKL)_n$, (b) $(IKKI)_n$ and (c) $(WKKW)_n$ in 25 mM SDS micelle solution, where n = 2, 2.5 and 3. Data are expressed as the mean of three runs per peptide.

7.2.2. Antimicrobial activity

The antimicrobial activity of the synthetic peptides was studied against a panel of clinically relevant Gram-positive and Gram-negative bacteria and the results are summarised in Table 7.2. The designed peptides effectively inhibited bacterial growth over a range of concentrations, with L12 and W12 emerging as the most potent antimicrobials. Both of these peptides recorded

the lowest GM of the MICs of 13.1 μM, followed by W10 with a value of 22.1 μM. The three least effective peptides, L8, I8 and I10 also exhibited the lowest α-helical conformation (Figure 7.2), suggesting that folding of peptides into amphipathic structures was essential for antimicrobial activity. This observation is supported by evidence that helix formation is a major driver of peptide insertion into the lipid bilayer [200]. In general, an increase in size of the continuous cationic and hydrophobic faces in the amphipathic helix corresponded with reduced MIC values. Upon closer examination, the choice of non-polar amino acid was a key determinant of the minimum number of residues required in each uninterrupted segment for peptide activity. Amongst the hydrophobic amino acids studied, the incorporation of Ile proved least effective, as a minimum of six residues in each of the continuous cationic and hydrophobic faces was necessary for activity. Even then, I12 recorded a 16- and 32-fold higher MIC against the Gram-positive *S. aureus* as compared to L12 and W12 respectively. For Leu-containing peptides, cationic and hydrophobic segments consisting of at least five amino acids were required to inhibit bacterial growth, in line with findings from previous reports [194, 201]. However, only four residues per segment were sufficient to render peptides, comprising of bulky Trp residues, active. The superior potency of Trp-containing amphiphiles could be attributed to the strong affinity of Trp for membrane interfaces, which facilitates peptide penetration and disruption of the lipid bilayer [197, 202]. Therefore, the inclusion of bulky Trp residues could prove effective in designing shorter and more potent helical peptides.

Table 7.2. MICs and SIs of peptides with idealised facial amphiphilicity against Gram-positive and Gram-negative bacteria.

AMP	MIC [µM]				GM[a] [µM]	HC$_{50}$ [µM]	SI[b]
	E. coli	*K. pneumoniae*	*P. aeruginosa*	*S. aureus*			
L8	500	> 500	> 500	> 500	-	>2000	-
L10	31.3	> 500	62.5	> 500	-	>2000	-
L12	7.81	31.3	7.81	15.6	13.1	>2000	152
I8	> 500	> 500	>500	> 500	-	>2000	-
I10	500	> 500	>500	> 500	-	>2000	-
I12	15.6	> 500	15.6	250	-	>2000	-
W8	31.3	250	>250	62.5	-	>2000	-
W10	15.6	62.5	15.6	15.6	22.1	>2000	91
W12	15.6	15.6	15.6	7.81	13.1	483	37

[a] The GM of the MICs for the 4 bacterial strains.
[b] SI is determined as follows: (HC$_{50}$/GM). The highest tested concentration of 2000 µM was used for SI calculations when less than 50% haemolysis was observed at this concentration.

7.2.3. Haemolytic activity and cell selectivity

The synthetic peptides were evaluated for their haemolytic activity using 4% (v/v) blood from two healthy donors and as shown in Figure 7.3, all peptides induced minimal haemolysis at their respective MICs. The Ile-containing peptides (I8, I10 and I12), and those consisting of two repeat units (L8, I8 and W8) displayed the lowest haemolysis of <1.5% even at 2000 µM. Notably, the most active peptide L12 only induced 16% haemolysis at 2000 µM, a concentration 150-fold greater than its GM MIC value. Trp incorporation (W8, W10 and W12) produced peptides with stronger haemolytic activity with W10 and W12 inducing haemolysis of 28% and 78% at 2000 µM, respectively. This corresponded to a far lower HC$_{50}$ value, defined as the lowest peptide concentration producing 50% haemolysis of RBCs, of 483 µM for W12 as compared to all other peptides (Table 7.2).

To enhance clinical utility of the amphipathic helical peptides, they should preferentially interact with microbial over mammalian cell membranes in

order to maximise antimicrobial efficacy while minimising toxicity. The SI, defined as the ratio of HC_{50} to GM MIC values, is one measure devised to aid in the selection of the best therapeutic candidates, with higher SI values deemed more desirable. Of the nine peptides designed, L12 displayed the highest SI of 152, followed by W10 and W12. Although both L12 and W12 emerged equally active against the panel of bacteria with similar GM values of 13.1 μM, the relatively low haemolytic activity displayed by L12 translated into a fourfold superior SI compared to W12 (Table 7.2). Among the Trp-containing peptides, W10 possessed the optimal composition with the highest SI of 97, despite recording a higher GM value of 22 μM as compared to W12. While increasing the number of lipophilic Trp residues increased both antimicrobial and haemolytic activities, the reduction in the HC_{50} value for W12 occurred to a far greater extent than the corresponding decrease in MICs. Thus, limiting the continuous hydrophobic face to ≤ 5 Trp residues may be crucial in designing more selective peptides, as the expansion of this uninterrupted segment beyond that proved detrimental to the SI.
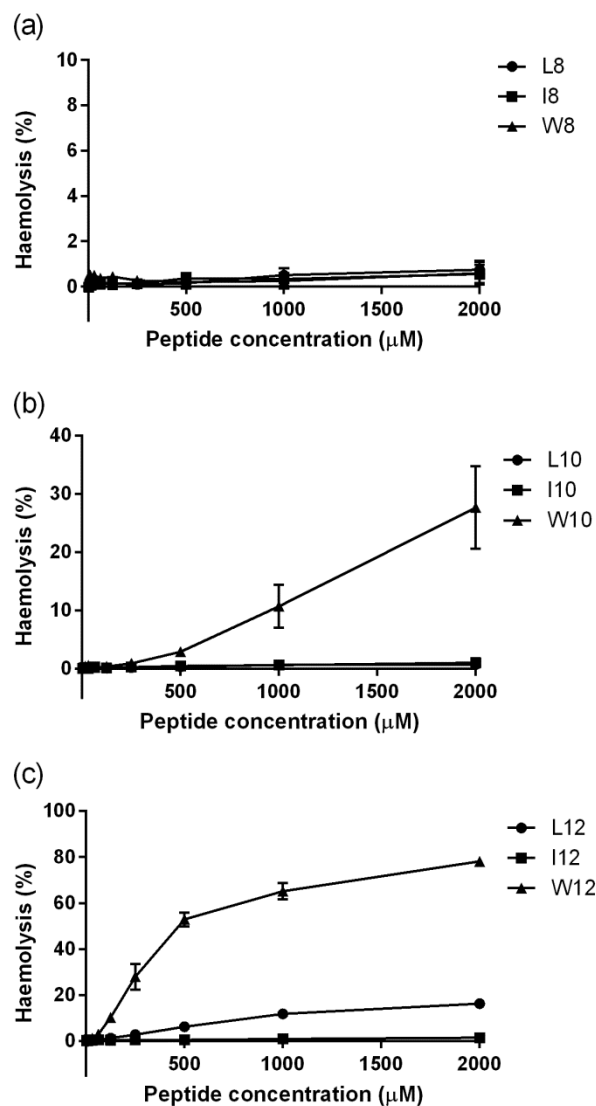
Figure 7.3. Haemolytic activity of synthetic α-helical peptides possessing (a) 2 repeat units, (b) 2.5 repeat units and (c) 3 repeat units tested against blood from two healthy donors. Peptides induced minimal haemolysis at concentrations corresponding to the respective MICs. Data are expressed as mean ± S.D. for two independent experiments.

7.2.4. Antimicrobial mechanisms

The bactericidal mechanisms of the synthetic peptides were evaluated by performing *in vitro* killing efficiency studies against a panel of Gram-positive and Gram-negative bacteria. L12 demonstrated killing efficiencies of > 99.9% at 2x MICs of all four species (Figure 7.4). The bactericidal activity was more

significant at 4x MIC with L12 achieving > 4 log reduction for *P. aeruginosa*, > 5 log reduction for *E. coli* and *K. pneumoniae*, and > 6 log reduction for *S. aureus*.
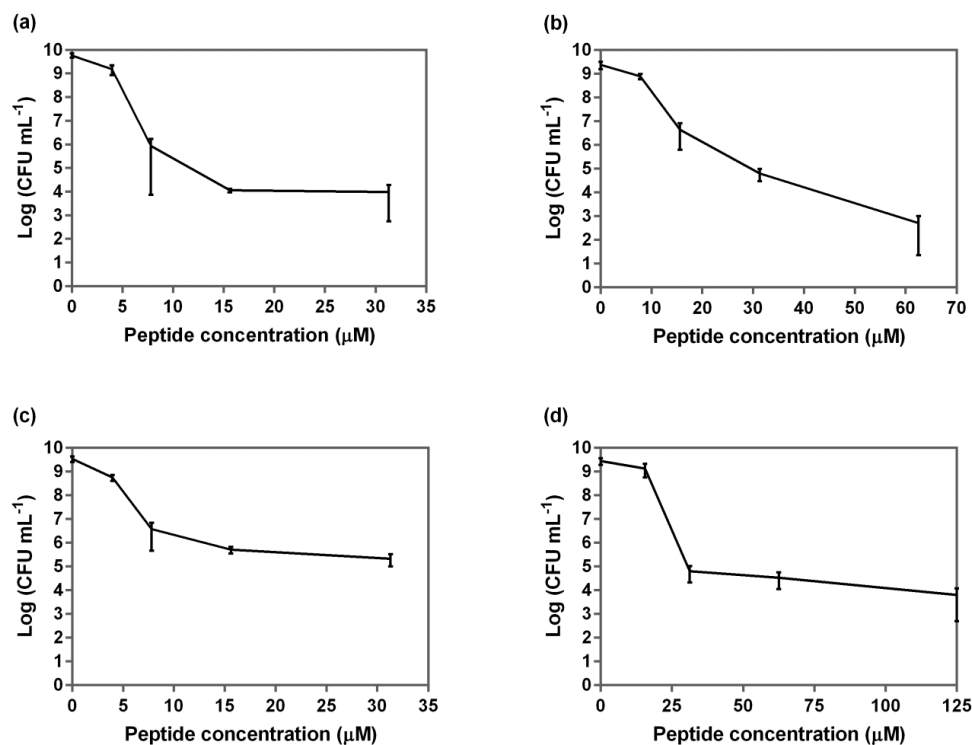
Figure 7.4. Killing efficiency of antimicrobial peptide L12 against (a) *E. coli*, (b) *S. aureus*, (c) *P. aeruginosa* and (d) *K. pneumoniae* following treatment for 18 h at concentrations corresponding to 0, 0.5x, 1x, 2x and 4x MIC. Data are expressed as mean ± S.D. for two independent experiments.

AMPs adopting amphipathic helical structures are recognised to interact with bacterial membranes in order to exert their antimicrobial effect by creating pores, or inducing widespread collapse of membrane structural integrity [22]. In this study, live-cell imaging of bacterial cells was performed using the CellASIC™ ONIX Microfluidic Platform to elucidate the antimicrobial mechanisms of the most selective peptide L12. The DNA intercalating dye PI was utilised to detect peptide-mediated membrane damaged to *E. coli* and *S. aureus* following treatment with L12 at concentrations up to 8x MIC. As

shown in Figure 7.5a, *E. coli* cells doubled continuously without taking up the fluorescent dye in the absence of L12. Under similar conditions, *S. aureus* cells also excluded PI and replicated uninterruptedly (Figure 7.5d). However, exposure of *E. coli* to L12 at 4x MIC rapidly induced fluorescent staining of bacterial cells within 15 min (Figure 7.5b). The effect was more pronounced at 8x MIC with PI uptake into bacterial cells occurring within 5 min of peptide treatment (Figure 7.5c). Similarly, *S. aureus* exhibited fluorescence within 15 min of peptide introduction at both 4x and 8x MIC (Figures 7.5e and f). Moreover, the replication of L12-treated *E. coli* and *S. aureus* cells was promptly halted after 25 min exposure to 8x MIC, suggesting that permeabilisation of bacterial membranes likely culminated in cell death. Live-cell imaging studies also provide a useful means of assessing the relative kinetics of the membrane-permeabilising activity of AMPs when comparing Gram-positive versus Gram-negative bacteria. Treatment of *S. aureus* with L12 at 8x MIC resulted in rapid fluorescent staining of > 90% and ~100% of cells within 15 and 35 min, respectively (Figure 7.5f). For *E. coli* however, membrane permeabilisation was far more gradual with ~65% of cells displaying fluorescence within 15 min and > 90% staining only achieved at 45 min (Figure 7.5c). The more rapid fluorescence observed for *S. aureus* is consistent with the fact that Gram-positive bacteria lack an outer membrane, hence binding of PI to intracellular DNA is readily achieved upon compromise of cytoplasmic membrane integrity. The presence of an outer membrane in Gram-negative bacteria necessitates that both outer and inner membranes are sequentially permeabilised before PI can gain access to DNA, thus slowing down the rate at which PI can diffuse into the bacterial cell.

(a)
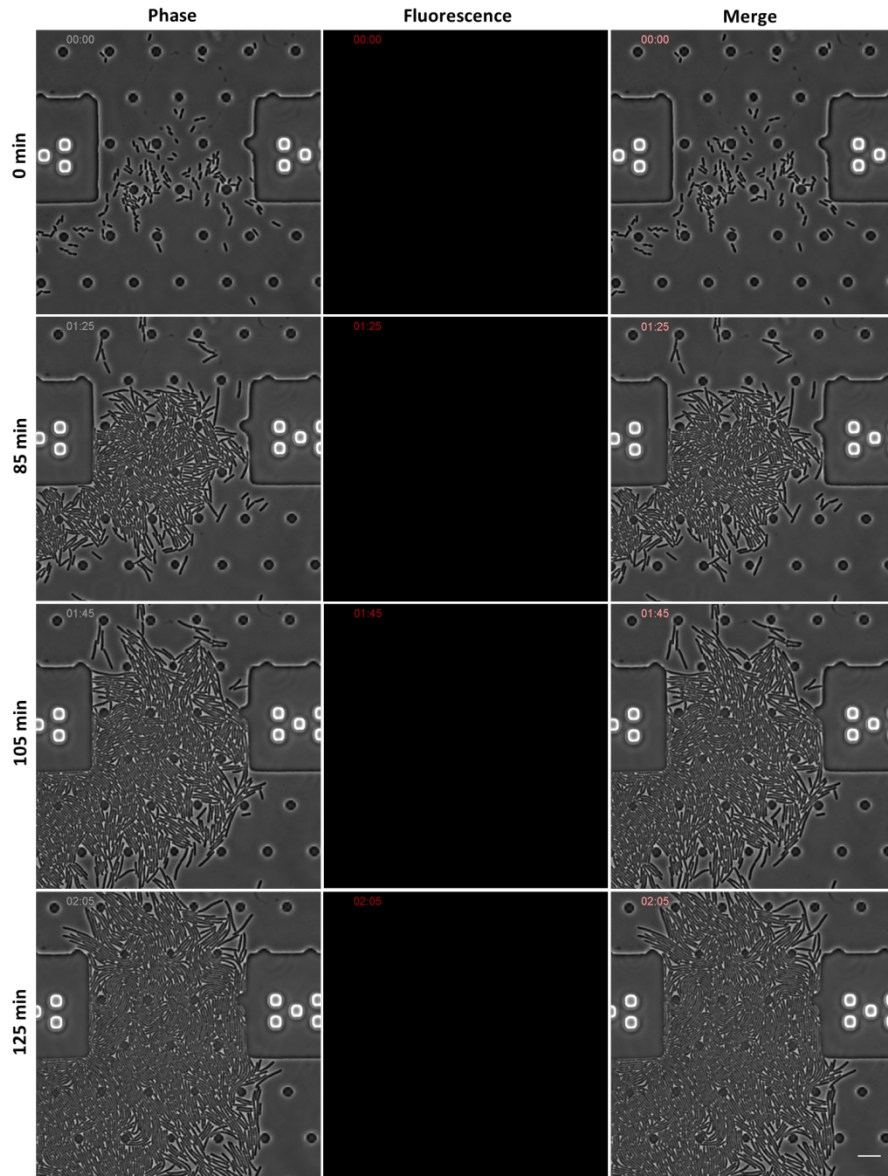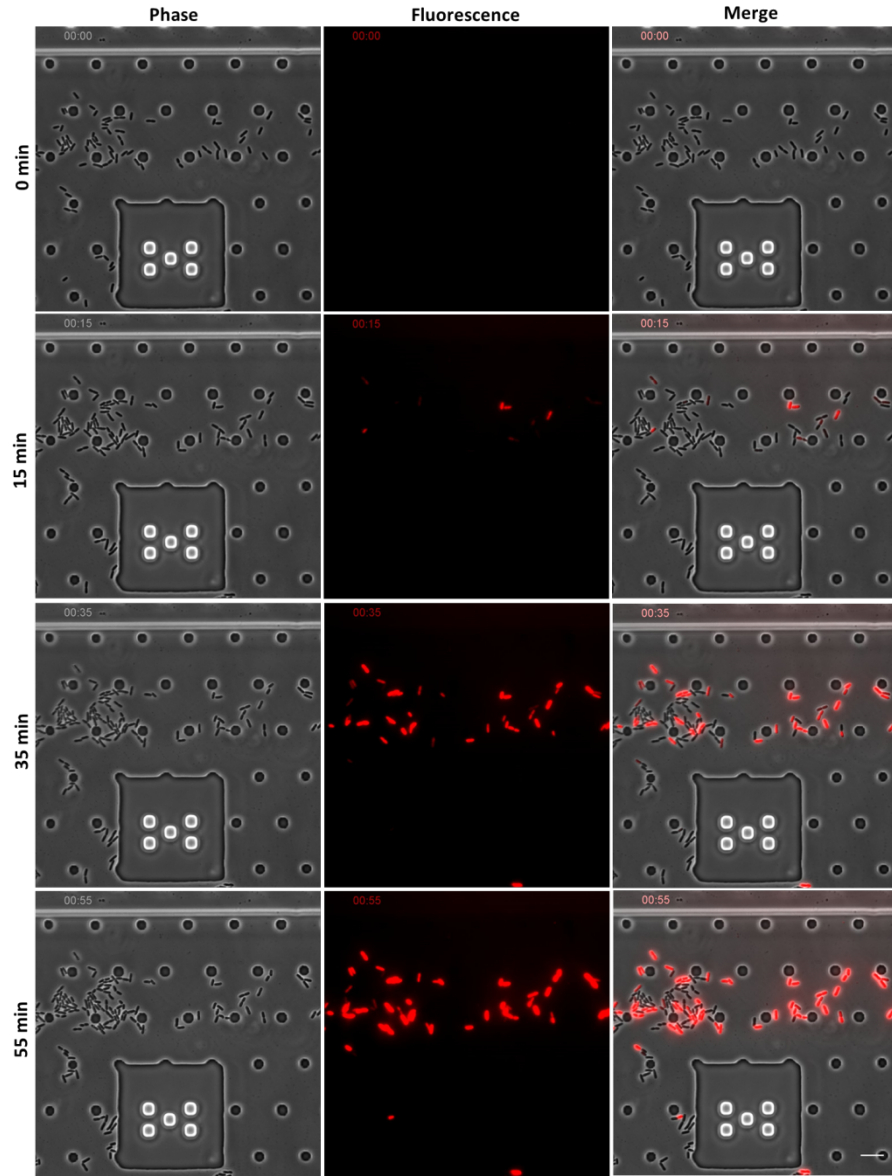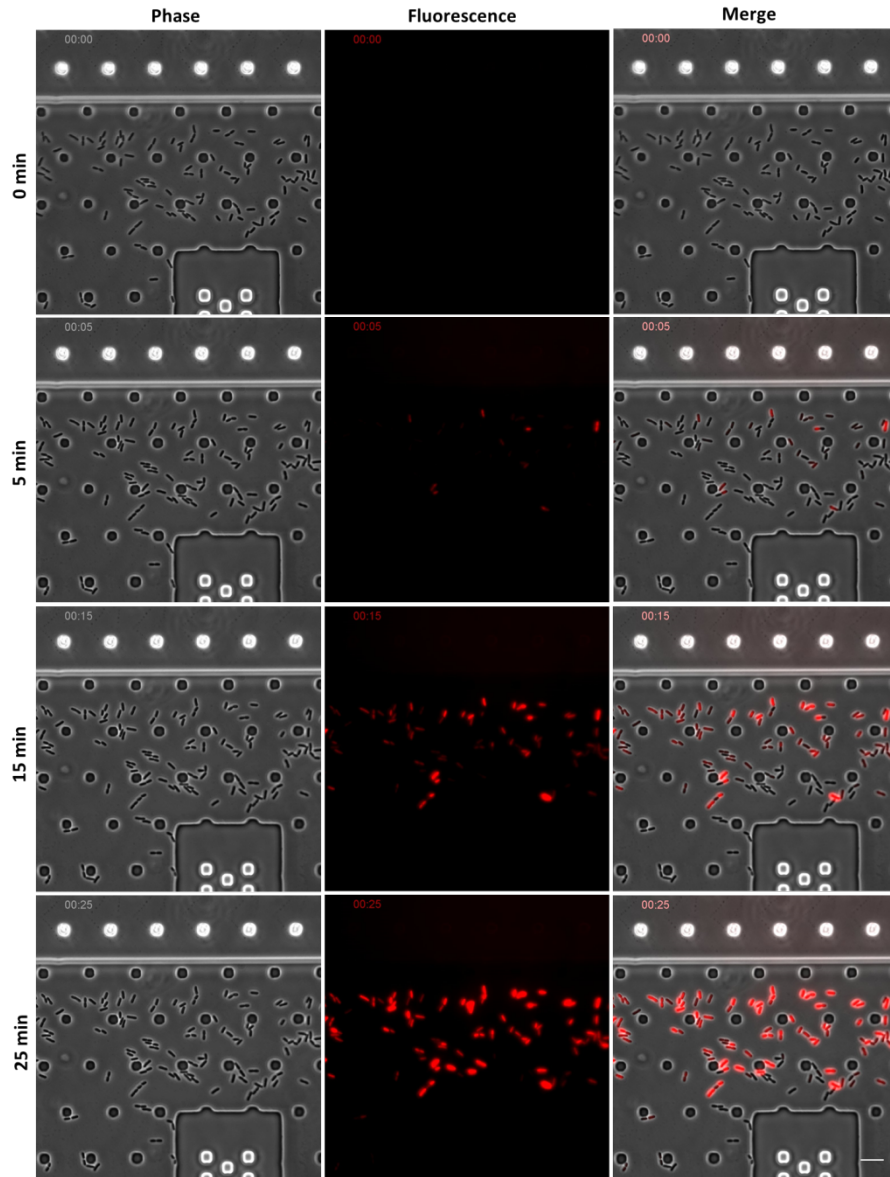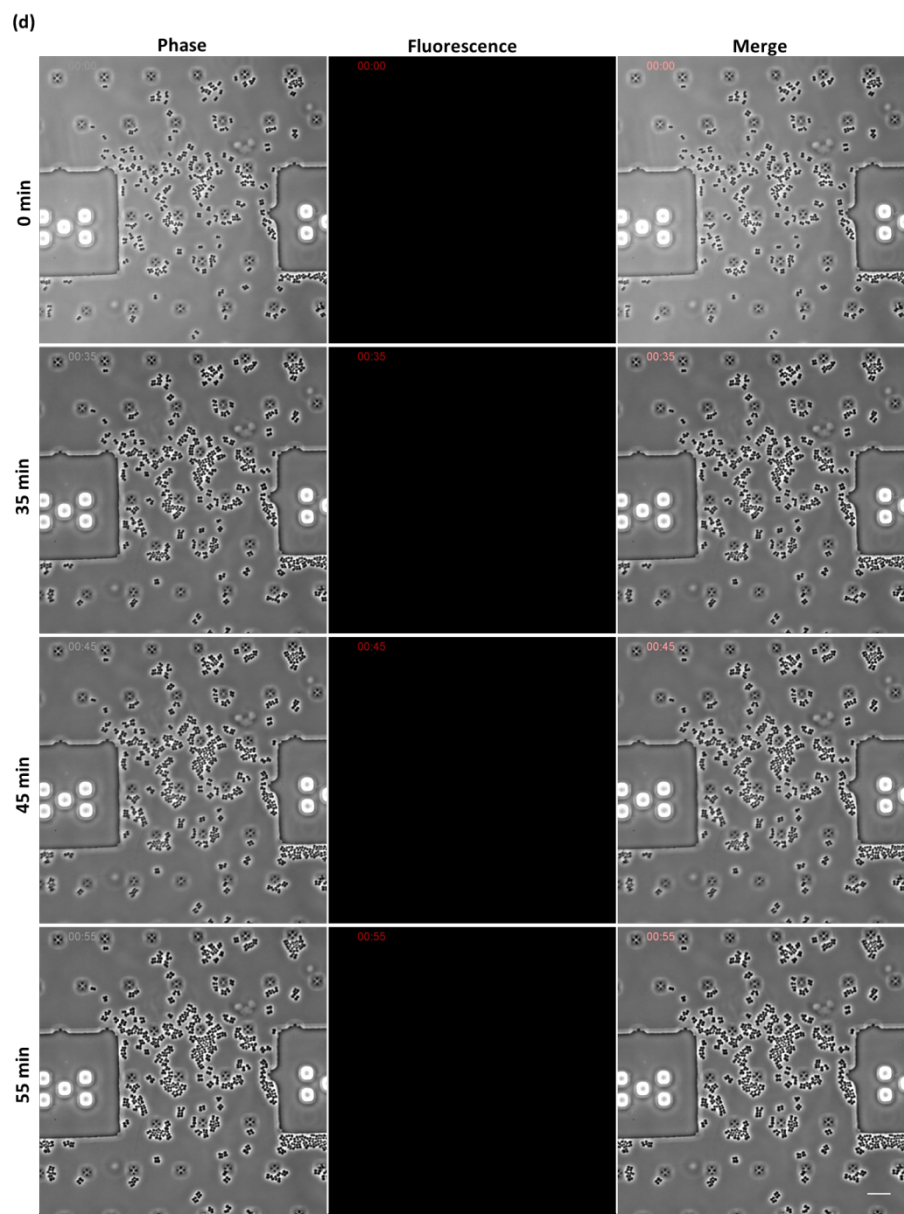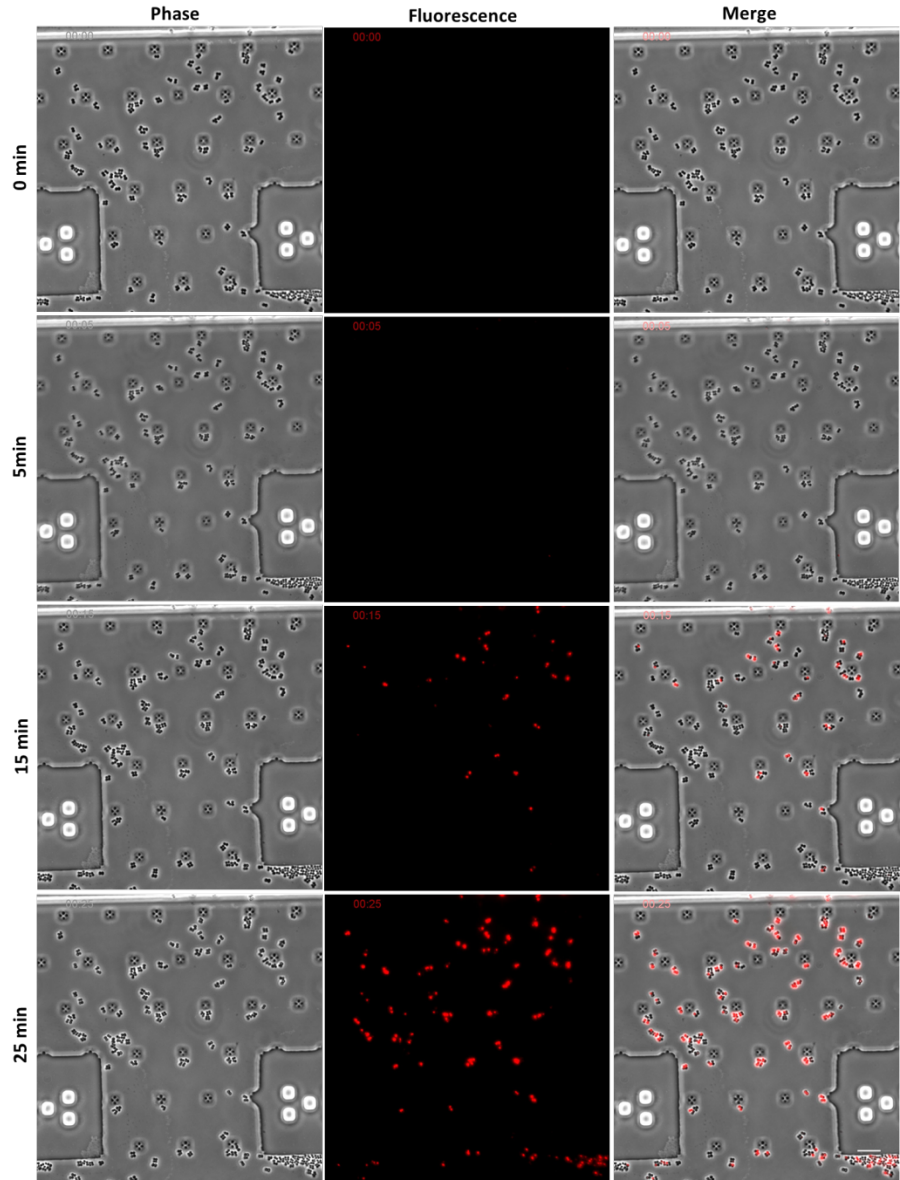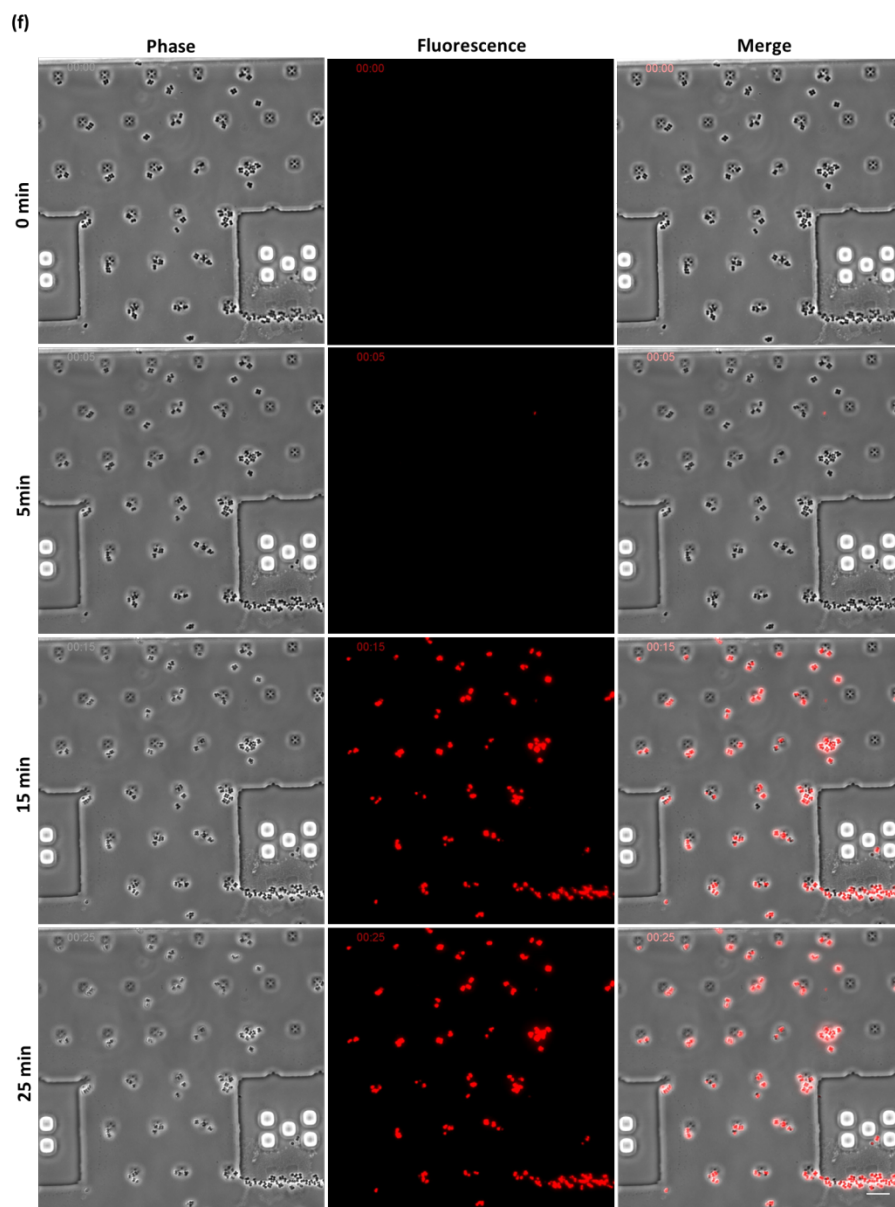
	Phase	Fluorescence	Merge
0 min	00:00	00:00	00:00
85 min	01:25	01:25	01:25
105 min	01:45	01:45	01:45
125 min	02:05	02:05	02:05

(b)

	Phase	Fluorescence	Merge
0 min			
15 min			
35 min			
55 min			

(c)

	Phase	Fluorescence	Merge

(d)

	Phase	Fluorescence	Merge
0 min			
35 min			
45 min			
55 min			

	Phase	Fluorescence	Merge
0 min			
5min			
15 min			
25 min			

Figure 7.5. Time-lapse fluorescence microscopy images of *E. coli* (a, b, c) and *S. aureus* (d, e, f) following treatment with (a and d) media alone, (b and e) L12 at 4x MIC and (c and f) L12 at 8x MIC in the presence of the membrane impermeable dye, PI. The uptake of PI into bacterial cells within minutes of exposure supports the rapid membrane-lytic antimicrobial mechanisms of the synthetic peptides. No uptake of PI was observed in negative controls while a concentration dependent increase in the proportion of fluorescent bacteria was evident with peptide treatment. Scale bar = 10 μm.

7.2.5. Inhibition of MDR bacteria and biofilms

The antimicrobial activity of the three most selective peptides was further
evaluated against drug-resistant bacteria including MRSA, and MDR clinical
isolates of both *P. aeruginosa* and *M. tuberculosis*. As shown in Table 7.3, the
synthetic peptides remained equally effective against drug-resistant pathogens,
with MICs ranging from 7.81 to 125 μM. While both 12-mers demonstrated
relatively similar activity against MDR *P. aeruginosa* and *M. tuberculosis*,
W12 recorded an 8-fold lower MIC than L12 against MRSA. The observed
retention of broad-spectrum inhibitory activity against drug-resistant bacteria
largely stems from the non-specific membrane-lytic mode of action displayed
by most AMPs [24].

Table 7.3. MICs of synthetic peptides against clinical isolates of MRSA 252,
MDR *M. tuberculosis* (CSU87), and MDR *P. aeruginosa* (PA-W1, PA-W14
and PA-W25).

Antimicrobial peptide	MIC [μM]				
	MRSA 252	PA-W1	PA-W14	PA-W25	CSU87
L12	62.5	15.6	15.6	15.6	62.5
W10	15.6	31.3	125	125	62.5
W12	7.81	15.6	31.3	15.6	62.5

Besides their efficacy against planktonic bacteria, AMPs could provide useful
alternatives to address challenging biofilm-related infections [191]. Thus, the
most selective peptide L12 was evaluated for its ability to inhibit biofilm
formation at sub and supra-MIC levels. As shown in Figure 7.6a, L12
prevented the development of both drug-susceptible and drug-resistant
biofilms to similar extents. Though ineffective at sub-MIC levels, L12
significantly reduced the biomass of PAO1 and PA-W25 biofilms by ~90% at
both 1x and 2x MIC ($p \leq 0.0001$). These findings were corroborated by
bioluminescent imaging of *P. aeruginosa* which revealed that L12 effectively

inhibited biofilm formation at 1x, 2x and 4x MIC (Figure 7.6b), with > 99% reduction in luminescence signal (Figure 7.6c). Unlike the inhibition of *P. aeruginosa* biofilms, the reduction in biomass of *S. aureus* biofilms occurred in a dose-dependent manner (Figure 7.6a). L12 inhibited MSSA and MRSA biofilms by ~37% and 39% at 0.25x MIC, respectively, and ~53% and 45% at 0.5x MIC, respectively. The anti-biofilm properties of AMPs are partly attributed to direct killing of planktonic bacteria, hence, the prevention of biofilm formation at sub-MIC suggests that alternative mechanisms could potentially be involved. It has been shown that coating AMPs onto surfaces reduces bacterial adherence in turn inhibiting biofilm formation and this may contribute here [121].

The treatment of mature biofilms also poses a significant clinical problem; hence L12 was further evaluated for its potential to disrupt pre-formed biofilms of drug-resistant pathogens. As shown in Figure 7.6d, L12 displayed significant concentration-dependent reduction in cell viabilities of pre-established biofilms of both MRSA and MDR PA-W25 at 8x and 16x MIC within 2 h of treatment ($p \leq 0.0001$). Bioluminescent imaging studies of pre-formed *P. aeruginosa* biofilms confirmed that L12 effectively eradicates mature biofilms at supra-MIC levels after 2 h (Figure 7.6e), accompanied by significant reductions in luminescence at 16x MIC ($p \leq 0.05$), and 32x and 64x MIC ($p \leq 0.01$) (Figure 7.6f). All in all, these findings underscore the potential utility of the *de novo* AMPs presented here in tackling the mounting problem of MDR biofilms and infections.

Figure 7.6. (a) Inhibition of drug-susceptible and drug-resistant *P. aeruginosa* and *S. aureus* biofilms formation following overnight exposure to L12. (b) IVIS imaging and (c) radiance quantification of biofilm growth inhibition of bioluminescent *P. aeruginosa* treated with L12 overnight. (d) Cell viabilities of pre-formed PA-W25 and MRSA 252 biofilms after treatment with L12 for 2 h. (e) IVIS imaging and (f) radiance quantification of pre-formed biofilm disruption of bioluminescent *P. aeruginosa* exposed to L12 for 2 h. Rows in (b) and (e) represent individual replicates. L12 inhibits biofilm formation at 1x and 2x MIC, and effectively disrupts pre-established biofilms at supra-MIC levels. (* $p \leq 0.05$, ** $p \leq 0.01$, *** $p \leq 0.001$, **** $p \leq 0.0001$).

7.2.6. Anti-endotoxin activity

Host innate immune responses during sepsis, elicited by exposure to the Gram-negative bacterial cell wall component, LPS, could lead to septic shock and eventually death if uncontrolled. The neutralisation of endotoxins by amphipathic peptides could provide an effective means of blocking the overproduction of inflammatory mediators induced by LPS. Thus, the LPS-binding abilities of the *de novo* peptides were evaluated from 3.9 to 31.3 μM using the LAL chromogenic assay, as cell viabilities were > 70% for all peptides, except L12 which recorded ~30% cell viability at the highest concentration (Figure 7.7c). As shown in Figure 7.7a, the most hydrophobic 12-mer, W12, bound LPS most effectively with ≥ 90% binding even at low peptide concentrations of 7.81 μM. In comparison, I12 and L12 only neutralised ~29% and 47% of LPS, respectively at similar concentrations. Increasing the number of repeat units by 0.5 contributed to stronger LPS-binding for W12 to W10 at all concentrations tested. Taken together, these findings suggest that both peptide length and hydrophobicity are important determinants of the LPS-neutralising properties of amphipathic peptides.

The overproduction of the pro-inflammatory mediator NO has been implicated in the pathogenesis of septic shock, inducing harmful effects including tissue damage and myocardial depression [203]. Hence, the ability of the peptides to restrict LPS-induced macrophage activation was assessed by quantifying nitrite production from LPS-stimulated RAW 264.7 cells treated with peptides. The most potent inhibitors L12 and W12 limited NO production to levels similar to controls even at the lowest peptide concentration of 3.9 μM (p

$\leq$ 0.0001) (Figure 7.7b). W10 and I12, however, demonstrated a dose-dependent reduction in NO release from macrophages. While NO production was enhanced > 6-fold in the absence of peptides, treatment with 7.81 μM of W10 and I12 suppressed NO production to concentrations ~2.7 and 2.5-fold, respectively, higher than that of controls. In general, there was close agreement between the LPS-binding and neutralising activities of the peptides, except for I12 which demonstrated similar LPS-blocking activity as W10 despite exhibiting the lowest LPS-binding affinity. This finding suggests that in addition to the direct binding of LPS by I12, other mechanisms may be involved in the suppression of pro-inflammatory responses induced by LPS [204, 205]. Overall, the short amphiphilic peptides presented in this study could potentially be developed as anti-inflammatory agents in the treatment of endotoxemia by blocking LPS-mediated induction of inflammatory mediators.
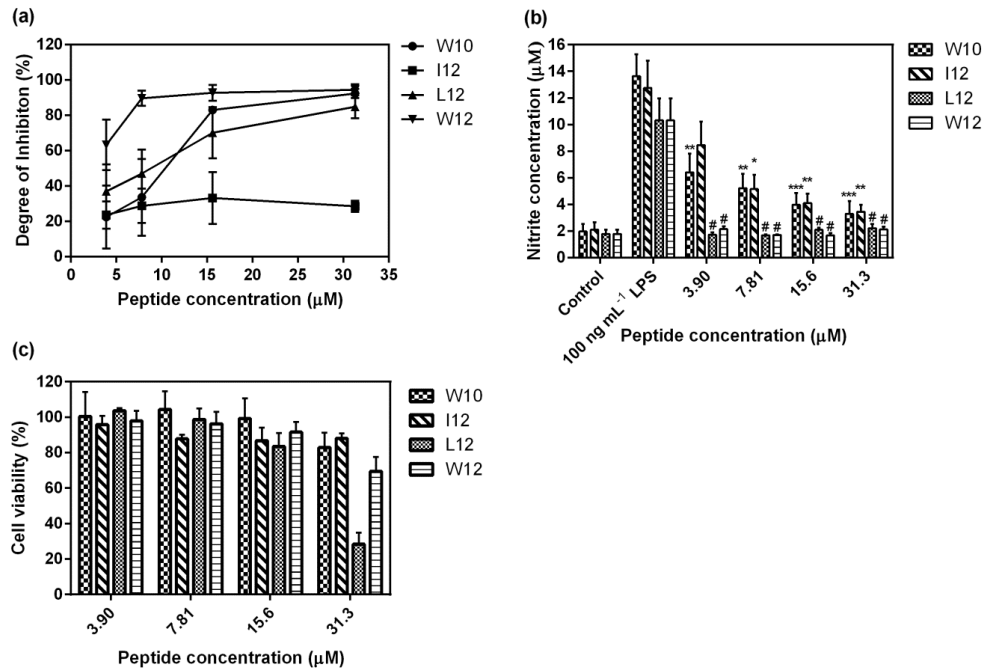
Figure 7.7. The ability of *de novo* designed peptides to (a) bind LPS within 30 min exposure and (b) restrict LPS-stimulated NO production following 24 h treatment with peptides at various concentrations. The synthetic peptides L12 and W12 strongly bound LPS and effectively inhibited NO production at sub-MIC concentrations of 3.9 μM. (* $p \leq 0.05$, ** $p \leq 0.01$, *** $p \leq 0.001$, # $p \leq 0.0001$). (c) The effect of synthetic peptides on viability of RAW 264.7 mouse macrophage cells following 24 h treatment with peptides at various concentrations. Data are expressed as mean ± S.E.M. for three independent experiments.

7.3. Conclusions

In summary, the design principles proposed in this study, with peptides comprising of the backbone sequence $(X_1Y_1Y_2X_2)_n$, were successful in producing broad-spectrum α-helical AMPs. Optimisation of peptide selectivity by varying the number of repeat units and choice of hydrophobic amino acid, found that the sequences $(LKKL)_3$ and $(WKKW)_{2.5}$ possessed the highest SIs of 152 and 91 respectively. The bactericidal activity of L12 was likely due to membrane-lysis, inducing rapid disruption of Gram-positive and Gram-negative bacterial membranes within minutes. L12 also effectively inhibited the formation, and promoted the disruption, of drug-resistant biofilms. Finally,

both L12 and W12 demonstrated potent suppression of LPS-induced pro-inflammatory mediators even at low peptide concentrations of 3.9 μM. All in all, the design strategies presented in this study could provide a useful tool for developing therapeutic peptides with broad-ranging clinical applications in the treatment and prevention of drug-resistant biofilms and endotoxemia.

CHAPTER 8: Conclusions and future perspectives

The overall aim of this thesis was to apply a *de novo* approach in the design of short synthetic AMPs to develop novel compounds for anti-infective applications. We tested the hypothesis that rationally designed synthetic AMPs, comprising of repeat sequences corresponding to the hydrophobic periodicity of natural α-helical peptides, could be safely and effectively applied in TB mono- and combination therapy, and in the treatment and prevention of drug-resistant biofilms and endotoxemia. In Chapter 4, we provided important evidence that short synthetic amphipathic α-helical peptides, of only eight to ten residues, could effectively inhibit both drug-susceptible and drug-resistant *M. tuberculosis*. While the presence of free thiol groups in Cys residues did not serve to enhance the anti-mycobacterial activity of the parent peptide $(LLKK)_2$, enhancement in hydrophobicity by incorporating Met residues was shown to be an effective strategy to improve activity. The most selective peptide, $M(LLKK)_2M$, was found to be minimally toxic at its MIC, and rapidly disrupted the mycobacterial membrane within 10 min of treatment. Notably, mycobacteria did not develop resistance after multiple exposures to sub-lethal doses of this peptide. In addition, AMPs displayed synergism in combination with rifampicin against both *M. smegmatis* and *M. bovis* BCG and additivity against *M. tuberculosis*. Moreover, such combination therapy was effective in delaying the emergence of rifampicin resistance, highlighting the potential utility of AMPs as adjuvants in combinatorial treatment regimens for TB.

In Chapter 5, the effect of key physicochemical parameters including hydrophobicity and helicity on anti-mycobacterial activity and synergism of our synthetic AMPs was investigated for the first time. The three most hydrophobic peptides (WW, MM and II) were the most active, and exhibited synergism with rifampicin. However, increasing hydrophobicity beyond a certain threshold was found to be detrimental to cell selectivity, with peptides possessing intermediate hydrophobicity displaying the highest SI. Flow cytometric analysis revealed that enhancements in hydrophobicity and helicity increased the rate and extent of peptide-mediated membrane permeabilisation. This finding corroborated the postulation that synergism between the peptides and rifampicin was likely mediated *via* peptide-induced pore formation. The rapid, concentration-dependent membrane depolarisation, leakage of intracellular ATP and calcein release from PE/PG LUVs supported the membrane-lytic mechanism of action of the peptides. Together, these findings suggest that hydrophobicity and helicity significantly impact anti-mycobacterial activity and optimisation of both parameters is necessary to develop synthetic analogues with superior selectivity indices and enhanced synergistic potential with conventional antibiotics.

In Chapter 6, unnatural amino acid-modified α-helical peptides were systematically evaluated in an attempt towards enhancing anti-mycobacterial activities and stability. Substitutions were well tolerated without an appreciable effect on toxicity profiles and secondary conformations, and the modified peptides withstood proteolytic digestion by trypsin. The most selective peptide II-D, the all D-amino acid analogue, exhibited a fourfold

increase in selectivity index in comparison to the unmodified L-amino acid peptide. This peptide also effectively reduced the intracellular bacterial burden of both drug-susceptible and MDR clinical isolates of *M. tuberculosis* after 4-days of treatment. Live-cell imaging studies with BCG provided evidence of the membrane-permeabilising mechanisms of II-D. Flow cytometric analysis of II-D treated H37Rv and CSU87 further corroborated the membrane-targeted mode of action of this peptide. Overall, unnatural amino acid modifications not only serve to decrease the susceptibility of peptides to proteases, but also enhance mycobacterial selectivity.

In Chapter 7, a new sequence-based approach is presented in the *de novo* design of α-helical peptides with idealised facial amphiphilicity. Synthetic amphiphiles composed of the backbone sequence $(X_1Y_1Y_2X_2)_n$, where X_1 and X_2 are hydrophobic residues (Leu or Ile or Trp), Y_1 and Y_2 are cationic residues (Lys), and n is the number repeat units (2 or 2.5 or 3), demonstrated potent broad-spectrum antimicrobial activities against clinical isolates of drug-susceptible and MDR bacteria. The most selective peptide, L12, promoted rapid permeabilisation of bacterial membranes. Importantly, L12 not only suppressed biofilm growth, but effectively disrupted mature biofilms after only 2 h of treatment. The peptides bound LPS, with L12 and W12 suppressing the production of LPS-induced pro-inflammatory mediators to levels of unstimulated controls at low micromolar concentrations. Thus, the proposed rational design strategy can be implemented to develop potent, selective and multifunctional α-helical peptides to eradicate drug-resistant biofilm-associated and endotoxemia.

In addition to providing insights into the rational design of short α-helical AMPs for broad-ranging clinical applications, the present study has helped identify possible new avenues for future research. While findings from the *in vitro* efficacy studies are promising, the clinical potential of the optimised lead compounds needs to be established *in vivo* using animal models of TB infection. Combinatorial drug regimens form the bedrock of successful TB chemotherapy, and hence new anti-tubercular agents are unlikely to obtain approval for use as monotherapy [206]. Thus, it is necessary for new or re-purposed drugs to be evaluated either as adjuncts to first-line anti-tubercular drugs or as part of a new combination regimen. As such, synergistic two, three or four drug combinations comprising of peptides plus rifampicin, isoniazid, ethambutol and pyrazinamde should first be evaluated for their intracellular bactericidal activity using macrophage cell lines. This can be done by enumeration of CFU after treatment with various drug combinations over four and seven days. For MDR-TB, synergistic interactions can be evaluated between peptides and second-line drugs including moxifloxacin, amikacin, kanamycin and streptomycin. Following this, promising drug combinations should be brought forward for further evaluation *in vivo*. Therapeutic efficacy of drug combinations can be determined by enumeration of CFU in the lungs and spleen, and histopathological evaluation of the degree of lung tissue damage [207].

Since the *in vivo* activity of AMPs is affected by the presence of salts, proteins and enzymes in serum, the route of administration could have a profound impact on the bioavailability and in turn, efficacy of peptides at the site of

infection [109]. While first-line anti-tubercular drugs are typically administered orally, therapeutic doses of AMPs have been delivered either subcutaneously, intranasally or intratracheally [32, 207-209]. Furthermore, variation in the dosing frequency and treatment duration between studies raises pertinent questions regarding the ideal therapeutic regimen for AMPs in TB chemotherapy. The pharmacokinetics of synthetic AMPs can be studied by measuring peptide concentrations in plasma, urine, liver, kidney and lung homogenates following administration via the different routes. Samples can be obtained at every 10 min intervals up to 90 min and quantification of peptides can be carried out using a HPLC system couple to a MS (LC-MS) [210]. This would provide information on the drug concentration immediately after administration, the maximum drug concentration achieved, the half-life, volume of distribution and clearance rate. The peptides should be evaluated at two different doses in order to determine which achieves a more favourable therapeutic range (period of time the drug concentration remains over the MIC). With a better understanding of how long a peptide remains in the therapeutic range, the dosing interval can then be adjusted accordingly. Such a systematic comparison of the effect of different administration routes and drug regimens on the dose requirements and pharmacokinetics of synthetic AMPs for effective clearance of TB infection *in vivo* is necessary. This would provide invaluable guidance for the preclinical testing of drug candidates and ensure that promising compounds are fairly evaluated under similar treatment conditions, according to robust and established protocols.

The spread of AMR has compelled the exploration of alternative anti-infective strategies, and modulation of host immunity using immunotherapies is one approach which holds promise [176]. This paradigm shift towards host-directed, rather than pathogen-directed therapies, is beneficial from the standpoint of avoiding selection pressure for microbial resistance development [176]. The use of immunomodulating AMPs, or their inducers, as therapeutic agents in the control of pulmonary TB has been proposed as a promising strategy [211]. As discussed in Chapter 5, the peptides presented in this study do not activate macrophages, implying that the observed intracellular activity was likely due to direct antimicrobial killing rather than immunomodulatory effects. Recently, N-formylation of synthetic peptides was found to significantly improve their immunomodulatory effects, which in turn enhanced H37Rv clearance *in vivo,* both alone and in combination with rifampicin and isoniazid [212]. Hence, this strategy could be exploited to impart the most selective α-helical peptides presented here with immunomodulatory properties. An investigation into the effect of N-formylation on the immunomodulatory activity of synthetic AMPs, followed by both intracellular and *in vivo* efficacy studies can be performed to determine the feasibility of this strategy in augmenting mycobacterial killing. N-formylated peptides including M(LLKK)2M and I(LLKK)2I can be evaluated in combination with rifampicin and isoniazid in animal models and their effectiveness determined by quantifying CFU in the lungs and spleen. Pulmonary histopathological changes following treatment with drug combinations should be compared to both monotherapy and untreated controls

in order to assess their effect on the size and distribution of TB lesions and the extent of granuloma formation.

In conclusion, the findings of this thesis have supported the hypothesis that rationally designed synthetic AMPs, adopting α-helical conformations, are safe and effective in TB mono- and combination therapy, and in the treatment and prevention of drug-resistant biofilms and endotoxemia. While there is immense therapeutic potential for synthetic AMPs in anti-infective applications, several issues including production costs, toxicity and stability need to be overcome. However, with advances in peptide synthesis and drug delivery, it may be sooner rather than later that the first HDP, or synthetic analogues thereof, makes it from the lab to the clinic.

REFERENCES

[1] WHO. Antimicrobial resistance: global report on surveillance 2014. Geneva: WHO; 2014.

[2] O'Neill J. Antimicrobial resistance: tackling a crisis for the health and wealth of nations. Review on antimicrobial resistance. London: Wellcome Trust; 2014.

[3] Ventola CL. The antibiotic resistance crisis: part 1: causes and threats. P T. 2015;40:277.

[4] Liu YY, Wang Y, Walsh TR, Yi LX, Zhang R, Spencer J, et al. Emergence of plasmid-mediated colistin resistance mechanism MCR-1 in animals and human beings in China: a microbiological and molecular biological study. Lancet Infect Dis. 2016;16:161-8.

[5] WHO. Global tuberculosis report 2015. Geneva: WHO; 2015.

[6] WHO. The end TB strategy. Geneva: WHO; 2015.

[7] Esposito S, Bianchini S, Blasi F. Bedaquiline and delamanid in tuberculosis. Expert Opin Pharmacother 2015;16:2319-30.

[8] WHO. Treatment of tuberculosis: guidelines. Geneva: WHO; 2010.

[9] Abubakar I, Zignol M, Falzon D, Raviglione M, Ditiu L, Masham S, et al. Drug-resistant tuberculosis: time for visionary political leadership. Lancet Infect Dis. 2013;13:529-39.

[10] Zumla AI, Gillespie SH, Hoelscher M, Philips PP, Cole ST, Abubakar I, et al. New antituberculosis drugs, regimens, and adjunct therapies: needs, advances, and future prospects. Lancet Infect Dis. 2014;14:327-40.

[11] Wong EB, Cohen KA, Bishai WR. Rising to the challenge: new therapies for tuberculosis. Trends Microbiol. 2013;21:493-501.

[12] Lewis K. Platforms for antibiotic discovery. Nat Rev Drug Discov. 2013;12:371-87.

[13] Brown ED, Wright GD. Antibacterial drug discovery in the resistance era. Nature. 2016;529:336-43.

[14] O'Neill J. Securing new drugs for future generations: the pipeline for antibiotics. Review on antimicrobial resistance. London: Wellcome Trust; 2015.

[15] The Pew Charitable Trusts. The critical need for new antibiotics. The Pew Charitable Trusts; 2016. Available from URL: http://www.pewtrusts.org/en/multimedia/data-visualizations/2016/the-critical-need-for-new-antibiotics.

[16] Hay M, Thomas DW, Craighead JL, Economides C, Rosenthal J. Clinical development success rates for investigational drugs. Nat Biotechnol. 2014;32:40-51.

[17] Steiner H, Hultmark D, Engström A, Bennich H, Boman HG. Sequence and specificity of two antibacterial proteins involved in insect immunity. Nature. 1981;292:246-8.

[18] Ganz T, Selsted ME, Szklarek D, Harwig SS, Daher K, Bainton DF, et al. Defensins. Natural peptide antibiotics of human neutrophils. J Clin Invest. 1985;76:1427.

[19] Zasloff M. Magainins, a class of antimicrobial peptides from Xenopus skin: isolation, characterization of two active forms, and partial cDNA sequence of a precursor. Proc Natl Acad Sci USA. 1987;84:5449-53.

[20] Jenssen H, Hamill P, Hancock RE. Peptide antimicrobial agents. Clin Microbiol Rev. 2006;19:491-511.

[21] Zasloff M. Antimicrobial peptides of multicellular organisms. Nature. 2002;415:389-95.

[22] Hancock RE, Sahl HG. Antimicrobial and host-defense peptides as new anti-infective therapeutic strategies. Nat Biotechnol. 2006;24:1551-7.

[23] Brogden KA. Antimicrobial peptides: pore formers or metabolic inhibitors in bacteria? Nat Rev Microbiol. 2005;3:238-50.

[24] Hancock RE, Patrzykat A. Clinical development of cationic antimicrobial peptides: from natural to novel antibiotics. Curr Drug Targets: Infect Disord. 2002;2:79-83.

[25] Peschel A, Sahl HG. The co-evolution of host cationic antimicrobial peptides and microbial resistance. Nat Rev Microbiol. 2006;4:529-36.

[26] Ong ZY, Wiradharma N, Yang YY. Strategies employed in the design and optimization of synthetic antimicrobial peptide amphiphiles with enhanced therapeutic potentials. Adv Drug Delivery Rev. 2014;78:28-45.

[27] Lai Y, Gallo RL. AMPed up immunity: how antimicrobial peptides have multiple roles in immune defense. Trends Immunol. 2009;30:131-41.

[28] Travis SM, Anderson NN, Forsyth WR, Espiritu C, Conway BD, Greenberg EP, et al. Bactericidal activity of mammalian cathelicidin-derived peptides. Infect Immun. 2000;68:2748-55.

[29] Feng X, Sambanthamoorthy K, Palys T, Paranavitana C. The human antimicrobial peptide LL-37 and its fragments possess both antimicrobial and antibiofilm activities against multidrug-resistant *Acinetobacter baumannii*. Peptides. 2013;49:131-7.

[30] Linde CM, Hoffner SE, Refai E, Andersson M. *In vitro* activity of PR-39, a proline-arginine-rich peptide, against susceptible and multidrug-resistant *Mycobacterium tuberculosis*. J Antimicrob Chemother. 2001;47:575-80.

[31] Sonawane A, Santos JC, Mishra BB, Jena P, Progida C, Sorensen OE, et al. Cathelicidin is involved in the intracellular killing of mycobacteria in macrophages. Cell Microbiol. 2011;13:1601-17.

[32] Rivas-Santiago B, Rivas Santiago CE, Castañeda-Delgado JE, León–Contreras JC, Hancock RE, Hernandez-Pando R. Activity of LL-37, CRAMP and antimicrobial peptide-derived compounds E2, E6 and CP26 against *Mycobacterium tuberculosis*. Int J Antimicrob Agents. 2013;41:143-8.

[33] Sharma S, Verma I, Khuller GK. Biochemical interaction of human neutrophil peptide-1 with *Mycobacterium tuberculosis* H37Ra. Arch Microbiol. 1999;171:338-42.

[34] Ogata K, Linzer BA, Zuberi RI, Ganz T, Lehrer RI, Catanzaro A. Activity of defensins from human neutrophilic granulocytes against *Mycobacterium avium-Mycobacterium intracellulare*. Infect Immun. 1992;60:4720-5.

[35] Sharma S, Verma I, Khuller GK. Antibacterial activity of human neutrophil peptide-1 against *Mycobacterium tuberculosis* H37Rv: *in vitro* and *ex vivo* study. Eur Respir J 2000;16:112-7.

[36] Sharma S, Verma I, Khuller GK. Therapeutic potential of human neutrophil peptide 1 against experimental tuberculosis. Antimicrob Agents Chemother. 2001;45:639-40.

[37] Singh PK, Jia HP, Wiles K, Hesselberth J, Liu L, Conway BA, et al. Production of β-defensins by human airway epithelia. Proc Natl Acad Sci USA. 1998;95:14961-6.

[38] Maisetta G, Batoni G, Esin S, Florio W, Bottai D, Favilli F, et al. In vitro bactericidal activity of human β-defensin 3 against multidrug-resistant nosocomial strains. Antimicrob Agents Chemother. 2006;50:806-9.

[39] Chen X, Niyonsaba F, Ushio H, Okuda D, Nagaoka I, Ikeda S, et al. Synergistic effect of antibacterial agents human β-defensins, cathelicidin LL-37 and lysozyme against *Staphylococcus aureus* and *Escherichia coli*. J Dermatol Sci. 2005;40:123-32.

[40] Nagaoka I, Hirota S, Yomogida S, Ohwada A, Hirata M. Synergistic actions of antibacterial neutrophil defensins and cathelicidins. Inflamm Res. 2000;49:73-9.

[41] Niyonsaba F, Iwabuchi K, Someya A, Hirata M, Matsuda H, Ogawa H, et al. A cathelicidin family of human antibacterial peptide LL-37 induces mast cell chemotaxis. Immunology. 2002;106:20-6.

[42] Yang D, Chertov O, Bykovskaia SN, Chen Q, Buffo MJ, Shogan J, et al. β-Defensins: linking innate and adaptive immunity through dendritic and T cell CCR6. Science. 1999;286:525-8.

[43] Yang D, Chen Q, Schmidt AP, Anderson GM, Wang JM, Wooters J, et al. LL-37, the neutrophil granule- and epithelial cell-derived cathelicidin, utilizes formyl peptide receptor-like 1 (FPRL1) as a receptor to chemoattract human peripheral blood neutrophils, monocytes, and T cells. J Exp Med. 2000;192:1069-74.

[44] Yang D, Chen Q, Chertov O, Oppenheim JJ. Human neutrophil defensins selectively chemoattract naive T and immature dendritic cells. J Leukoc Biol. 2000;68:9-14.

[45] Territo MC, Ganz T, Selsted ME, Lehrer R. Monocyte-chemotactic activity of defensins from human neutrophils. J Clin Invest. 1989;84:2017.

[46] Grigat J, Soruri A, Forssmann U, Riggert J, Zwirner J. Chemoattraction of macrophages, T lymphocytes, and mast cells is evolutionarily conserved within the human α-defensin family. J Immunol. 2007;179:3958-65.

[47] Scott MG, Davidson DJ, Gold MR, Bowdish D, Hancock RE. The human antimicrobial peptide LL-37 is a multifunctional modulator of innate immune responses. J Immunol. 2002;169:3883-91.

[48] Chaly YV, Paleolog EM, Kolesnikova TS, Tikhonov I, Petratchenko EV, Voitenok NN. Neutrophil α-defensin human neutrophil peptide modulates cytoline production in human monocytes and adhesion molecule expression in endothelial cells. Eur Cytokine Netw. 2000;11:257-66.

[49] Niyonsaba F, Ushio H, Nakano N, Ng W, Sayama K, Hashimoto K, et al. Antimicrobial peptides human β-defensins stimulate epidermal keratinocyte migration, proliferation and production of proinflammatory cytokines and chemokines. J Invest Dermatol. 2006;127:594-604.

[50] Haney EF, Hancock RE. Peptide design for antimicrobial and immunomodulatory applications. Biopolymers. 2013;100:572-83.

[51] Yeung AT, Gellatly SL, Hancock RE. Multifunctional cationic host defence peptides and their clinical applications. Cell Mol Life Sci. 2011;68:2161-76.

[52] Marr AK, Gooderham WJ, Hancock RE. Antibacterial peptides for therapeutic use: obstacles and realistic outlook. Curr Opin Pharmacol. 2006;6:468-72.

[53] Ge Y, MacDonald DL, Holroyd KJ, Thornsberry C, Wexler H, Zasloff M. *In vitro* antibacterial properties of pexiganan, an analog of magainin. Antimicrob Agents Chemother. 1999;43:782-8.

[54] Steinberg DA, Hurst MA, Fujii CA, Kung AH, Ho JF, Cheng FC, et al. Protegrin-1: a broad-spectrum, rapidly microbicidal peptide with *in vivo* activity. Antimicrob Agents Chemother. 1997;41:1738-42.

[55] Perron GG, Zasloff M, Bell G. Experimental evolution of resistance to an antimicrobial peptide. Proc Biol Sci. 2006;273:251-6.

[56] Fox JL. Antimicrobial peptides stage a comeback. Nat Biotechnol. 2013;31:379-82.

[57] Kollef M, Pittet D, Sanchez Garcia M, Chastre J, Fagon JY, Bonten M, et al. A randomized double-blind trial of iseganan in prevention of ventilator-associated pneumonia. Am J Respir Crit Care Med. 2006;173:91-7.

[58] van Saene H, van Saene J, Silvestri L, de la Cal M, Sarginson R, Zandstra D. Iseganan failure due to the wrong pharmaceutical technology. Chest. 2007;132:1412.

[59] Zasloff M. Antimicrobial peptides: Do they have a future as therapeutics? In: Harder J, Schröder JM, editors. Antimicrobial peptides: Role in human health and disease. Switzerland: Springer International Publishing; 2016. p. 147-54.

[60] Ashby M, Petkova A, Hilpert K. Cationic antimicrobial peptides as potential new therapeutic agents in neonates and children: a review. Curr Opin Infect Dis. 2014;27:258-67.

[61] Khara JS, Ee PL. Nature-inspired multifunctional host defense peptides with dual antimicrobial-immunomodulatory activities. In: Santambrogio L, editor. Biomaterials in Regenerative Medicine and the Immune System. Switzerland: Springer International Publishing; 2015. p. 95-112.

[62] Uhlig T, Kyprianou T, Martinelli FG, Oppici CA, Heiligers D, Hills D, et al. The emergence of peptides in the pharmaceutical business: From exploration to exploitation. EuPA Open Proteom. 2014;4:58-69.

[63] Salunke DB, Hazra BG, Pore VS. Steroidal conjugates and their pharmacological applications. Curr Med Chem. 2006;13:813-47.

[64] Rozansky R, Bachrach U, Grossowicz N. Studies on the antibacterial action of spermine. J Gen Microbiol. 1954;10:11-6.

[65] Bucki R, Leszczyńska K, Byfield FJ, Fein DE, Won E, Cruz K, et al. Combined antibacterial and anti-inflammatory activity of a cationic disubstituted dexamethasone-spermine conjugate. Antimicrob Agents Chemother. 2010;54:2525-33.

[66] Wang Y, Ke XY, Khara JS, Bahety P, Liu S, Seow SV, et al. Synthetic modifications of the immunomodulating peptide thymopentin to confer anti-mycobacterial activity. Biomaterials. 2014;35:3102-9.

[67] Majerle A, Kidrič J, Jerala R. Enhancement of antibacterial and lipopolysaccharide binding activities of a human lactoferrin peptide fragment by the addition of acyl chain. J Antimicrob Chemother. 2003;51:1159-65.

[68] Liu Y, Xia X, Xu L, Wang Y. Design of hybrid β-hairpin peptides with enhanced cell specificity and potent anti-inflammatory activity. Biomaterials. 2013;34:237-50.

[69] Bhunia A, Mohanram H, Domadia PN, Torres J, Bhattacharjya S. Designed β-boomerang antiendotoxic and antimicrobial peptides: structures and activities in lipopolysaccharide J Biol Chem. 2009;284:21991-2004.

[70] Mohanram H, Bhattacharjya S. Resurrecting inactive antimicrobial peptides from the lipopolysaccharide trap. Antimicrob Agents Chemother. 2014;58:1987-96.

[71] Scudiero O, Galdiero S, Cantisani M, Di Noto R, Vitiello M, Galdiero M, et al. Novel synthetic, salt-resistant analogs of human beta-defensins 1 and 3 endowed with enhanced antimicrobial activity. Antimicrob Agents Chemother 2010;54:2312-22.

[72] Beckloff N, Laube D, Castro T, Furgang D, Park S, Perlin D, et al. Activity of an antimicrobial peptide mimetic against planktonic and biofilm cultures of oral pathogens. Antimicrob Agents Chemother. 2007;51:4125-32.

[73] Hua J, Scott RW, Diamond G. Activity of antimicrobial peptide mimetics in the oral cavity: II. Activity against periopathogenic biofilms and anti-inflammatory activity. Mol Oral Microbiol. 2010;25:426-32.

[74] Leszczyńska K, Namiot D, Byfield FJ, Cruz K, Żendzian-Piotrowska M, Fein DE, et al. Antibacterial activity of the human host defence peptide LL-37 and selected synthetic cationic lipids against bacteria associated with oral and upper respiratory tract infections. J Antimicrob Chemother. 2013;68:610-8.

[75] Murugan RN, Jacob B, Ahn M, Hwang E, Sohn H, Park HN, et al. *De novo* design and synthesis of ultra-short peptidomimetic antibiotics having dual antimicrobial and anti-Inflammatory activities. PloS One. 2013;8:e80025.

[76] Padhee S, Smith C, Wu H, Li Y, Manoj N, Qiao Q, et al. The development of antimicrobial α-AApeptides that suppress proinflammatory immune responses. Chembiochem. 2014;15:688-94.

[77] Matsuzaki K. Control of cell selectivity of antimicrobial peptides. Biochim Biophys Acta. 2009;1788:1687-92.

[78] Lee EK, Kim YC, Nan YH, Shin SY. Cell selectivity, mechanism of action and LPS-neutralizing activity of bovine myeloid antimicrobial peptide-18 (BMAP-18) and its analogs. Peptides. 2011;32:1123-30.

[79] Nan YH, Bang JK, Jacob B, Park IS, Shin SY. Prokaryotic selectivity and LPS-neutralizing activity of short antimicrobial peptides designed from the human antimicrobial peptide LL-37. Peptides. 2012;35:239-47.

[80] Wang G, Elliott M, Cogen AL, Ezell EL, Gallo RL, Hancock RE. Structure, dynamics, and antimicrobial and immune modulatory activities of human LL-23 and its single-residue variants mutated on the basis of homologous primate cathelicidins. Biochemistry. 2012;51:653-64.

[81] Lee E, Kim JK, Shin S, Jeong KW, Lee J, Lee DG, et al. Enantiomeric 9-mer peptide analogs of protaetiamycine with bacterial cell selectivities and anti-inflammatory activities. J Pept Sci. 2011;17:675-82.

[82] Wang P, Nan YH, Yang ST, Kang SW, Kim Y, Park IS, et al. Cell selectivity and anti-inflammatory activity of a Leu/Lys-rich α-helical model antimicrobial peptide and its diastereomeric peptides. Peptides. 2010;31:1251-61.

[83] Wei L, Wu J, Liu H, Yang H, Rong M, Li D, et al. A mycobacteriophage-derived trehalose-6, 6'-dimycolate-binding peptide containing both antimycobacterial and anti-inflammatory abilities. FASEB J. 2013;27:3067-77.

[84] Chan DI, Prenner EJ, Vogel HJ. Tryptophan-and arginine-rich antimicrobial peptides: structures and mechanisms of action. Biochim Biophys Acta. 2006;1758:1184-202.

[85] Park KH, Nan YH, Park Y, Kim JI, Park IS, Hahm KS, et al. Cell specificity, anti-inflammatory activity, and plausible bactericidal mechanism of designed Trp-rich model antimicrobial peptides. Biochim Biophys Acta. 2009;1788:1193-203.

[86] Strøm MB, Rekdal Ø, Svendsen JS. Antimicrobial activity of short arginine-and tryptophan-rich peptides. J Pept Sci. 2002;8:431-7.

[87] Strøm MB, Haug BE, Skar ML, Stensen W, Stiberg T, Svendsen JS. The pharmacophore of short cationic antibacterial peptides. J Med Chem. 2003;46:1567-70.

[88] Loose C, Jensen K, Rigoutsos I, Stephanopoulos G. A linguistic model for the rational design of antimicrobial peptides. Nature. 2006;443:867-9.

[89] Pauling L, Corey RB, Branson HR. The structure of proteins: two hydrogen-bonded helical configurations of the polypeptide chain. Proc Natl Acad Sci USA. 1951;37:205-11.

[90] Eisenberg D, Weiss RM, Terwilliger TC. The hydrophobic moment detects periodicity in protein hydrophobicity. Proc Natl Acad Sci USA. 1984;81:140-4.

[91] DeGrado WF, Lear JD. Induction of peptide conformation at apolar water interfaces. 1. A study with model peptides of defined hydrophobic periodicity. J Am Chem Soc. 1985;107:7684-9.

[92] O'Neil KT, DeGrado WF. A thermodynamic scale for the helix-forming tendencies of the commonly occurring amino acids. Science. 1990;250:646-51.

[93] Wiradharma N, Khoe U, Hauser CA, Seow SV, Zhang S, Yang YY. Synthetic cationic amphiphilic α-helical peptides as antimicrobial agents. Biomaterials. 2011;32:2204-12.

[94] Yomogida S, Nagaoka I, Yamashita T. Involvement of cysteine residues in the biological activity of the active fragments of guinea pig neutrophil cationic peptides. Infect Immun. 1995;63:2344-6.

[95] Wiradharma N, Khan M, Yong LK, Hauser CA, Seow SV, Zhang S, et al. The effect of thiol functional group incorporation into cationic helical peptides on antimicrobial activities and spectra. Biomaterials. 2011;32:9100-8.

[96] Javadpour MM, Juban MM, Lo WC, Bishop SM, Alberty JB, Cowell SM, et al. *De novo* antimicrobial peptides with low mammalian cell toxicity. J Med Chem. 1996;39:3107-13.

[97] Ong ZY, Gao SJ, Yang YY. Short synthetic β-sheet forming peptide amphiphiles as broad spectrum antimicrobials with antibiofilm and endotoxin neutralizing capabilities. Adv Funct Mater. 2013;23:3682-92.

[98] Dong N, Ma Q, Shan A, Lv Y, Hu W, Gu Y, et al. Strand length-dependent antimicrobial activity and membrane-active mechanism of arginine- and valine-rich β-hairpin-like antimicrobial peptides. Antimicrob Agents Chemother. 2012;56:2994-3003.

[99] Dong N, Zhu X, Chou S, Shan A, Li W, Jiang J. Antimicrobial potency and selectivity of simplified symmetric-end peptides. Biomaterials. 2014;35:8028-39.

[100] Chou S, Shao C, Wang J, Shan A, Xu L, Dong N, et al. Short, multiple-stranded β-hairpin peptides have antimicrobial potency with high selectivity and salt resistance. Acta Biomater. 2016;30:78-93.

[101] Frecer V, Ho B, Ding JL. *De novo* design of potent antimicrobial peptides. Antimicrob Agents Chemother. 2004;48:3349-57.

[102] Fjell CD, Hiss JA, Hancock RE, Schneider G. Designing antimicrobial peptides: form follows function. Nat Rev Drug Discov. 2011;11:37-51.

[103] Bratt CL, Kohlgraf KG, Yohnke K, Kummet C, Dawson DV, Brogden KA. Communication: antimicrobial activity of SMAP28 with a targeting domain for *Porphyromonas gingivalis*. Probiotics Antimicrob Proteins. 2010;2:21-5.

[104] Bell G, Gouyon PH. Arming the enemy: the evolution of resistance to self-proteins. Microbiology. 2003;149:1367-75.

[105] Hancock RE, Lehrer R. Cationic peptides: a new source of antibiotics. Trends Biotechnol. 1998;16:82-8.

[106] Ong ZY, Cheng J, Huang Y, Xu K, Ji Z, Fan W, et al. Effect of stereochemistry, chain length and sequence pattern on antimicrobial properties of short synthetic β-sheet forming peptide amphiphiles. Biomaterials. 2014;35:1315-25.

[107] Baltzer SA, Brown MH. Antimicrobial peptides:promising alternatives to conventional antibiotics. J Mol Microbiol Biotechnol. 2011;20:228-35.

[108] Brogden NK, Brogden KA. Will new generations of modified antimicrobial peptides improve their potential as pharmaceuticals? Int J Antimicrob Agents. 2011;38:217-25.

[109] Silva JP, Appelberg R, Gama FM. Antimicrobial peptides as novel anti-tuberculosis therapeutics. Biotechnol Adv. 2016;35:924-40.

[110] Snewin VA, Gares MP, Gaora PO, Hasan Z, Brown IN, Young DB. Assessment of immunity to mycobacterial infection with luciferase reporter constructs. Infect Immun. 1999;67:4586-93.

[111] Carroll P, Schreuder LJ, Muwanguzi-Karugaba J, Wiles S, Robertson BD, Ripoll J, et al. Sensitive detection of gene expression in mycobacteria under replicating and non-replicating conditions using optimized far-red reporters. PLoS One. 2010;5:e9823.

[112] Parish T, Stoker NG. Electroporation of mycobacteria. In: Parish T, Stoker NG, editors. Mycobacteria Protocols. Totowa, NJ, USA: Humana Press; 1998. p. 129-44.

[113] Liu L, Xu K, Wang H, Tan PJ, Fan W, Venkatraman SS, et al. Self-assembled cationic peptide nanoparticles as an efficient antimicrobial agent. Nat Nanotechnol. 2009;4:457-63.

[114] Wang H, Xu K, Liu L, Tan JP, Chen Y, Li Y, et al. The efficacy of self-assembled cationic antimicrobial peptide nanoparticles against *Cryptococcus neoformans* for the treatment of meningitis. Biomaterials. 2010;31:2874-81.

[115] Rand K, Houck H, Brown P, Bennett D. Reproducibility of the microdilution checkerboard method for antibiotic synergy. Antimicrob Agents Chemother. 1993;37:613-5.

[116] Jacobs DS, DeMott WR, Oxley DK. Jacobs & DeMott laboratory test handbook with key word index. 5th ed. Hudson, OH: Lexi Comp; 2001.

[117] Eliopoulos GM, Moellering RC. Antibiotic combinations. 3rd ed. Baltimore, MD: The Williams & Wilkins Co.; 1991.

[118] Wilkinson RJ, Patel P, Llewelyn M, Hirsch CS, Pasvol G, Snounou G, et al. Influence of polymorphism in the genes for the interleukin (IL)-1 receptor antagonist and IL-1β on tuberculosis. J Exp Med. 1999;189:1863-74.

[119] Kim H, Jang JH, Kim SC, Cho JH. *De novo* generation of short antimicrobial peptides with enhanced stability and cell specificity. J Antimicrob Chemother. 2014;69:121-32.

[120] Haney EF, Mansour SC, Hilchie AL, de la Fuente-Núñez C, Hancock RE. High throughput screening methods for assessing antibiofilm and immunomodulatory activities of synthetic peptides. Peptides. 2015;71:276-85.

[121] Segev-Zarko L, Saar-Dover R, Brumfeld V, Mangoni ML, Shai Y. Mechanisms of biofilm inhibition and degradation by antimicrobial peptides. Biochem J. 2015;468:259-70.

[122] Karsi A, Menanteau-Ledouble S, Lawrence ML. Development of bioluminescent *Edwardsiella ictaluri* for noninvasive disease monitoring. FEMS Microbiol Lett. 2006;260:216-23.

[123] Koshlukova SE, Lloyd TL, Araujo MW, Edgerton M. Salivary histatin 5 induces non-lytic release of ATP from *Candida albicans* leading to cell death. J Biol Chem. 1999;274:18872-9.

[124] Lienkamp K, Madkour AE, Kumar KN, Nüsslein K, Tew GN. Antimicrobial polymers prepared by ring-opening metathesis polymerization: manipulating antimicrobial properties by organic counterion and charge density variation. Chemistry. 2009;15:11715-22.

[125] EMD Millipore Corporation. User Guide CellASIC® ONIX B04A-03 Microfluidic Bacteria Plates. EMD Millipore Corporation; 2014.

[126] Matsuzaki K. Why and how are peptide-lipid interactions utilized for self-defense? Magainins and tachyplesins as archetypes. Biochim Biophys Acta. 1999;1462:10.

[127] Shai Y. Mechanism of the binding, insertion and destabilization of phospholipid bilayer membranes by a-helical antimicrobial and cell non-selective membrane-lytic peptides. Biochim Biophys Acta. 1999;1462:55-70.

[128] Yang L, Weiss TM, Lehrer RI, Huang HW. Crystallization of antimicrobial pores in membranes: magainin and protegrin. Biophys J. 2000;79:2002-9.

[129] Corrales-Garcia L, Ortiz E, Castañeda-Delgado J, Rivas-Santiago B, Corzo G. Bacterial expression and antibiotic activities of recombinant variants of human β-defensins on pathogenic bacteria and *M. tuberculosis*. Protein Expres Purif. 2013;89:33-43.

[130] Fattorini L, Gennaro R, Zanetti M, Tan D, Brunori L, Giannoni F, et al. In vitro activity of protegrin-1 and beta-defensin-1, alone and in combination with isoniazid, against *Mycobacterium tuberculosis*. Peptides. 2004;25:1075-7.

[131] Chingaté S, Delgado G, Salazar LM, Soto CY. The ATPase activity of the mycobacterial plasma membrane is inhibited by the LL37-analogous peptide LLAP. Peptides. 2015;71:222-8.

[132] Ernst WA, Thoma-Uszynski S, Teitelbaum R, Ko C, Hanson DA, Clayberger C, et al. Granulysin, a T cell product, kills bacteria by altering membrane permeability. J Immunol. 2000;165:7102-8.

[133] Nguyen LT, Chau JK, Perry NA, De Boer L, Zaat SA, Vogel HJ. Serum stabilities of short tryptophan-and arginine-rich antimicrobial peptide analogs. PLoS One. 2010;5:e12684.

[134] Dos Santos Cabrera MP, Arcisio-Miranda M, Costa SB, Konno K, Ruggiero JR, Procopio J, et al. Study of the mechanism of action of anoplin, α-helical antimicrobial decapeptide with ion channel-like activity, and the role of the amidated C-terminus. J Pept Sci. 2008;14:661-9.

[135] Estieu-Gionnet K, Guichard G. Stabilized helical peptides: overview of the technologies and therapeutic promises. Expert Opin Drug Discov. 2011;6:937-63.

[136] Chen Y, Mant CT, Farmer SW, Hancock RE, Vasil ML, Hodges R. Rational design of alpha-helical antimicrobial peptides with enhanced activities and specificity/therapeutic index. J Biol Chem. 2005;280:12316-29.

[137] Chen Y, Guarnieri MT, Vasil AI, Vasil ML, Mant CT, Hodges RS. Role of peptide hydrophobicity in the mechanism of action of α-helical antimicrobial peptides. Antimicrob Agents Chemother. 2007;51:1398-406.

[138] Guerrero E, Saugar JM, Matsuzaki K, Rivas L. Role of positional hydrophobicity in the leishmanicidal activity of magainin 2. Antimicrob Agents Chemother. 2004;48:2980-6.

[139] Lee DG, Kim HN, Park Y, Kim HK, Choi BH, Choi CH, et al. Design of novel analogue peptides with potent antibiotic activity based on the antimicrobial peptide, HP (2-20), derived from N-terminus of *Helicobacter pylori* ribosomal protein L1. Biochim Biophys Acta. 2002;1598:185-94.

[140] Dathe M, Schümann M, Wieprecht T, Winkler A, Beyermann M, Krause E, et al. Peptide helicity and membrane surface charge modulate the balance of electrostatic and hydrophobic interactions with lipid bilayers and biological membranes. Biochemistry. 1996;35:12612-22.

[141] Ramaswamy S, Musser JM. Molecular genetic basis of antimicrobial agent resistance in *Mycobacterium tuberculosi*s: 1998 update. Tuber Lung Dis. 1998;79:3-29.

[142] Barry AL, Craig WA, Nadler H, Reller LB, Sanders CC, Swenson JM. Methods for determining bactericidal activity of antimicrobial agents; approved guideline. NCCLS document M26-A. 1999;19.

[143] Sader HS, Fedler KA, Rennie RP, Stevens S, Jones RN. Omiganan pentahydrochloride (MBI 226), a topical 12-amino-acid cationic peptide: spectrum of antimicrobial activity and measurements of bactericidal activity. Antimicrob Agents Chemother. 2004;48:3112-8.

[144] Anantharaman A, Rizvi MS, Sahal D. Synergy with rifampin and kanamycin enhances potency, kill kinetics, and selectivity of *de novo*-designed antimicrobial peptides. Antimicrob Agents Chemother. 2010;54:1693-9.

[145] Cirioni O, Silvestri C, Ghiselli R, Orlando F, Riva A, Mocchegiani F, et al. Protective effects of the combination of α-helical antimicrobial peptides and rifampicin in three rat models of *Pseudomonas aeruginosa* infection. J Antimicrob Chemother. 2008;62:1332-8.

[146] Mangoni ML, Rinaldi AC, Di Giulio A, Mignogna G, Bozzi A, Barra D, et al. Structure-function relationships of temporins, small antimicrobial peptides from amphibian skin. Eur J Biochem. 2000;267:1447-54.

[147] Fu LM, Fu-Liu CS. Is *Mycobacterium tuberculosis* a closer relative to Gram-positive or Gram–negative bacterial pathogens? Tuberculosis. 2002;82:85-90.

[148] Brennan PJ, Nikaido H. The envelope of mycobacteria. Annu Rev Biochem. 1995;64:29-63.

[149] Hett EC, Rubin EJ. Bacterial growth and cell division: a mycobacterial perspective. Microbiol Mol Biol Rev. 2008;72:126-56.

[150] Cook GM, Berney M, Gebhard S, Heinemann M, Cox RA, Danilchanka O, et al. Physiology of mycobacteria. Adv Microb Physiol. 2009;55:81-319.

[151] Favrot L, Ronning DR. Targeting the mycobacterial envelope for tuberculosis drug development. Expert Rev Anti Infect Ther. 2012;10:1023-36.

[152] Trias J, Benz R. Permeability of the cell wall of *Mycobacterium smegmatis*. Mol Microbiol. 1994;14:283-90.

[153] Yajko DM, Sanders CA, Nassos PS, Hadley WK. In vitro susceptibility of *Mycobacterium avium* complex to the new fluoroquinolone sparfloxacin (CI-978; AT-4140) and comparison with ciprofloxacin. Antimicrob Agents Chemother. 1990;34:2442-4.

[154] Haemers A, Leysen DC, Bollaert W, Zhang MQ, Pattyn SR. Influence of N substitution on antimycobacterial activity of ciprofloxacin. Antimicrob Agents Chemother. 1990;34:496-7.

[155] Rastogi N, Goh KS. Action of 1-isonicotinyl-2-palmitoyl hydrazine against the *Mycobacterium avium* complex and enhancement of its activity by m-fluorophenylalanine. Antimicrob Agents Chemother. 1990;34:2061-4.

[156] Meng H, Kumar K. Antimicrobial activity and protease stability of peptides containing fluorinated amino acids. J Am Chem Soc. 2007;129:15615-22.

[157] Radzishevsky IS, Rotem S, Zaknoon F, Gaidukov L, Dagan A, Mor A. Effects of acyl versus aminoacyl conjugation on the properties of antimicrobial peptides. Antimicrob Agents Chemother. 2005;49:2412-20.

[158] Jiang Z, Higgins MP, Whitehurst J, Kisich KO, Voskuil MI, Hodges RS. Anti-tuberculosis activity of α-helical antimicrobial peptides: *de novo* designed L- and D-enantiomers versus L-and D-LL37. Protein Pept Lett. 2011;18:241.

[159] Dathe M, Wieprecht T. Structural features of helical antimicrobial peptides: their potential to modulate activity on model membranes and biological cells. Biochim Biophys Acta. 1999;1462:71-87.

[160] Chin DH, Woody RW, Rohl CA, Baldwin RL. Circular dichroism spectra of short, fixed-nucleus alanine helices. Proc Natl Acad Sci USA. 2002;99:15416-21.

[161] Shepherd NE, Hoang HN, Abbenante G, Fairlie DP. Single turn peptide alpha helices with exceptional stability in water. J Am Chem Soc. 2005;127:2974-83.

[162] Luo P, Baldwin RL. Mechanism of helix induction by trifluoroethanol: a framework for extrapolating the helix-forming properties of peptides from trifluoroethanol/water mixtures back to water. Biochemistry. 1997;36:8413-21.

[163] Jiang Z, Kullberg BJ, Van Der Lee H, Vasil AI, Hale JD, Mant CT, et al. Effects of hydrophobicity on the antifungal activity of α-helical antimicrobial peptides. Chem Biol Drug Des. 2008;72:483-95.

[164] Zimmerman SS, Scheraga HA. Influence of local interactions on protein structure. I. Conformational energy studies of N-acetyl-N'-methylamides of Pro-X and X-Pro dipeptides. Biopolymers. 1977;16:811-43.

[165] Piela L, Némethy G, Scheraga HA. Proline-induced constraints in α-helices. Biopolymers. 1987;26:1587-600.

[166] Kumar S, Bansal M. Dissecting α-helices: position-specific analysis of α-helices in globular proteins. Proteins. 1998;31:460-76.

[167] Kim MK, Kang YK. Positional preference of proline in α-helices. Protein Sci 1999;8:1492-9.

[168] Giangaspero A, Sandri L, Tossi A. Amphipathic α helical antimicrobial peptides. Eur J Biochem. 2001;268:5589-600.

[169] Vermeer LS, Lan Y, Abbate V, Ruh E, Bui TT, Wilkinson LJ, et al. Conformational flexibility determines selectivity and antibacterial, antiplasmodial, and anticancer potency of cationic α-helical peptides. J Biol Chem. 2012;287:34120-33.

[170] Tachi T, Epand RF, Epand RM, Matsuzaki K. Position-dependent hydrophobicity of the antimicrobial magainin peptide affects the mode of peptide-lipid interactions and selective toxicity. Biochemistry. 2002;41:10723-31.

[171] Wieprecht T, Dathe M, Beyermann M, Krause E, Maloy WL, MacDonald DL, et al. Peptide hydrophobicity controls the activity and selectivity of magainin 2 amide in interaction with membranes. Biochemistry. 1997;36:6124-32.

[172] Jacob B, Park IS, Bang JK, Shin SY. Short KR-12 analogs designed from human cathelicidin LL-37 possessing both antimicrobial and antiendotoxic activities without mammalian cell toxicity. J Pept Sci. 2013;19:700-7.

[173] Gabriel GJ, Madkour AE, Dabkowski JM, Nelson CF, Nüsslein K, Tew GN. Synthetic mimic of antimicrobial peptide with nonmembrane-disrupting antibacterial properties. Biomacromolecules. 2008;9:2980-3.

[174] Wu M, Hancock RE. Interaction of the cyclic antimicrobial cationic peptide bactenecin with the outer and cytoplasmic membrane. J Biol Chem. 1999;274:29-35.

[175] Travis J, Potempa J, Maeda H. Are bacterial proteinases pathogenic factors? Trends Microbiol. 1995;3:405-7.

[176] Hancock RE, Nijnik A, Philpott DJ. Modulating immunity as a therapy for bacterial infections. Nat Rev Microbiol. 2012;10:243-54.

[177] Schmidtchen A, Frick IM, Andersson E, Tapper H, Björck L. Proteinases of common pathogenic bacteria degrade and inactivate the antibacterial peptide LL-37. Mol Microbiol. 2002;46:157-68.

[178] Sieprawska-Lupa M, Mydel P, Krawczyk K, Wójcik K, Puklo M, Lupa B, et al. Degradation of human antimicrobial peptide LL-37 by *Staphylococcus aureus*-derived proteinases. Antimicrob Agents Chemother. 2004;48:4673-9.

[179] Wade D, Boman A, Wåhlin B, Drain C, Andreu D, Boman HG, et al. All-D amino acid-containing channel-forming antibiotic peptides. Proc Natl Acad Sci USA. 1990;87:4761-5.

[180] Merrifield R, Juvvadi P, Andreu D, Ubach J, Boman A, Boman HG. Retro and retroenantio analogs of cecropin-melittin hybrids. Proc Natl Acad Sci USA. 1995;92:3449-53.

[181] Hong SY, Oh JE, Lee KH. Effect of D-amino acid substitution on the stability, the secondary structure, and the activity of membrane-active peptide. Biochem Pharmacol. 1999;58:1775-80.

[182] Falciani C, Lozzi L, Pollini S, Luca V, Carnicelli V, Brunetti J, et al. Isomerization of an antimicrobial peptide broadens antimicrobial spectrum to Gram-positive bacterial pathogens. PLoS One. 2012;7: e46259.

[183] Strömstedt AA, Pasupuleti M, Schmidtchen A, Malmsten M. Evaluation of strategies for improving proteolytic resistance of antimicrobial peptides by using variants of EFK17, an internal segment of LL-37. Antimicrob Agents Chemother. 2009;53:593-602.

[184] Silva T, Magalhães B, Maia S, Gomes P, Nazmi K, Bolscher JG, et al. Killing of *Mycobacterium avium* by lactoferricin peptides: improved activity of arginine-and D-amino-acid-containing molecules. Antimicrob Agents Chemother. 2014;58:3461-7.

[185] Raynaud C, Etienne G, Peyron P, Lanéelle MA, Daffé M. Extracellular enzyme activities potentially involved in the pathogenicity of *Mycobacterium tuberculosis*. Microbiology. 1998;144:577-87.

[186] Carmona G, Rodriguez A, Juarez D, Corzo G, Villegas E. Improved protease stability of the antimicrobial peptide Pin2 substituted with D-amino acids. Protein J. 2013;32:456-66.

[187] Park CB, Yi KS, Matsuzaki K, Kim MS, Kim SC. Structure–activity analysis of buforin II, a histone H2A-derived antimicrobial peptide: the proline hinge is responsible for the cell-penetrating ability of buforin II. Proc Natl Acad Sci USA. 2000;97:8245-50.

[188] Park CB, Kim HS, Kim SC. Mechanism of action of the antimicrobial peptide buforin II: buforin II kills microorganisms by penetrating the cell membrane and inhibiting cellular functions. Biochem Biophy Res Commun. 1998;244:253-7.

[189] Sharma A, Pohane AA, Bansal S, Bajaj A, Jain V, Srivastava A. Cell penetrating synthetic antimicrobial peptides (SAMPs) exhibiting potent and selective killing of *Mycobacterium* by targeting its DNA. Chemistry. 2015;21:3540-5.

[190] Hilchie AL, Wuerth K, Hancock RE. Immune modulation by multifaceted cationic host defense (antimicrobial) peptides. Nat Chem Biol. 2013;9:761-8.

[191] de la Fuente-Núñez C, Reffuveille F, Fernández L, Hancock RE. Bacterial biofilm development as a multicellular adaptation: antibiotic resistance and new therapeutic strategies. Curr Opin Microbiol. 2013;16:580-9.

[192] Hall-Stoodley L, Costerton JW, Stoodley P. Bacterial biofilms: from the natural environment to infectious diseases. Nat Rev Microbiol. 2004;2:95-108.

[193] Costerton JW, Stewart PS, Greenberg EP. Bacterial biofilms: a common cause of persistent infections. Science. 1999;284:1318-22.

[194] Wiradharma N, Sng M, Khan M, Ong ZY, Yang YY. Rationally designed α-helical broad-spectrum antimicrobial peptides with idealized facial amphiphilicity. Macromol Rapid Commun. 2013;34:74-80.

[195] Deslouches B, Phadke SM, Lazarevic V, Cascio M, Islam K, Montelaro RC, et al. De novo generation of cationic antimicrobial peptides: influence of length and tryptophan substitution on antimicrobial activity. Antimicrob Agents Chemother. 2005;49:316-22.

[196] Xiong H, Buckwalter BL, Shieh HM, Hecht MH. Periodicity of polar and nonpolar amino acids is the major determinant of secondary structure in

self-assembling oligomeric peptides. Proc Natl Acad Sci USA. 1995;92:6349-53.

[197] Yau WM, Wimley WC, Gawrisch K, White SH. The preference of tryptophan for membrane interfaces. Biochemistry. 1998;37:14713-8.

[198] Hu J, Chen C, Zhang S, Zhao X, Xu H, Zhao X, et al. Designed antimicrobial and antitumor peptides with high selectivity. Biomacromolecules. 2011;12:3839-43.

[199] Deslouches B, Steckbeck JD, Craigo JK, Doi Y, Mietzner TA, Montelaro RC. Rational design of engineered cationic antimicrobial peptides consisting exclusively of arginine and tryptophan, and their activity against multidrug-resistant pathogens. Antimicrob Agents Chemother. 2013;57:2511-21.

[200] Wieprecht T, Apostolov O, Beyermann M, Seelig J. Thermodynamics of the α-helix-coil transition of amphipathic peptides in a membrane environment: implications for the peptide-membrane binding equilibrium. J Mol Biol. 1999;294:785-94.

[201] Blondelle SE, Houghten RA. Design of model amphipathic peptides having potent antimicrobial activities. Biochemistry. 1992;31:12688-94.

[202] Andrushchenko VV, Vogel HJ, Prenner EJ. Interactions of tryptophan-rich cathelicidin antimicrobial peptides with model membranes studied by differential scanning calorimetry. Biochim Biophys Acta. 2007;1768:2447-58.

[203] Cobb JP, Danner RL. Nitric oxide and septic shock. JAMA. 1996;275:1192-6.

[204] Scott MG, Vreugdenhil AC, Buurman WA, Hancock RE, Gold MR. Cutting edge: cationic antimicrobial peptides block the binding of lipopolysaccharide (LPS) to LPS binding protein. J Immunol. 2000;164:549-53.

[205] Mookherjee N, Wilson HL, Doria S, Popowych Y, Falsafi R, Yu JJ, et al. Bovine and human cathelicidin cationic host defense peptides similarly suppress transcriptional responses to bacterial lipopolysaccharide. J Leukocyte Biol. 2006;80:1563-74.

[206] Woodcock J, Griffin JP, Behrman RE. Development of novel combination therapies. N Engl J Med. 2011;364:985-7.

[207] Rivas-Santiago B, Castañeda-Delgado JE, Santiago CE, Waldbrook M, González-Curiel I, León-Contreras JC, et al. Ability of innate defence regulator peptides IDR-1002, IDR-HH2 and IDR-1018 to protect against *Mycobacterium tuberculosis* infections in animal models. PLoS One. 2013;8:e59119.

[208] Llamas-González YY, Pedroza-Roldán C, Cortés-Serna MB, Márquez-Aguirre AL, Gálvez-Gastélum FJ, Flores-Valdez MA. The synthetic cathelicidin HHC-10 inhibits *Mycobacterium bovis* BCG in vitro and in C57BL/6 mice. Microb Drug Resist. 2013;19:124-9.

[209] Kalita A, Verma I, Khuller GK. Role of human neutrophil peptide-1 as a possible adjunct to antituberculosis chemotherapy. J Infect Dis. 2004;190:1476-80.

[210] Schmidt R, Ostorházi E, Wende E, Knappe D, Hoffmann R. Pharmacokinetics and in vivo efficacy of optimized oncocin derivatives. J Antimicrob Chemother. 2016;71:1003-11.

[211] Rivas-Santiago CE, Hernández-Pando R, Rivas-Santiago B. Immunotherapy for pulmonary TB: antimicrobial peptides and their inducers. Immunotherapy. 2013;5:1117-26.

[212] Mir SA, Sharma S. Immunotherapeutic potential of N-formylated peptides of ESAT-6 and glutamine synthetase in experimental tuberculosis. Int Immunopharmacol. 2014;18:298-303.